

## **EXPLORATION OF STRUCTURE-SWITCHING RNA APTAMER SENSORS**



**EXPLORATION OF STRUCTURE-SWITCHING IN THE DESIGN OF RNA  
APTAMER SENSORS**

**By**

**PUI SAI LAU, B.Sc.**

**A Thesis**

**Submitted to the School of Graduate Studies**

**in Partial Fulfillment of the Requirements**

**for the Degree**

**Doctor of Philosophy**

**McMaster University**

**© Copyright Pui Sai Lau, December 2013**

DOCTOR OF PHILOSOPHY (2013)  
(Biochemistry and Biomedical Sciences)

McMaster University  
Hamilton, Ontario

TITLE: Exploration of Structure-Switching in the Design of RNA Aptamer Sensors

AUTHOR: Pui Sai Lau, B.Sc. (McMaster University)

SUPERVISOR: Dr. Yingfu Li

NUMBER OF PAGES: xix, 182

## ABSTRACT

The process of “structure-switching” enables biomolecular switches to function as effective biosensing tools. Biomolecular switches can be activated or inactivated by binding to a specific target that triggers a precise conformational change in the biomolecules involved. Examples of aptamer-based biomolecular switches can be found in nature. Furthermore, efforts have been made in the last decade to engineer structure-switching sensors using DNA aptamers whereby, the aptamer is coupled to a signal transduction method to generate a readout signal upon target binding to the aptamer domain. Conversely, RNA aptamers have been relatively underexplored for sensor development, largely due to its susceptibility to nuclease degradation and chemical instability. Despite these shortcomings, many RNA aptamers possess superior sensing capabilities, and the abundance of RNA aptamers provides new opportunities to further advance the field. In effect, this thesis uses a structure-switching design to demonstrate the power of RNA aptamers for fluorescence-based sensor development. Herein, we demonstrate generalizable structure-switching strategies to make use of the abundance of RNA aptamers, monitor the quality control of detection and correct detection error, as well as enhance RNA aptamer sensing capability by using regulated graphene adsorption. Furthermore, our findings have expanded for secondary applications involving collaborations with other research labs. In one application, we demonstrate that entrapment of structure-switching RNA aptamers in sol-gel material confers protection against nuclease degradation and chemical instability. In another application, we further validate the use of riboswitches, or natural structure-switching RNA aptamers, as

potential targets for drug discovery. Overall, these results demonstrate the capability of RNA aptamers for sensor development. We conclude with a discussion of possible areas for further inquiry, as well as future applications for the advancement of structure-switching RNA aptamers.

## ACKNOWLEDGEMENTS

First and foremost, I would like to thank my supervisor Dr. Yingfu Li for giving me the opportunity to further expand my mind. After finishing my undergraduate degree, I firmly believed that I had reached my full learning potential. Now at the end of my Ph.D. studies, I realize that I was wrong. I have learned a great deal from Dr. Li, who has immensely shaped my development as a scientist. Most of all, I have learned that I still have yet to reach my full potential. I look forward to many future learning opportunities.

I would also like to thank my co-supervisor and supervisory committee member Dr. Brian Coombes for his valuable suggestions and support, especially during my practice seminars, journal club presentations, and committee meetings. His depth of knowledge has been truly inspirational to me. I would also like to thank my supervisory committee member, Dr. John Brennan. His challenging questions and practical advice during my committee meetings have helped me address immediate issues in my research, as well as anticipate future issues.

The Li lab members have also provided a supportive network for discussion. I would especially like to recognize Monsur Ali, Jimmy Gu, Jinping Song, Jeffrey Lam, Sergio Aguirre, and Wendy Mok for their helpful discussions, and assistance. I would also like to thank Carmen Carrasquilla and Christy Hui from the Brennan lab who have helped me learn a lot about sol-gel derived materials.

I would like to acknowledge McMaster University for being a wonderful home-away-from-home for me. I have truly enjoyed my time at this school, especially the

vibrant community, positive campus environment, recreational swimming and Phoenix fries.

On a more personal note, I would like to thank my parents, who have nurtured my love of learning from an early age, and my brother for helping me develop my competitive edge. Lastly, but certainly not least, I would like to thank Trevor, my best friend and partner for life, for his unconditional love and support.

*“My flesh and my heart may fail, but God is the strength of my heart and my portion forever.”*

*Psalm 73:26*

## TABLE OF CONTENTS

<b>Abstract</b> .....	iii
<b>Acknowledgements</b> .....	v
<b>List of Figures</b> .....	xiv
<b>List of Schemes</b> .....	xvii
<b>List of Tables</b> .....	xvii
<b>List of Abbreviations</b> .....	xvii
<b>Chapter 1. A General Introduction</b> .....	1
<b>1.1 Author’s Preface</b> .....	1
<b>1.2 Overview of Structure-Switching Sensors</b> .....	2
<b>1.3 The Origin of Structure-Switching DNA Aptamers</b> .....	4
1.3.1 Structure-switching DNA aptamers in fluorescent sensors.....	8
1.3.2 Structure-switching DNA aptamers in electrochemical sensors.....	14
1.3.3 Structure-switching DNA aptamers in colorimetric sensors.....	19
<b>1.4 Structure-Switching RNA Aptamers</b> .....	22
1.4.1 Natural aptamers for small molecules: metabolite-sensing riboswitches.....	22
1.4.2 Synthetic riboswitches for small molecules.....	26
<b>1.5 RNA Aptamers Created Through SELEX</b> .....	27
<b>1.6 The Limitations of RNA for Detection</b> .....	29
<b>1.7 Research Objectives and Thesis Organization</b> .....	32
<b>Chapter 2. A General Approach to the Construction of Structure-Switching Reporters from RNA Aptamers</b> .....	35
<b>2.1 Author’s Preface</b> .....	35
<b>2.2 Abstract</b> .....	36

<b>2.3 Introduction</b> .....	37
<b>2.4 Materials and Methods</b> .....	39
2.4.1 Materials.....	39
2.4.2 Polymerase Chain Reaction.....	40
2.4.3 RNA transcription.....	41
2.4.4 Fluorescence measurements.....	41
2.4.5 Signaling rate calculation.....	41
<b>2.5 Results and Discussion</b> .....	42
2.5.1 Creation of an aptamer reporter for theophylline.....	42
2.5.2 Sensing capability of the theophylline reporter.....	44
2.5.3 Creation of an aptamer reporter for TPP.....	45
2.5.4 Sensing capability of the TPP reporter.....	46
<b>2.6 Conclusions</b> .....	48
<b>2.7 Acknowledgements</b> .....	51
<b>2.8 References</b> .....	51
<b>Chapter 3. Quality Control Certification of RNA Aptamer-Based Detection</b> .....	53
<b>3.1 Author’s Preface</b> .....	53
<b>3.2 Abstract</b> .....	54
<b>3.3 Introduction</b> .....	55
<b>3.4 Materials and Methods</b> .....	57
3.4.1 Materials.....	57
3.4.2 Polymerase Chain Reaction.....	58
3.4.3 RNA transcription.....	58
3.4.4 Fluorescence measurements.....	59

<b>3.5 Results and Discussion</b> .....	60
3.5.1 Construction of an aptamer reporter for thrombin.....	60
3.5.2 Sensing performance of the thrombin reporter.....	61
3.5.3 Functionality test of the QC element.....	62
3.5.4 Construction of an aptamer reporter for theophylline.....	63
3.5.5 Sensing capability of the theophylline reporter.....	64
3.5.6 Test of QC element function within the theophylline reporter.....	64
3.5.7 Elimination of false-positive signals guided by QC element.....	66
<b>3.6 Conclusions</b> .....	67
<b>3.7 Acknowledgements</b> .....	69
<b>3.8 References</b> .....	70
<b>Chapter 4. A General Strategy to Create RNA Aptamer Sensors Using Regulated Graphene Oxide Adsorption</b> .....	72
<b>4.1 Author’s Preface</b> .....	72
<b>4.2 Abstract</b> .....	73
<b>4.3 Introduction</b> .....	73
<b>4.4 Materials and Methods</b> .....	77
4.4.1 Materials.....	77
4.4.2 Polymerase Chain Reaction.....	78
4.4.3 RNA transcription.....	79
4.4.4 Fluorescence measurements.....	79
<b>4.5 Results and Discussion</b> .....	80
4.5.1 Creation of an aptamer reporter for theophylline.....	80
4.5.2 Sensing capability of theophylline reporter.....	84
4.5.3 Creation of an aptamer reporter for TPP.....	85

4.5.4 Sensing capability of TPP reporter.....	87
<b>4.6 Conclusions.....</b>	<b>88</b>
<b>4.7 Acknowledgements.....</b>	<b>89</b>
<b>4.8 References.....</b>	<b>90</b>
<b>Chapter 5. Secondary Application #1: Stabilizing Structure-Switching Signaling RNA Aptamers by Entrapment in Sol-Gel Derived Materials for Solid-Phase Assays.....</b>	<b>92</b>
<b>5.1 Author’s Preface.....</b>	<b>92</b>
<b>5.2 Abstract.....</b>	<b>93</b>
<b>5.3 Introduction.....</b>	<b>94</b>
<b>5.4 Results and Discussion.....</b>	<b>97</b>
5.4.1 Characterization of sol-gel derived materials.....	97
5.4.2 Leaching of aptamers from sol-gel derived materials.....	98
5.4.3 Signal generation from entrapped RNA aptamer reporters.....	99
5.4.4 Sensitivity and selectivity of entrapped RNA aptamer reporters.....	102
5.4.5 RNA aptamer sensitivity to ribonucleases.....	104
5.4.6 Effects of long-term storage on RNA aptamer activity.....	105
<b>5.5 Conclusions.....</b>	<b>108</b>
<b>5.6 References.....</b>	<b>109</b>
<b>Chapter 6. Secondary Application #2: Synthesis and Evaluation of Glucosamine-6-Phosphate as Activators of glmS Riboswitch.....</b>	<b>112</b>
<b>6.1 Author’s Preface.....</b>	<b>112</b>
<b>6.2 Abstract.....</b>	<b>113</b>
<b>6.3 Introduction.....</b>	<b>113</b>
<b>6.4 Results and Discussion.....</b>	<b>115</b>

<b>6.5 Conclusions.....</b>	<b>121</b>
<b>6.6 References.....</b>	<b>122</b>
<b>Chapter 7. Discussion and Future Directions.....</b>	<b>124</b>
<b>Appendix 1.....</b>	<b>132</b>
<b>Chapter 2. Supplementary Information.....</b>	<b>132</b>
<b>Chapter 3. Supplementary Information.....</b>	<b>135</b>
<b>Chapter 4. Supplementary Information.....</b>	<b>139</b>
<b>Appendix 2. Development of Tandem DNA Aptamers for the Detection of <i>L. Monocytogenes</i>.....</b>	<b>141</b>
<b>Author’s Preface.....</b>	<b>141</b>
<b>Abstract.....</b>	<b>142</b>
<b>Introduction.....</b>	<b>142</b>
<b>Materials and Methods.....</b>	<b>145</b>
Materials.....	145
Growth of bacterial strains.....	146
Growth of <i>L. monocytogenes</i> biofilm.....	146
Preparation of dimeric/trimeric DNA libraries.....	147
Polymerase Chain Reaction.....	149
Biofilm SELEX procedure.....	150
Cell SELEX procedure.....	151
<b>Results and Discussion .....</b>	<b>153</b>
Creation of dimeric and trimeric DNA libraries.....	153
Optimization of biofilm growth of <i>L. monocytogenes</i> .....	155

Progress of SELEX.....	156
Analysis of dimeric and trimeric sequence data.....	160
<b>Future Directions.....</b>	<b>162</b>
<b>Acknowledgements.....</b>	<b>163</b>
<b>References for Appendix 2.....</b>	<b>164</b>
<b>References.....</b>	<b>166</b>

## LIST OF FIGURES

### Chapter 1

<b>Figure 1-1.</b> Variations of the structure-switching design strategy.....	5
<b>Figure 1-2.</b> Application of SELEX to develop structure-switching reporters.....	6
<b>Figure 1-3.</b> Fluorescent signal amplification strategies for structure-switching design...	10
<b>Figure 1-4.</b> Structure-switching design for electrochemical detection.....	14
<b>Figure 1-5.</b> Labeled and label-free formats of electrochemical detection.....	16
<b>Figure 1-6.</b> Structure-switching reporter for colorimetric detection.....	21
<b>Figure 1-7.</b> A list of targets for which riboswitches have been discovered.....	23
<b>Figure 1-8.</b> Regulatory mechanisms of riboswitches.....	25
<b>Figure 1-9.</b> A list of targets for which RNA aptamers have been discovered through SELEX.....	29
<b>Figure 1-10.</b> General mechanism of RNA cleavage by intramolecular transesterification.....	30

### Chapter 2

<b>Figure 2-1.</b> General strategy for designing fluorescent RNA aptamer reporters.....	39
<b>Figure 2-2.</b> Structure-switching reporter for theophylline.....	43
<b>Figure 2-3.</b> Specificity and sensitivity of the theophylline reporter.....	44
<b>Figure 2-4.</b> Structure-switching reporter for TPP.....	47

### Chapter 3

<b>Figure 3-1.</b> Structure-switching RNA aptamers with a quality control element.....	57
<b>Figure 3-2.</b> A thrombin reporter.....	61
<b>Figure 3-3.</b> False-positive signal reporting.....	63
<b>Figure 3-4.</b> A theophylline reporter.....	65

## Chapter 4

<b>Figure 4-1.</b> RNA aptamer sensors based on regulated graphene oxide adsorption.....	77
<b>Figure 4-2.</b> Creation of the theophylline reporter.....	83
<b>Figure 4-3.</b> BDNA mechanism for signal enhancement.....	84
<b>Figure 4-4.</b> Sensing capability of the theophylline reporter.....	85
<b>Figure 4-5.</b> Creation of the TPP reporter.....	86
<b>Figure 4-6.</b> Sensing capability of the TPP reporter.....	87

## Chapter 5

<b>Figure 5-1.</b> Leaching of the anti-theophylline and anti-TPP RNA aptamer reporter constructs from various sol-gel derived materials.....	99
<b>Figure 5-2.</b> Fluorescence signaling ability of RNA aptamer reporters in solution and in various sol-gel derived materials.....	100
<b>Figure 5-3.</b> Sensitivity of the sol-gel entrapped RNA aptamer reporters.....	103
<b>Figure 5-4.</b> Changes in emission intensity of RNA aptamer reporters upon exposure to RNase A or RNase H.....	105
<b>Figure 5-5.</b> Structure-switching and signaling ability of RNA aptamer reporters after different storage time.....	106

## Chapter 6

<b>Figure 6-1.</b> The structures of three GlcN6P analogues.....	114
<b>Figure 6-2.</b> The MTPA plane of <i>S</i> - and <i>R</i> -MTPA esters.....	118
<b>Figure 6-3.</b> The MTPA plane of <i>S</i> -MTPA esters 14a and 14b made from 12a and 12b.....	119
<b>Figure 6-4.</b> Cleavage of <i>glmS</i> RNA with and without compounds.....	120

## Appendix 1: Supplementary Information

<b>Figure S2-1.</b> Secondary structures of the theophylline and TPP aptamers.....	132
<b>Figure S2-2.</b> The initially designed structure-switching reporter from the theophylline RNA aptamer.....	133
<b>Figure S2-3.</b> Detection sensitivity of the theophylline reporter made of FDNA1, QDNA2 and TRA1.....	134
<b>Figure S2-4.</b> Nucleotide sequences of TPP aptamer and a mutant aptamer.....	134
<b>Figure S3-1.</b> Thermal denaturation profiles of duplexes made from Q <sub>2</sub> DNA13-16 with mfRNA, F <sub>1</sub> DNAF <sub>2</sub> and Q <sub>1</sub> DNA for thrombin and theophylline reporters.....	135
<b>Figure S3-2.</b> Wildtype multifunctional RNA aptamer sequences and their mutated aptamer sequences for thrombin and theophylline reporters.....	136
<b>Figure S3-3.</b> Detection sensitivity of structure-switching RNA aptamer reporters made up of corresponding mfRNA, Q <sub>1</sub> DNA, F <sub>1</sub> DNAF <sub>2</sub> , and Q <sub>2</sub> DNA13.....	137
<b>Figure S3-4.</b> Error detection and correction using thrombin structure-switching reporter with a quality control element.....	138
<b>Figure S4-1.</b> Optimization of conditions for RNA aptamer sensor using classic GO adsorption method.....	139
<b>Figure S4-2.</b> Sequences of theophylline and TPP mutant aptamers.....	140

## Appendix 2

<b>Figure 1.</b> Overview of objectives to develop tandem DNA aptamers for detection of <i>L. monocytogenes</i> .....	145
<b>Figure 2.</b> Scheme of creating the homo-tandem DNA library.....	154
<b>Figure 3.</b> Creation of the homo-tandem DNA library.....	154
<b>Figure 4.</b> Biofilm growth of <i>L. monocytogenes</i> 568.....	155
<b>Figure 5.</b> Overview of biofilm-SELEX.....	157
<b>Figure 6.</b> Finding optimal conditions for biofilm-SELEX.....	157

<b>Figure 7.</b> Progress of SELEX using tandem dimeric and trimeric DNA pools.....	158
<b>Figure 8.</b> Overview of cell-SELEX.....	159
<b>Figure 9.</b> Sequencing results of the dimer DNA pool after 17 round of SELEX.....	161

## LIST OF SCHEMES

### Chapter 6

<b>Scheme 6-1.</b> Synthesis of carba-sugar 1.....	115
<b>Scheme 6-2.</b> Synthesis of GlcN6P analogues 2 and 3.....	117
<b>Scheme 6-3.</b> Synthesis of <i>R</i> - and <i>S</i> - Mosher esters from compound 12a.....	118

## LIST OF TABLES

### Chapter 6

<b>Table 6-1.</b> Effect of synthetic compounds on <i>glmS</i> riboswitch.....	120
--	-----

## LIST OF ABBREVIATIONS

APTES	3-(aminopropyl)triethoxysilane
ATP	adenosine 5'-triphosphate
AuNP	gold nanoparticle
BDNA	blocking DNA
bp	base-pair
DABCYL	4-([4-(dimethylamino)phenyl]-azo)-benzoic acid succinimidyl ester
dATP	2'-deoxyadenosine 5'-triphosphate
DGS	diglycerylsilane
DNA	2'-deoxyribonucleic acid

DNase	deoxyribonuclease
dNTP	2'-deoxyribonucleoside 5'-triphosphate
ds	double-stranded
FAM	6-carboxyfluorescein
FDNA	fluorophore labeled DNA
F <sub>1</sub> DNA <sub>2</sub>	dual fluorophore labeled DNA
FRET	fluorescence resonance energy transfer
GlcN6P	glucosamine-6-phosphate
GO	graphene oxide
K <sub>d</sub>	dissociation constant
mRNA	multifunctional RNA
mRNA	messenger RNA
MSQ	methylsilsesquioxane
MTMS	methyltrimethoxysilane
nt	nucleotide
NTP	nucleoside 5'-triphosphate
PAGE	polyacrylamide gel electrophoresis
PCR	polymerase chain reaction
QC	quality control
QDNA	quencher-labeled DNA
RF	relative fluorescence
RNA	ribonucleic acid
RNase	ribonuclease
SELEX	systematic evolution of ligands by exponential enrichment
ss	single-stranded
SS	sodium silicate

T4 PNK	T4 polynucleotide kinase
TMOS	tetramethylorthosilicate
TMP	thiamine monophosphate
TPP	thiamine pyrophosphate
TPPRNA	extended TPP RNA aptamer
TRA	extended theophylline RNA aptamer
WT	wild-type

## CHAPTER 1

### A GENERAL INTRODUCTION

#### 1.1 Author's Preface

The following introductory sections are intended to provide background information underlying structure-switching aptamer-based sensors in the broader context of sensor development. Specifically, sections 1.2 and 1.3 are a modified version of a published book chapter, which I primarily wrote with suggestions from Dr. Yingfu Li (first citation below). Section 1.4 is an excerpt from a previously published review, which I co-wrote with Dr. Yingfu Li (second citation below). Collectively, the introductory sections lead up to the overall objective of this thesis, which is found in section 1.7.

Lau PS, Li Y (in press) Exploration of structure-switching in the design of aptamer biosensors. *Adv Biochem Engin/Biotechnol*. DOI: 10.1007/10\_2013\_223.

Lau PS, Li Y (2011) Functional nucleic acids as molecular recognition elements for small organic and biological molecules. *Curr Org Chem* 15: 557-75.

## 1.2 Overview of Structure-Switching Sensors

Nature has evolved biomolecular switches in all domains of life as biosensing tools to monitor its complex environmental surroundings. Made of nucleic acids or proteins, biomolecular switches effectively detect specific chemical signals (targets) to carry out precise biochemical functions within a cell. Through “structure-switching”, nature’s biosensors can become active/inactive, by target binding that induces specific conformational change of the biomolecules involved [1].

To date, the only known group of natural nucleic acid-based biomolecular switches are riboswitches. Discovered by Breaker’s group in 2002, riboswitches are RNA-based regulatory systems found in diverse organisms that respond to specific small molecules to regulate gene expression [2]. Typically composed of a molecular recognition element (aptamer domain) that binds to a specific target and a downstream expression domain, riboswitches operate through structure-switching events whereby target binding to the aptamer domain results in an overall change in the structure of the designated RNA to switch the expression domain to the “on” or “off” state.

Although the number of novel classes of riboswitches that respond to different metabolites continues to grow [3-5], many research groups have successfully engineered artificial riboswitches to broaden the versatility of controlling gene expression by RNA switches [6-14]. Interestingly, even before the discovery of riboswitches, the laboratories of Szostak and Gold independently developed a method to derive artificial aptamers in 1990 [15, 16]. Termed systematic evolution of ligands by exponential enrichment, or

SELEX, this test-tube-based selection technique has been extensively used to isolate aptamers specific to a target of choice from random-sequence DNA or RNA libraries [17, 18]. Through the mechanism of structure-switching, many of these aptamers have been coupled to a signal transduction method to relay a readout signal produced by target binding to the aptamer domain [19, 20].

Exploration of structure-switching for the design of aptamer-based biosensors is attractive for two particular reasons. First, structure-switching processes can ensure high detection specificity; that is because structure-switching can only be induced through specific target-aptamer interactions (which are difficult to imitate by non-cognate targets). Second, structure-switching is highly compatible with a variety of signal transduction mechanisms for signal generation; the aptamer-ligand binding also brings about pronounced structural/physical rearrangement of the aptamer, which can be effortlessly coupled to many prevailing signal production mechanisms for the generation of an easily detectable signal, such as a change in fluorescence intensity, color appearance and electrochemical readout.

The exploration of aptamers for engineering biosensors also comes with a number of advantages that reflect the innate properties of nucleic acids. These include the chemical stability of DNA, intricate folding capability of DNA and RNA, tendency of both DNA and RNA to form predictable duplex structural elements, ease of immobilization of DNA and RNA onto solid supports, and their amenability to various chemical modifications [21].

### 1.3 The Origin of Structure-Switching DNA Aptamers

Early accounts of engineered structure-switching aptamer sensors began using DNA aptamers. Inspired by natural biomolecular switches and motivated to improve upon previous aptamer sensor designs that lacked wide applicability towards diverse aptamers, our group developed structure-switching DNA aptamers [22]. This approach takes advantage of the ability of aptamers to form both an aptamer–target complex and a DNA–DNA duplex with complementary sequences. By creating a DNA duplex composed of an extended DNA aptamer strand partly hybridized to complementary strands of fluorophore-labeled DNA (FDNA) and quencher-labeled DNA (QDNA), low fluorescent signal is obtained due to the close proximity of the fluorophore and quencher moieties (the “off” mode). The addition of target, however, facilitates formation of the target–aptamer complex and subsequent displacement of QDNA, generating high fluorescent signal (the “on” mode) (Figure 1-1a). In this way, signaling reporters were successfully created for both anti-ATP [23] and anti-thrombin [24] aptamers.

The ATP reporter exhibited target specificity comparable to the original aptamer (which primarily recognizes the common adenosine group), and generated 10- to 14-fold fluorescence increase in the presence of adenosine and related analogs such as ATP, ADP, AMP, and dATP. Expectedly, no fluorescence increase was generated in the presence of CTP, UTP, or GTP. Similarly, the thrombin reporter only recognized the thrombin target, produced ~12-fold fluorescence increase, but exhibited no signal for BSA and human factors Xa and IXa. The structure-switching design served well despite

differences in binding affinity and size of the aptamers tested, thus demonstrating generality of the strategy [22].

To further extend the generality, our group developed three other structure-switching designs [22]. These alternative designs include the attachment of the fluorophore to the end of an aptamer (Figure 1-1b) or at an internal nucleotide (Figure 1-1c), and the hybridization of FDNA and QDNA with an aptamer without the addition of extra nucleotides (Figure 1-1d). Notably, there are also examples of sensing strategies that make use of target-induced structure-switching, but do not involve the dissociation of a complementary oligonucleotide [25, 26].

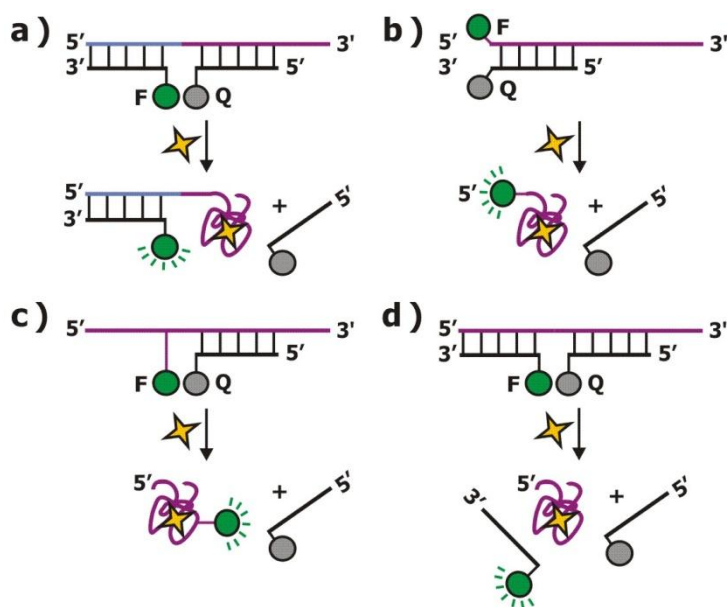


**Figure 1-1.** Variations of the structure-switching design strategy. All examples make use of the ability of a DNA aptamer (purple) to form a duplex with a complementary DNA sequence, or a complex with a designated target (star). F and Q signify fluorophore and quencher, respectively. See main text for details.

Aptamers are artificially created through the SELEX process [15, 16]. In this technique, a randomized library of  $\sim 10^{15}$  single-stranded DNA or RNA sequences is subjected to a selective pressure to separate molecules that pass a functional test (i.e. target binding) from those that do not. Successful sequences are copied, and used to carry out the same procedure for another round. Through iterative rounds of selection and amplification, functional molecules “evolve”, so that only the most effective sequences survive in the end (Figure 1-2a).

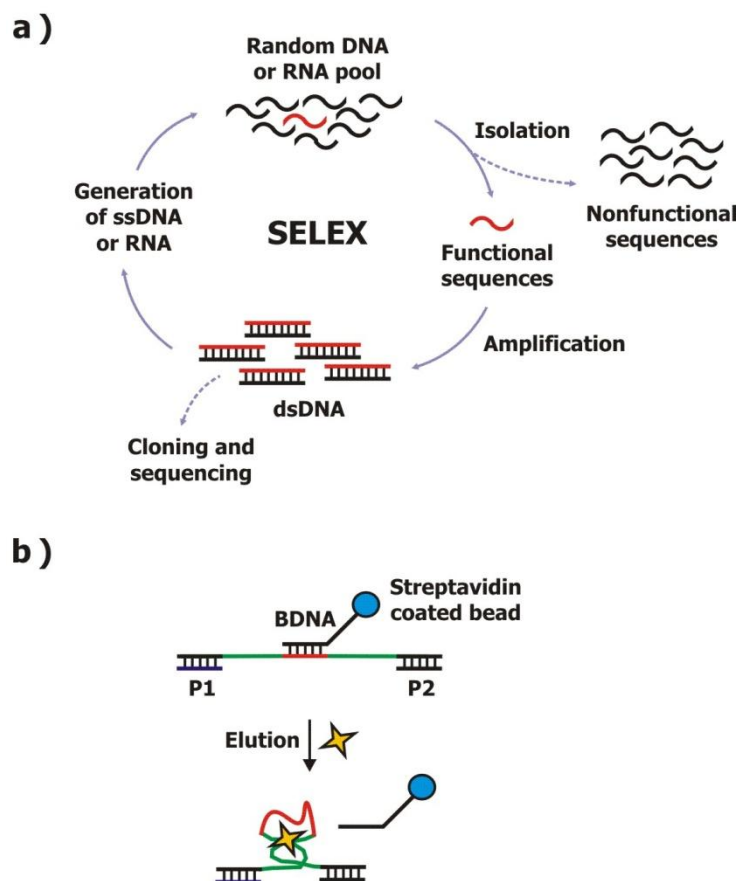


**Figure 1-2.** **a)** General SELEX scheme. **b)** Application of SELEX to develop structure-switching reporters. Isolation step is depicted: DNA sequences are designed with two randomized sites (green) and fixed regions that hybridize with primers (P1, P2), and biotinylated DNA (BDNA). Only sequences capable of target (star) binding, and thus

structure-switching, are eluted from the streptavidin beads and carried on for further SELEX rounds.

Our group has developed a strategy to create structure-switching reporters directly through SELEX [27]. The potential advantage of this approach is that post-SELEX modification and optimization steps do not need to be taken to convert the selected aptamer into a signaling probe. In this study, the DNA library was specially designed to contain a central fixed-sequence domain flanked by two random-sequence domains, each of which was further flanked by a primer-binding sequence. The central fixed-sequence domain was purposely designed to be complementary to an antisense oligonucleotide biotinylated at its 5'-end (BDNA), which permitted immobilization of the DNA library onto streptavidin-coated beads. The immobilized DNA duplex was then exposed to a solution containing the target of interest. Oligonucleotides that were able to form the DNA/target complex were separated from the beads and were released into solution. These molecules were then collected, amplified by PCR and processed for the next round of enrichment (Figure 1-2b). Interestingly, all classes of ATP-binding aptamers obtained contained the previously isolated ATP-binding aptamer, which reinforces that SELEX often finds the same solution to a given problem. Other groups have also independently reported selection of the same ATP-binding motif [23, 28], despite differences in library designs and SELEX strategies used. Additionally, conserved nucleotides were also found outside of the target-binding sites, suggesting that these regions are important for the structure-switching process. All selected reporters readily responded to ATP, however, the fluorescence increase was only ~4.5-fold. A possible explanation for this may lie in

the finding that all selected aptamers acquired one or two nucleotide mutations in the site that binds to BDNA. Although a weaker aptamer-BDNA duplex enabled easier structure-switching throughout the course of SELEX, it also contributed to higher background signal of the aptamer-based sensor. Therefore, improved structure-switching reporters may be developed in the future by using a more stringent SELEX design (i.e. elevated temperature during the functional selection step to eliminate weaker duplex structures) [27].

Since conception, structure-switching DNA aptamers have been expanded to detect various targets including GTP [27], mercury [29, 30], quinine [31], cocaine [32], arginine [33], IgE [34], L-tyrosinamide [35], cathepsin D [36], lysozyme [37], and PDGF [38], although most studies to date have predominantly focused on the anti-ATP and anti-thrombin DNA aptamers, which have become model systems for biosensor development. Moreover, the versatility of the structure-switching design has been adapted to function with other signal transduction methods including electrochemical and colorimetric platforms. In the following sections, we discuss some of the key advancements of structure-switching sensors using fluorescent, colorimetric and electrochemical signal transduction mechanisms. To facilitate comparative analysis, we examine examples primarily based on the well-characterized anti-ATP and anti-thrombin DNA aptamers.

### **1.3.1 Structure-Switching DNA Aptamers in Fluorescent Sensors**

Fluorescence is a commonly used method of signal transduction for aptamer sensors due to the ease of conjugation of various fluorophores and quenchers to DNA,

and the convenience of detection conferred by widely available commercial instruments. Using the classic structure-switching design [22], our lab discovered that the ATP reporter produced a  $K_d$  of  $\sim 600 \mu\text{M}$  [22], which is 60-fold lower in affinity than the original aptamer ( $K_d = \sim 10 \mu\text{M}$ ) [23]. The thrombin reporter produced a  $K_d$  of  $\sim 400 \text{nM}$  [22], which is a 2-fold reduction in affinity compared to the original aptamer ( $K_d = 200 \text{nM}$ ) [24]. These findings suggest that the QDNA displacement step affects the target-binding affinity of aptamers with inherently low affinity more so than those with high affinity. Possible explanations for the reduced affinities of the structure-switching reporters include: (i) QDNA hybridization partially blocks the aptamer site, so the target must compete with QDNA for binding, and (ii) the low level of fluorescence generated from the signaling duplex (extended aptamer-FDNA-QDNA) itself may make it difficult to detect small increases in fluorescence from low target concentrations, which may be obscured within the background fluorescence associated with a large excess of unswitched duplex.

To enhance detection sensitivity, signal amplification methods can provide solutions. A commonly used assay format based on structure-switching involves a capture probe to bind a desired ligand at one site for immobilization, and a signaling probe to bind the ligand at another site for detection (Figure 1-3a). In this way, Qu and colleagues have created an assay that makes use of fluorescent silica nanoparticles (FNPs), which can entrap many fluorophores in a single particle [39]. Compared with traditional fluorophores, FNPs are advantageous as they provide fluorescent signal amplification and higher photostability. The design by the Qu group involved use of magnetic silica

microspheres functionalized with DNA that hybridizes to a part of the anti-ATP aptamer (capture probe), and FNPs functionalized with DNA that hybridizes to another part of the aptamer (signaling probe). In the absence of the target, the capture probe-aptamer-signaling probe complex was separated from the solution magnetically, which resulted in low fluorescence in solution. However, when the target was introduced, the binding of the target to the aptamer resulted in a structure-switching event that separated FNPs from the complex and produced a high level of fluorescence in solution. This method exhibited a much improved detection limit of 0.1  $\mu\text{M}$ .

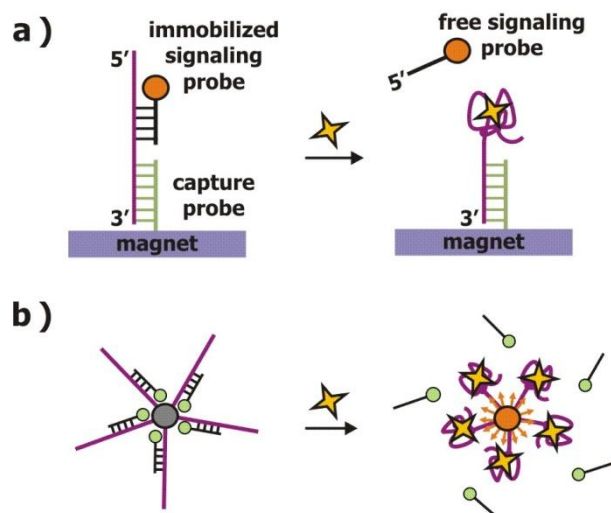


**Figure 1-3. a)** A structure-switching assay for fluorescence-based detection. The capture probe immobilizes the aptamer, and the signaling probe anneals to provide a readout signal upon target induced structure-switching. Only the signal in solution from displaced signaling probes is measured after the magnetic separation step. **b)** Quantum dots for multiplex detection; use of multiple aptamers, for many target-induced structure-switching events and high increase in fluorescent signal.

Quantum dots (QDs) have also been explored for the purpose of signal amplification. From a molecular recognition perspective, the surface of QDs can be easily

functionalized with multiple oligonucleotides to facilitate multiple binding interactions (Figure 1-3b). From a signaling perspective, QDs provide higher photostability, sharper emission bands, and versatility for multiplex detection (QDs respond to the same excitation wavelength, but can be tuned to emit at different wavelengths). The Ellington group has designed a strategy whereby QDs were functionalized with multiple copies of an extended thrombin aptamer [40]. Hybridization of a complementary, quencher-modified DNA to the QD-aptamer resulted in low fluorescence due to the close proximity of the QD and quencher. The addition of thrombin however, led to multiple target-aptamer binding interactions, and displacement of many quencher-modified DNA strands. The result of multiple structure-switching events generated signal amplification and a 19-fold fluorescence enhancement.

The Lu group has taken QDs one step further for simultaneous detection of multiple targets within one pot [41]. Their design takes advantage of a number of properties of gold nanoparticles (AuNPs): the ability of AuNPs to quench fluorescence when in close proximity to QDs, the tunability of fluorescence quenching by controlling the aggregation or dispersal state of AuNPs, and the color changes associated with aggregation or dispersal of AuNPs due to surface plasmon resonance. In brief, when no target was added, AuNPs and QDs functionalized with complementary DNA sequences hybridized to an extended aptamer sequence. In this state, the AuNP-QD-aptamer complex aggregated to generate low fluorescence (due to close proximity of QD and AuNP), as well as a blue color from the AuNPs. In the presence of target, however, target-aptamer binding occurred, which caused the functionalized QDs and AuNPs to

dehybridize and disperse the aggregate. This subsequently led to high fluorescence signaling (separation of QD from AuNP), and a color change to red. Using this design, two different aptamer-based reporters were created to detect ATP, and cocaine, respectively. The associated QDs for each reporter emitted at characteristic wavelengths of 525 and 585 nm, although the same excitation wavelength was used for both systems. ATP and cocaine were accurately detected simultaneously in the same solution using fluorescent and colorimetric means.

Over the last few years, structure-switching fluorescent reporters have started to move into the realm of more “real-life” detection involving use of automation and complex samples. For drug discovery, our group implemented a structure-switching assay to search for enzyme inhibitors in a high throughput screen (HTS) [42]. The therapeutic target used in this case was adenosine deaminase (ADA), a problematic metabolic enzyme in severe combined immunodeficiency diseases that irreversibly converts adenosine into inosine [43]. The well-established anti-ATP structure-switching aptamer reporter provided a suitable solution as a screening assay since the aptamer has high affinity for adenosine, but does not bind inosine [23]. In the presence of adenosine, the target-aptamer complex formed and structure-switching occurred to generate high fluorescent signaling. However, in the presence of inosine (after ADA conversion of adenosine), the fluorescein-labeled aptamer bound to the complementary QDNA sequence, and fluorescence was quenched. The use of this screening assay resulted in the identification of small-molecule inhibitors of ADA out of a collection of 44,400 compounds [42].

Another automated approach that was demonstrated to be highly amenable with structure-switching sensors is fluorescence activated cell sorting (FACS), a method which can sort fluorescent cells faster than  $10^4$  cells a second [44]. Liu and colleagues immobilized the anti-ATP structure-switching aptamer onto magnetic microparticles, and implemented FACS to sort out microparticles that underwent target-induced structure-switching (high fluorescence) from those that retained the duplex of fluorescein-labeled aptamer and QDNA (low fluorescence) [45]. Furthermore, sorting was also demonstrated in serum without significant change in the performance of the reporter. In another FACS-based study, Mirkin's group functionalized AuNPs with duplexes made of the ATP aptamer hybridized to a fluorophore-modified complementary DNA sequence, forming the aptamer "nanoflare" [46]. In this state, the close proximity of fluorophore to the AuNP resulted in fluorescence quenching. However, the addition of ATP resulted in target-aptamer complex formation and the release of fluorophore-modified complementary DNA (high fluorescence from reporter "flares"). This reporter was readily taken up by living cells, and FACS was implemented to measure fluorescence intensity and quantify intracellular levels of ATP.

Other efforts have also resulted in the successful immobilization of structure-switching reporters in sol-gel- [47, 48], hydrogel- [49], and cellulose- [50] based materials, which have shown comparable sensing capabilities as solution-based studies. These findings will help extend the utility of structure-switching sensors towards real-world applications in medical diagnostics, environmental monitoring, and food safety.

### 1.3.2 Structure-Switching DNA Aptamers in Electrochemical Sensors

Electrochemistry has become another well-established signal transduction method for structure-switching designs (Figure 1-4a). Some of the major advantages include high sensitivity and selectivity, fast and accurate detection, requirement of only simple instrumentation, and possible miniaturization for portability [51]. Signals generated by aptamer-based electrochemical sensors involve the transfer of electrons between redox-active moieties in an electrically conductive medium (electrolyte) and a conductive support (electrode) to which the aptamer is typically immobilized. The electrical changes produced by target binding to the aptamer can be measured based on changes in voltage (potentiometric), current (amperometric) or the ability to transport charge (conductometric) [52].

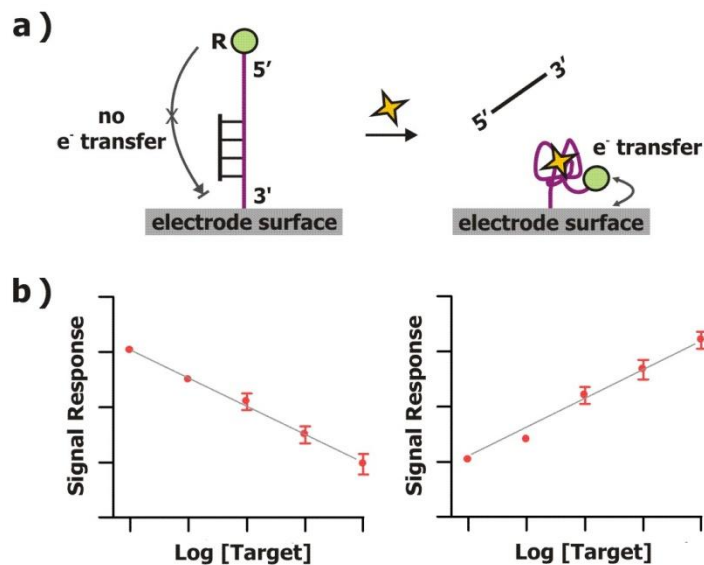


**Figure 1-4.** a) Structure-switching design for electrochemical detection. b) Sensor “off” switch involves a decrease in signal upon target detection (left). Sensor “on” switch involves signal increase upon target addition (right).

Electrochemical sensors can be classified as “signal-off” or “signal-on” sensor types depending on whether target binding decreases or increases the measured electrochemical signal (Figure 1-4b). One of the earlier signal-off sensor designs involved hybridization of an immobilized anti-ATP aptamer with a complementary DNA sequence labeled with a redox-tag [53]. In this state, the close proximity of the redox-tag to the electrode surface facilitated electron transfer and an intense electrochemical signal. However, in the presence of ATP, the aptamer sequence binds to its target, and displaces the redox-tag-labeled DNA strand. The separation of the redox-tag from the electrode resulted in substantial signal reduction. Alternatively, in a reported signal-on design, the anti-ATP aptamer was labeled with the redox-tag [54]. When the aptamer sequence formed a duplex structure with the complementary DNA strand, a low electrochemical signal was produced due to the rather large distance of the redox-tag from the electrode surface. The presence of target however, resulted in target-aptamer complex formation, and displacement of the complementary DNA. In this state, the redox tag was brought in close proximity to the electrode surface for electron transfer to occur. The aforementioned designs are considered to be “labeled” methods as they involve direct labeling of the aptamer or aptamer-related sequence with a redox tag (Figure 1-5a). “Label-free” structure-switching designs on the other hand, have also been demonstrated and involve a free redox mediator in solution; the aptamer and aptamer-related sequences are free of any direct labeling (Figure 1-5b). One notable label-free example involved hybridization of an extended anti-ATP aptamer sequence to a complementary DNA segment that was immobilized to an electrode support [55]. Methylene blue was used as the free redox

indicator, as it has the ability to interact with guanine to form a complex. This way, methylene blue molecules effectively tag the aptamer sequence. As a signal-off design, the high electrochemical signal generated in this state was significantly reduced upon addition of ATP, as structure-switching resulted in displacement of the target-aptamer complex, as well as methylene blue molecules away from the electrode surface.

Whether classified as signal-off or signal-on, labeled or label-free, electrochemical structure-switching designs based on the anti-ATP aptamer produce detection limits in the  $\mu\text{M}$  to nM range [53-55], which is an improvement to fluorescence-based designs. Nevertheless, signal amplification methods have also been successfully applied to lower the limit of detection further. Dong and colleagues have designed an assay using AuNPs functionalized with multiple copies of a complementary DNA sequence in duplex with the anti-ATP aptamer [56]. Methylene blue molecules interca-

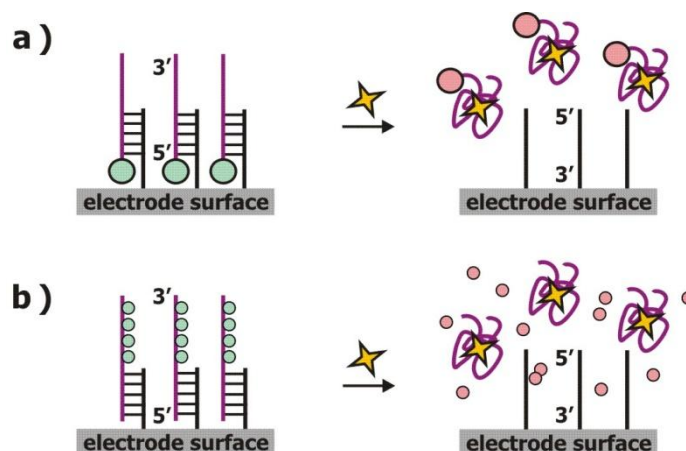


**Figure 1-5.** a) Electrochemical detection with “labeled” design involves direct coupling of the aptamer or aptamer-related sequence with a signaling molecule. b) A “label-free” design involves the use of a free signaling molecule in solution.

late along the DNA sequences immobilized to the electrode surface for redox tagging. The intense electrochemical signal produced in this state was significantly reduced when ATP was added to induce multiple structure-switching events, and subsequent displacement of multiple target-aptamer complexes, as well as methylene blue indicators. The detection limit was determined to be 100 pM, which is well below the reported  $K_d$  value of the original aptamer. Another notable signal amplification method involved a three-step procedure and made use of silver microspheres (SMSs) as a separation element, and graphene-mesoporous silica AuNP hybrids (GSGHs) to enhance the performance of the electrode surface [57]. In a first step, SMSs were functionalized with the anti-ATP aptamer, which formed a duplex with a complementary DNA sequence (blocker strand). In the presence of ATP, the blocker strand was displaced through structure-switching. SMSs linked with the aptamer-target complexes were then removed, leaving only the blocker strands in solution. In step two, hairpin probes that were complementary in sequence to the blocker strand were incorporated. The blocker strands opened the hairpin probes by the well-established toehold-based strand displacement strategy to generate an accumulation of duplex donor probes. In the last step, the duplex donor probes were captured to form  $\text{Ag}^+$ -stabilized DNA triplex structures with ssDNA acceptor probes that were immobilized onto the GSGH-electrode platform. Given the numerous DNA triplex structures formed and the enhanced nature of the electrode surface implemented, this design provided substantial signal amplification and yielded an incredible detection limit of ~23 pM.

In addition to continual advancements in sensing capabilities for electrochemistry-based detection, many sensing designs have been applied in complex sample matrices including serum [58], urine [59], and cell extracts [60]. Furthermore, the structure-switching design has also been used towards multiplex detection. Through implementation of a bifunctional aptamer, whereby the anti-ATP aptamer was linked to the anti-thrombin aptamer, parallel detection of both targets was effectively demonstrated [61]. Arguably, the most successful commercially available electrochemical sensor to date is the glucose sensor, which is widely used by diabetic patients around the world [62, 63]. Taking advantage of the convenience, portability, and low cost of personal glucose meters (PGMs), Lu's group strategically adapted commercially available PGMs and the structure-switching design to quantify adenosine among other non-glucose related targets [64]. In this approach, magnetic beads were functionalized with the designated aptamer in duplex with a complementary DNA sequence labeled with invertase enzyme. The addition of target resulted in structure-switching: the aptamer-target-bead complexes were separated magnetically, while the invertase-labeled DNA strands were left in solution. Invertase was then able to catalyze the conversion of sucrose into glucose for detection by the PGM. Because the concentration of released invertase-labeled DNA is directly proportional to the concentration of target, the readings produced by the PGM can be used for target quantification. Although this integrated method of detection is not as simple as current usage of PGMs, further progress towards automation can perhaps take this prototype system into mainstream usage for convenient medical and environmental monitoring in the near future.

### 1.3.3 Structure-Switching DNA Aptamers in Colorimetric Sensors

Colorimetric detection is an attractive option for biosensor development as a simple color change in the presence of the target is readily observable by the naked eye without the use of complex instruments (Figure 1-6). This advantage is particularly useful for on-site qualitative analysis in resource-limited regions. As nucleic acids do not absorb light in the visible spectrum, colorimetry-based detection requires coupling aptamers to a color-producing molecule to generate a color change upon target binding. For structure-switching designs, AuNPs (10-50 nm in diameter) have been a popular choice. Due to the optical phenomenon of surface plasmon resonance, the color of AuNPs in aqueous solution can be reversibly changed from a red (dispersed state) to a blue color (aggregated state). The surface of AuNPs can be easily functionalized to immobilize desired DNA sequences, which allows the tunability of color changes by target-aptamer interactions.

A “cross-linking” design was created by Lu’s group, whereby AuNPs were functionalized with one of two DNA sequences that were complementary to different sites of an extended anti-ATP aptamer [65]. Once all components were hybridized to each other, the extended aptamer cross-linked both types of functionalized AuNPs to form an aggregate and produce a blue color. Upon the addition of adenosine, target-aptamer binding occurred to induce structure-switching and subsequent displacement of functionalized AuNPs. Dispersal of AuNPs produced a red color. Although this method is a clear demonstration of technology transfer of the original structure-switching design into a novel signal transduction platform, the obtained sensitivity was not as high as for typical fluorescent-based designs, and generated a detection limit of 300  $\mu$ M.

Our group has improved the sensitivity of the ATP structure-switching reporter by applying a “non-cross-linking” strategy [66]. This design makes use of AuNPs functionalized with a segment of DNA to hybridize to the ATP aptamer. Under specific salt conditions, the aptamer-AuNPs remained well dispersed and produced a red color. The addition of target however, resulted in a structure-switching event, which led to aggregation of the AuNPs and a color change to blue. The detection limit was determined to be  $\sim 10 \mu\text{M}$ , which is identical to the reported  $K_d$  of the original aptamer [23]. Alternatively, a “label-free” method of structure-switching was also demonstrated to provide improved detection sensitivity. Developed by Fan and colleagues, this design makes use of the anti-ATP aptamer in duplex with its complementary sequence [67]. In a mixture of DNA duplex and AuNPs, the addition of salt resulted in aggregation of the AuNPs (blue color). However, when ATP was initially added to the duplex DNA and AuNP mixture, the target-aptamer complex formation resulted in structure-switching and displacement of the complementary DNA strand. The free DNA strand was then able to adsorb onto the surface of AuNPs, which provided protection and stability against the effect of salt. As a result, the AuNPs remained dispersed and appeared red in color. The reported detection limit was  $\sim 0.6 \mu\text{M}$ .

Although less extensively studied than fluorescence- and electrochemistry-based structure-switching aptamer reporters, AuNPs have also started to move into the realm of real-world applications. AuNPs using the cross-linking strategy have been successfully applied for multiplex detection, which enables the detection of multiple targets within the same environmental conditions and the investigation of co-operative binding. Based on

the original cross-linking system, Lu's group created design variations whereby AuNPs were functionalized with multiple complementary DNA sequences to hybridize to designated sites on the anti-ATP and anti-cocaine aptamers [68]. The aggregated state of the AuNPs resulted in a blue color. Depending on the system, the AuNP aggregates were dispersed to produce a red colour change, by the addition of both ATP and cocaine targets (high co-operativity), or simply by either one of the targets alone (no co-operativity).

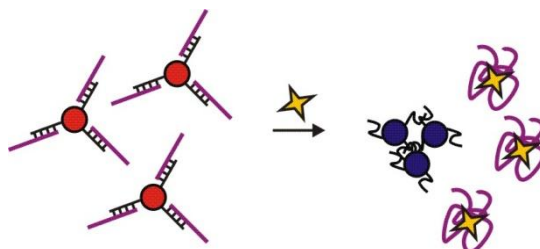


**Figure 1-6.** Structure-switching reporter for colorimetric detection. A gold nanoparticle (AuNP)-based system is illustrated. See main text for details.

To take one step further towards practical application, the cross-linking design has also been applied to a “dip-stick” assay format using lateral flow to separate dispersed aptamer-linked AuNPs from those aggregated [69]. This adaptation enhances the user-friendliness of detection, and the use of effective separation was also shown to provide better sensitivity than solution-based tests due to lower background interference. Furthermore, the assay retained function even in complex sample matrices, such as blood serum.

## **1.4 Structure-Switching RNA Aptamers**

### **1.4.1 Natural Aptamers for Small Molecules: Metabolite-Sensing Riboswitches**

Riboswitches are regulatory elements in mRNA that control gene expression by responding to a specific small molecule in cells. These RNA elements are typically composed of a well conserved aptamer domain that recognizes a specific metabolite and an expression domain that converts the aptamer-ligand interaction into a change in the level of gene expression [70, 71]. The small-molecule metabolites for which a riboswitch has been discovered include nucleobases [72-74] and their derivatives [75-84], amino acids [85-88] and their derivatives [89-95], vitamins [2, 96, 97], sugar derivatives [98], and even metal ions [99, 100] (see Figure 1-7). The binding of small molecule to these regulatory RNA elements typically alters the expression of genes associated with the biosynthesis, transport or utilization of the ligand that is directly involved. Remarkably, riboswitches can recognize its cognate target with superior specificity in a complex cellular environment and with an affinity typically in the picomolar to micromolar range. Moreover, riboswitches can effectively modulate gene expression without the need of any protein effector. Riboswitches that have been found in prokaryotes have been shown to regulate gene expression primarily at the transcriptional or translational levels. Commonly, these RNA systems function as genetic “off” switches as the binding of the designated small molecule often results in the repression of gene expression. For transcriptional control, small molecule interaction with the aptamer domain characteristically results in the formation of a terminative hairpin in the expression domain, which prematurely terminates transcription [71, 74, 77, 78, 90, 91, 93, 96, 97,

101]. In the absence of ligand, the segments that make up the hairpin are separated and instead, the anti-terminator structure forms to permit the continuation of transcription (Figure 1-8a).

Metabolites that have riboswitches	<b>AMINO ACIDS</b>
	L-glycine
	L-lysine
	<b>NUCLEOTIDES</b>
	adenine
	cyclic di-guanosine monophosphate (di-GMP)
	guanine
	pre-queuosine1 (preQ1)
	<b>CARBOHYDRATES</b>
	glucosamine-6-phosphate (GlcN6P)
	<b>COFACTORS</b>
	cyanocobalamin (VB12)
	nicotinamide mononucleotide (FMN)
	S-adenosylhomocysteine (SAH)
	S-adenosylmethionine (SAM)
thiamine pyrophosphate (TPP)	
<b>IONS</b>	
magnesium	
fluoride	

**Figure 1-7.** A list of targets for which riboswitches have been discovered.

Alternatively, small molecule interaction with riboswitches that utilize translational control often involves the formation of a sequestering structure that blocks the ribosomal binding site (RBS) and consequently, impedes translation. In the absence of ligand, the elements that form the sequestering structure are disassembled and the RBS becomes available for ribosomal binding and for translation to proceed (Figure 1-8b) [2, 78, 83, 87, 92, 96]. As regulation at the transcriptional level can effectively suppress gene expression at an early stage, regulation at the translational level may appear to be a slow and wasteful mechanism of control [102]. In spite of this observation, many riboswitches have been found to regulate translationally [2, 76, 78, 83, 87, 89, 92, 96, 102]. It may be the

case that regulation at the translational level is the first step of a more complicated process to regulate gene expression. In one hypothesis, the binding of ligand to terminate translation may allow the free 5' end of the newly produced transcript to be recognized by Rho, a protein that causes ATP dependent termination of transcription [103]. The orchestration of a number of regulatory steps that may not appear interconnected at first glance could potentially be in place to produce an overall, highly efficient control mechanism. Another apparent peculiarity in prokaryotic riboswitches is the existence of genetic “on” switches whereby, the binding of metabolite leads to the formation of an anti-terminator structure to activate transcription [73, 85, 102] or an anti-sequestering structure to activate translation [102]. The rarity of on-switches may be accounted for by the observation that most known riboswitches regulate genes that synthesize or transport more of the designated small molecule and hence high levels of that ligand logically signal repression of expression. However, in the case of the glycine riboswitch in *Bacillus subtilis*, operation by an on-switch mechanism may be preferable since it regulates genes involved in glycine degradation. High level of the glycine may make the organism aware that ligand is available for usage [85]. Alternatively, riboswitches have also been discovered to regulate gene expression through catalytic activity. In prokaryotes, a riboswitch that responds to glucosamine-6-phosphate (GlcN6P) exists to repress the biosynthesis of the monosaccharide ligand when cell wall production is not needed. Binding of GlcN6P activates self-cleavage of the ribozyme (the *glmS* ribozyme) and terminates further gene expression (Figure 1-8c) [98].

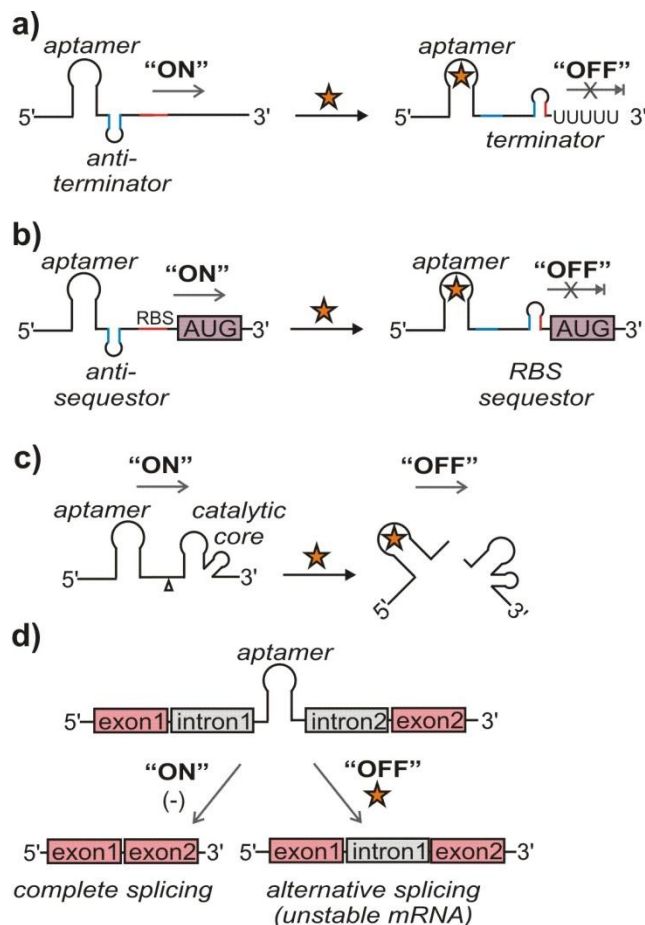


**Figure 1-8.** Riboswitches can regulate gene expression through **a)** transcription, **b)** translation (RBS = ribosomal binding site), **c)** catalytic cleavage, or **d)** alternative splicing. For simplicity, only genetic “off” switches are presented, whereby metabolite binding represses gene expression. Though not illustrated, systems whereby metabolite binding activates expression (“on” switches) also exist.

Eukaryotic organisms have also been discovered to implement similar RNA systems for regulatory control. Notably, thiamine pyrophosphate (TPP) riboswitches in many species of fungi and plants, have been found to use alternative RNA splicing to control gene expression (Figure 1-8d). Depending on the specific organism and the particular gene involved in regulation, TPP interaction has been shown to be able to activate or repress gene expression [79]. A common theme appears to entail off-switch regulation whereby

TPP binding leads to the production of a truncated or unstable transcript through alternative splicing, which consequently, causes down-regulation in expression of the gene of interest. Conversely, at low levels of TPP, a different splicing pattern or no splicing event occurs in the mRNA, which leads to the production of a functional protein [79-82].

### **1.4.2 Synthetic Riboswitches for Small Molecules**

Similar to natural riboswitches, synthetic counterparts have been engineered to regulate gene expression through small molecule binding. However, although natural riboswitches typically regulate the expression of metabolic genes, synthetic riboswitches can be designed to regulate virtually any gene in response to any small molecule that can bind to RNA [6]. Since the discovery that synthetic aptamers can be inserted into mRNA to regulate gene expression in a variety of organisms [7-11, 104, 105], substantial developments have been made to isolate effective synthetic riboswitches through high-throughput screens and selections [12, 106, 107]. Gallivan and his colleagues provided the first example of a synthetic riboswitch to function in *E. coli*, whereby the activity of the theophylline-sensing riboswitch was coupled with the chromogenic state of the bacterial cells. When theophylline bound to the aptamer domain, expression of the downstream  $\beta$ -galactosidase reporter gene was activated and the cells produced a blue color. However, in the absence of theophylline, translation of the reporter gene was repressed and the cells appeared white. This study also provided a proof of principle that unique synthetic riboswitches can be isolated from a library of non-functional sequences [11]. In a later study, partially randomized pools of the theophylline-sensing synthetic

riboswitch were applied in an automated high-throughput screen to select for sequences with enhanced function [108]. The screen led to the isolation of improved theophylline-sensing riboswitches that produced lower background levels of  $\beta$ -galactosidase expression when theophylline was absent and increases in reporter gene expression in the presence of theophylline. Moreover, the sequence information from this screen helped provide deeper insight into the possible mechanism of the isolated riboswitches [108]. Additionally, synthetic riboswitches have also been successfully implemented to “reprogram” bacteria to follow new chemical signals. In another study by the same group, the theophylline-sensing synthetic riboswitch was used to control the motility of *E. coli* cells when the aptamer domain was strategically placed upstream of *cheZ*, a gene which encodes for a protein factor that plays a critical role in bacterial chemotaxis. The presence of theophylline activated expression of the reporter gene, which consequentially enabled controlled movement of the cells toward the chemical stimulus [13]. As an extension of this work, cell motility was shown to be a readout response to monitor the progress of high-throughput screens. In contrast to the commonly used  $\beta$ -galactosidase reporter assay, a cell motility-based assay that simply measures the distance of cell migration on semisolid media, is relatively inexpensive, and can also provide rapid results [14]. Further progression in the development of synthetic riboswitches may pave the way for possible applications in bioremediation, bionanotechnology and synthetic biology [14].

### **1.5 RNA Aptamers Created Through SELEX**

The power of SELEX continues to generate novel aptamers that showcase the ability of nucleic acid probes to recognize a diverse range of targets. To date, there are at

least 130 RNA aptamers (Figure 1-9), which provides many opportunities for sensor development. These RNA aptamers can recognize a variety of targets including cofactors [109-114], small molecule drugs [115-118] and antibiotics [119-126], amino acids [127-134] and their derivatives [135, 136], nucleotides [137-139] and their derivatives [140-142], organic dyes [15, 143, 144], toxins [145], metal ions [146, 147], biomarkers of cancer [148-151] and neurological disease [152-158], as well as protein and non-protein factors related to microorganisms [159-165], viruses [16, 166-183], blood regulation [184-189], cell adhesion [187, 190-194], translation regulation [195-198], cell regulation [187, 199-216], and immunology [217-230].

Similar to naturally occurring RNA aptamers, many artificially developed RNA aptamers also possess superior target-binding characteristics. The RNA aptamer for keratinocyte growth factor for example, possess a  $K_d$  of 0.3 pM [199], which is the highest affinity of an artificially created aptamer known to date. Furthermore, several RNA aptamers possess remarkable binding specificity. For instance, the theophylline aptamer can bind theophylline ~10 000 times better than caffeine, a structural analog that only contains an additional methyl group [115]. Similarly, the arginine-binding RNA aptamer is highly enantioselective, and can recognize the L-form of arginine ~12 000 times better than the D-form [128]. Additionally, RNA aptamers have also demonstrated to discriminate against different redox states of the same target, as exemplified by the nicotinamide mononucleotide (NMN)-binding aptamer, which preferentially binds the oxidized state (NAD<sup>+</sup>) over the reduced state (NADH) of its target [109].



**Figure 1-9.** A list of targets for which RNA aptamers have been discovered through SELEX.

## 1.6 The Limitations of RNA for Detection

Despite the abundance of RNA aptamers, and the superior binding characteristics that many exhibit, RNA aptamers are relatively underexplored for sensor development.

The main reason for this is due to RNA's inherent chemical instability and susceptibility to degradation. Spontaneous cleavage of the phosphodiester bonds that connect the sugar-phosphate backbone of RNA commonly occurs through intramolecular transesterification reactions [231]. The source of instability stems from the characteristic 2'-hydroxyl group found on the ribose sugar of RNA. Absent in DNA, the 2'-hydroxyl group can readily act as a nucleophile to attack the adjacent phosphodiester linkage in the backbone of RNA, resulting in cleavage (Figure 1-10) [231]. This key chemical difference makes RNA ~100 000 times less stable than DNA under physiological conditions [232].

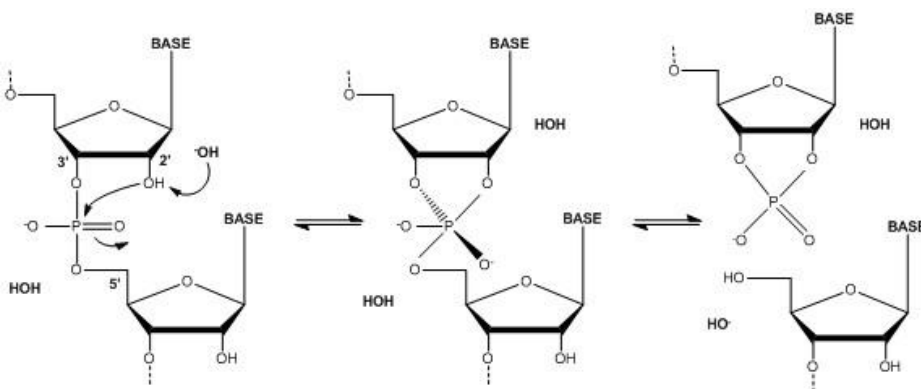


**Figure 1-10.** General mechanism of RNA cleavage by intramolecular transesterification. Ribose sugar possesses a 2'-hydroxyl group that can readily act as a nucleophile to attack the adjacent phosphodiester linkage, resulting in cleavage of the RNA.

A number of factors can also accelerate the rate of RNA transesterification. These factors are discussed below:

**pH.** Under basic conditions, specific base catalysis plays a predominant role to accelerate RNA cleavage as deprotonation of the 2'-hydroxyl group results in an increase in the

formation of the more nucleophilic 2'-oxyanion group [232]. In contrast, under acidic conditions, specific acid catalysis occurs, whereby both a non-bridging phosphate oxygen, as well as the 5'-oxyanion leaving group become protonated to accelerate cleavage reaction [233].

***Position of chemical groups involved in cleavage.*** To enable RNA cleavage, the 2'-oxygen nucleophile must be precisely positioned in-line with the 5'-oxyanion leaving group, in such a way that the leaving group is on the opposite side of the central phosphate relative to the nucleophile [234-236].

***Metal ions.*** The presence of metal ions can enhance transesterification by stabilizing specific RNA conformations that favor in-line positioning of the chemical groups conducive for cleavage [236]. Additionally, metal ions can also speed up transesterification by acting as a specific base catalyst to form metal-hydrates, or a specific acid catalyst to form complexes with oxygen atom(s) [237].

***RNA structure.*** Single-stranded RNA (ss RNA) is more prone to degradation than RNA in duplex form. While some ss RNA can fold up upon itself to form intramolecular duplex-like structures, these structures tend to be relatively weak; the greater conformational flexibility of ss RNA means greater sampling of different conformations including the position for in-line attack [238-240]. Phosphodiester linkages located at the termini of RNA helices are also more prone to cleavage relative to internally situated linkages, due to easier accessibility of degrading agents [241-243]. However, RNAs that

fold into highly complex structures are not necessarily protected against the effects of transesterification if the adopted conformations are favorable for in-line attack [236, 241].

**Temperature.** High temperature can also substantially speed up RNA cleavage by breaking up chemical bonds. In a reported study testing RNA degradation in conditions ranging from 4 to 50°C, the rate of RNA degradation increased by 3-fold at higher temperature [232].

**Nucleases.** Nucleases are another source of RNA degradation, and the majority of these protein enzymes target RNA rather than DNA [231]. Many nucleases catalyze transesterification using a combination of mechanisms described above. For example, bovine pancreatic ribonuclease A (RNase A) implements a combination of general acid and base catalysis [244], along with precise in-line positioning of the RNA phosphodiester linkage to the nuclease active site for cleavage [245]. As a result of effectively implementing all three methods, RNase A can catalyze RNA transesterification with a rate enhancement  $10^{12}$ -fold higher than the uncatalyzed RNA cleavage rate [246].

## **1.7 Research Objectives and Thesis Organization**

As discussed in the preceding sections, RNA aptamers inherently possess many useful properties for sensor development including immense functional capacity, conformational flexibility, as well as superior binding affinity and specificity in many examples. Furthermore, the abundance of naturally occurring and artificially developed RNA aptamers provides relatively untapped sources of molecular recognition elements

for sensor development and new opportunities to further advance the field. In effect, the overall objective of this thesis is to harness the power of RNA aptamers for fluorescence-based sensor development using a structure-switching design. While the concept of structure-switching has demonstrated to be highly versatile and effective in sensor development using DNA aptamers and riboswitches, it has not been applied towards RNA aptamers. The work presented in this thesis is the first to demonstrate this novel discovery.

The first research project establishes a general strategy to create structure-switching sensors based on RNA aptamers, and sets the foundation for all subsequent work in this thesis. Regardless of the origin, size or affinity of the aptamers tested, the presented sensing strategy demonstrates to be effective, and widely applicable (Chapter 2). To enhance user confidence against concerns of RNA aptamer instability and degradation, the second research project describes a novel structure-switching sensing strategy that can monitor the quality control of detection and distinguish between true-positive and false-positive signals (Chapter 3). By using this strategy to pin-point defective samples, remedy methods to correct a false-positive signal are also demonstrated in this section (Chapter 3). In the third research project, the versatility of the structure-switching approach using RNA aptamers is demonstrated by adapting the design for sensor development on graphene material (Chapter 4). For the fourth and fifth research projects, structure-switching RNA aptamers are further explored in secondary applications. In collaboration with the Brennan group, the established RNA aptamer-based sensors are successfully entrapped in sol-gel materials for solid-assay development.

Furthermore, this work also demonstrates that sol-gel entrapment provides a general method to protect RNA aptamers against nucleases, and chemical instability (Chapter 5). Additionally, in collaboration with the Ye group, the glmS ribozyme, a natural structure-switching RNA aptamer found in numerous Gram-positive bacteria has been further explored as a potential drug target for antibiotic development. Chemical synthesis of different metabolite analogues has resulted in one particular analogue that may be a potential lead for drug design (Chapter 6).

References for this Introductory Chapter, as well as for the final thesis chapter on Discussion and Future Directions (Chapter 7) are found at the end of this thesis. References pertaining to specific research projects (Chapters 2-6) are found at the end of each of these sections, respectively.

## CHAPTER 2

### A GENERAL APPROACH TO THE CONSTRUCTION OF STRUCTURE- SWITCHING REPORTERS FROM RNA APTAMERS

#### 2.1 Author's Preface

The first research project establishes a general strategy to create structure-switching sensors based on RNA aptamers. At the beginning of this project, RNA aptamers were highly underexplored for sensor development. This study provides the first sensing strategy that is widely applicable towards various RNA aptamers, and sets the foundation for all subsequent work in this thesis.

This chapter has been published, and a modified version is presented for this thesis (see full citation below). I am the first author of this publication. I was mainly responsible for project design, and performed all experiments, and analyses. I wrote the manuscript with significant assistance from Dr. Yingfu Li and Dr. Brian Coombes. Supplementary information is found in Appendix 1.

Lau PS, Coombes BK, Li Y (2010) A general approach to the construction of structure-switching reporters from RNA aptamers. *Angew Chem Int Ed Engl* 49: 7938-7942.

## 2.2 Abstract

Aptamers are unique molecular probes made up of single-stranded DNA or RNA that can fold into a defined tertiary structure to bind a designated target. Despite the wide availability, RNA aptamers remain underexplored for biosensor development. Herein, we present a general strategy to create fluorescent reporters from existing RNA aptamers. Based on a structure-switching design, this strategy exploits the dual ability of RNA aptamers: i) to form an RNA-DNA duplex by binding to its complementary sequence and ii) to form an RNA-target complex by binding to its designated target. In the reporter off mode, the fluorophore labeled RNA aptamer forms a duplex with quencher labeled DNA (denoted as QDNA). The close proximity of the fluorophore and quencher results in maximal fluorescence quenching. The addition of target displaces the QDNA to facilitate complex formation with the aptamer. As a result, the separation of fluorophore and quencher allows high fluorescence generation as the reporter is turned on. This fluorescent tagging strategy is attractive as it circumvents the need for the chemical synthesis of modified RNA, and the structure-switching reporters can be used to distinguish targets that have very similar chemical structures. We demonstrate the generality and simplicity of our approach with the creation of two novel reporters based on RNA aptamers that recognize theophylline drug, and thiamine pyrophosphate (TPP), respectively.

## 2.3 Introduction

Aptamers are single-stranded DNA or RNA molecules that are capable of ligand binding and have been widely investigated as molecular tools for a variety of applications.<sup>[1]</sup> For example, aptamers have become popular recognition elements in various biosensor platforms in which the aptamer–target binding event is reported by an optical, acoustic, mechanical, or electric signal.<sup>[2]</sup>

Biosensing by fluorescence is one of the most popular methods for the design of aptamer-based assays, largely because of ease of detection.<sup>[3]</sup> Our research group has previously reported a “structure-switching” approach to engineering fluorescent reporters from DNA aptamers.<sup>[4]</sup> This approach takes advantage of the ability of aptamers to form both an aptamer–target complex and a DNA–DNA duplex with a complementary sequence. Thus, a DNA duplex with a fluorophore-labeled aptamer and a quencher-labeled complementary strand can function as a reporter: the addition of target would release the complementary sequence from the aptamer, accompanied by an increase of fluorescence intensity.

The structure-switching approach was initially demonstrated using an anti-ATP aptamer (ATP = adenosine triphosphate) and an anti-thrombin aptamer,<sup>[4]</sup> and was further used to design reporters for other targets including guanosine triphosphate (GTP), cocaine, arginine, and the platelet-derived growth factor (PDGF).<sup>[5]</sup> Subsequent work has also expanded the utility of structure-switching aptamers in secondary

applications to monitor enzymatic reactions, facilitate high-throughput screening, and develop nanodevices and solid-phase assays.<sup>[6]</sup> The structure-switching approach has also been exploited to design aptamer sensors that function by colorimetric, electrochemical, or other reporting mechanisms.<sup>[7]</sup>

A large number of RNA aptamers have been isolated for diverse targets<sup>[8]</sup> through systematic evolution of ligands by exponential enrichment (SELEX) experiments.<sup>[9]</sup> Moreover, many metabolite-binding RNA aptamers exist in cells as part of riboswitches to regulate gene expression.<sup>[10]</sup> The availability of versatile RNA aptamers represents a superior opportunity to develop RNA-aptamer-based biosensors. However, the potential of RNA aptamers for bioanalytical applications is still underexplored. For example, only a few studies have investigated the use of RNA aptamers in the development of fluorescence assays.<sup>[11]</sup> To expand the exploration of RNA aptamers in bioanalysis, in this study we sought to devise a generalizable, structure-switching-based approach for the rational design of fluorescent reporters from known RNA aptamers.

Since DNA oligonucleotides are more readily available and more stable than synthetic RNA oligonucleotides, our proposed strategy began with the polymerase chain reaction (PCR) to produce double-stranded (ds) DNA from a synthetic, aptamer-encoding DNA template (purple line, Figure 2-1) using two primers. Primer 1 contains a T7 promoter at the 5'- end so that the resultant dsDNA can be used to synthesize an RNA molecule using T7 RNA polymerase by in vitro transcription. The RNA was

designed to have a sequence extension (red line) at the 5'-end so that this RNA can be used to assemble a three-component duplex structure with a fluorophore (F)-labeled DNA strand (denoted FDNA) and a quencher (Q)-labeled DNA oligonucleotide (QDNA) that has a complementary sequence to part of the RNA aptamer. This signaling duplex was expected to exhibit low fluorescence because of the proximity of the fluorophore and quencher. However, addition of the target should promote dissociation of QDNA from the duplex in favor of the target-aptamer complex formation, thus leading to the generation of a fluorescent signal. Two RNA aptamers were examined in this study: a synthetic aptamer that recognizes theophylline,<sup>[9a]</sup> and a naturally occurring aptamer that binds thiamine pyrophosphate (TPP).<sup>[12]</sup>

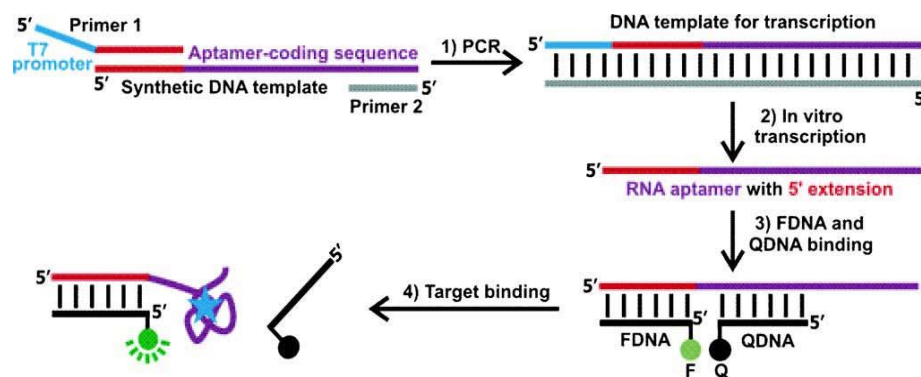


**Figure 2-1.** The proposed strategy for designing fluorescent RNA aptamer reporters that switch structures from a weakly fluorescent duplex to strongly fluorescent complex upon target binding. The aptamer sequence, shown in purple and produced by PCR and in vitro transcription, is linked to a sequence element that binds FDNA. The blue star represents the target for the aptamer.

## 2.4 Materials and Methods

**2.4.1 Materials.** All DNA oligonucleotides were synthesized using automated DNA synthesis (Integrated DNA Technologies, Coralville, IA) following the standard

phosphoramidite chemistry. FDNAs contain a 5'-fluorescein introduced using 5'-fluorescein phosphoramidite; QDNAs contain 3'-DABCYL introduced using 3'-DABCYL derivatized controlled pore glass (CPG). DNA oligonucleotides and purified by 10% denaturing PAGE before use. The fluorescently labeled DNA oligonucleotides were purified by HPLC. Unless otherwise noted, all other materials were purchased from Sigma (Oakville, Canada) and used without further purification.

**2.4.2 Polymerase Chain Reaction.** The synthetic DNA template for the theophylline reporter has the sequence of 5'-GAATT CTAAT ACGAC TCACT ATAGG CCTGC CACGC TCCGC TCACT GGGCG ATACC AGCCG AAAGG CCCTT GGCAG CGTCC AACAC ATCG-3'. It was amplified by PCR with 5'-GAATT CTAAT ACGAC TCACT ATA-3' and 5'-CGATG TGTTG GACGC-3' as forward and reverse primers. The sequence of the TPP aptamer template is 5'-GAATT CTAAT ACGAC TCACT ATAGG GCTGC CACGC TCCGA CGCTA TCACT CTATG CCACT AGGGG TGCTT GTTGT GCTGA GAGAG GAATA ATCCT TAACC CTTAT AACAC CTGAT CTAGG TAATA CTAGC GAAGG GAAGT GGCAA CAGAA GC-3', which was amplified with 5'-GAATT CTAAT ACGAC TCACT ATA-3' (forward primer) and 5'-GCTTC TGTTG CCACT-3' (reverse primer). PCR was conducted in 75 mM Tris-HCl (pH 9.0), 2 mM MgCl<sub>2</sub>, 50 mM KCl, 20 mM (NH<sub>4</sub>)<sub>2</sub>SO<sub>4</sub>, each primer at 0.5 μM, the template at 3 nM, each dNTP at 0.5 mM, and 5 units of Taq DNA polymerase (Biotools, Madrid, Spain). Thermal cycling steps were: 94°C for 1 min, 20 cycles of 94°C-45°C-72°C (30 s for each temperature), and finally 72°C for 8 min.

**2.4.3 RNA transcription.** The transcription reaction was conducted at 37°C for 2 h in 150  $\mu$ L of 40 mM Tris-HCl, pH7.9, 6 mM MgCl<sub>2</sub>, 10 mM DTT, 10 mM NaCl, 2 mM spermidine, 25 pmol PCR amplified DNA, 2.5 mM each of GTP, CTP, UTP, ATP, 1.07 units/ $\mu$ L RiboLock Ribonuclease Inhibitor and 1.33 units/ $\mu$ L T7 RNA polymerase (MBI Fermentas). The transcription mixture was then treated with DNase I (3 units) in the presence of 0.2 mM CaCl<sub>2</sub> at 37°C. The transcribed RNA was subsequently purified by 10% denaturing PAGE and quantified by absorbance at 260 nm.

**2.4.4 Fluorescence measurements.** The signaling mixture contained 50 mM Tris-HCl (pH 7.5), 20 mM MgCl<sub>2</sub>, 40 nM of FDNA, 80 nM extended RNA aptamer and 120 nM QDNA. The mixture was first heated at 65°C for 2 min, cooled at room temperature for 10 min, and stored at 4°C until analysis. Fluorescence measurements were performed at 37°C (unless stated otherwise) on Cary Eclipse (Varian) with an excitation/emission at 490/520 nm. To obtain the thermal denaturation profiles, each signaling mixture was incubated at 65°C for 5 min in the fluorimeter before temperature was decreased to 20°C at a rate of 1°C/min.

**2.4.5 Signaling rate calculation.** We estimated the signaling rate for each solution referred to in Figure 2-4c by using data taken from within the linear signaling phase of the experiment. Each data series was normalized by using the equation  $x = (F - F_0)/(F_{\max} - F_0)$ , where  $F_{\max}$  is the maximal fluorescence intensity observed with 100  $\mu$ M TPP (which gave highest level of fluorescence),  $F_0$  is the fluorescence reading taken for a TPP-containing solution immediately before TPP was added, and  $F$  is the fluorescence reading of the same solution at a given time after the TPP addition. On the assumption that the structure

switching reaction is a first-order reaction,  $x$  is equivalent to the fraction of the FDNA-aptamer-TPP complex at a defined TPP concentration at a given time point, and  $(1-x)$  is the fraction of the unswitched FDNA-QDNA-aptamer at the point. A plot of  $\ln(1-x)$  versus the reaction time should be linear and the negative slope of the line represents the reaction rate ( $k_r$ ). The signaling rate ( $k_s$ ), defined as fraction increase/min, for each TPP concentration is calculated as  $(k_r - k_0)/(k_F - k_0)$  where  $k_F$  is the reaction rate at the highest TPP concentration tested (i.e. 1000  $\mu\text{M}$ ) and  $k_0$  is the reaction rate without TPP.

## 2.5 Results and Discussion

### 2.5.1 Creation of an aptamer reporter for theophylline

The theophylline aptamer (see Figure S2-1 in Appendix 1, Supporting Information for the secondary structure) was chosen as the first model aptamer. This aptamer is well-characterized, exhibits remarkable specificity, and has been used in several biosensor engineering studies.<sup>[9a,13]</sup> We assessed different combinations of FDNA, the extended theophylline RNA aptamer (TRA) and QDNA in preliminary experiments (one example is provided in Figure S2-2 in Appendix 1, Supporting Information). Based on these investigations, we decided to investigate a system consisting of FDNA1, TRA1, and QDNA2 (Figure 2-2). TRA1 was designed to have several sequence elements, each of which served a defined purpose (see also Figure S2-1 in Appendix 1, Supporting Information):  $G_1G_2$  to facilitate RNA transcription,  $C_3-A_{22}$  for FDNA1 binding,  $U_{23}$  to create a suitable distance between F and Q for optimal quenching,<sup>[4]</sup>  $C_{24}-A_{39}$  for QDNA2

binding, G<sub>33</sub>–C<sub>65</sub> (letters in blue) is the actual recognition element, and c<sub>66</sub>–g<sub>75</sub> (lowercase letters) as part of 3'-primer binding site in the DNA template for PCR. C<sub>24</sub>–G<sub>32</sub> were added as a “extension domain” to allow the formation of a stable QDNA–TRA duplex without sequestering many nucleotides in the actual aptamer sequence, a feature modeled after the design of structure-switching DNA aptamers.<sup>[4]</sup>

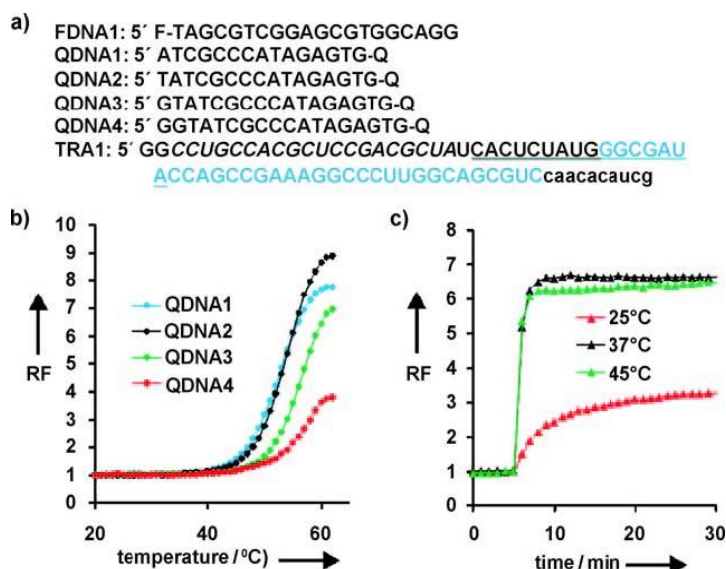


**Figure 2-2.** Structure-switching reporter for theophylline. a) Sequences of FDNA1, TRA1, and QDNA1–4. b) Thermal denaturation profiles of the duplexes made from QDNA1–4 with TRA1 and FDNA1. c) Target induced fluorescence response at 25°C, 37°C, and 45°C. RF=relative fluorescence. The duplex was incubated for 5 min followed by addition of 1 mM theophylline. The average values of two independent experiments (with less than 20% variations) are shown (the same applies to other figures below if not specified otherwise). Experimental details are provided in the Supporting Information.

To derive an optimal QDNA, four different QDNA sequences (Figure 2-2a) were examined for thermal denaturation profiles in the duplex with FDNA1 and TRA1 (Figure 2-2b). The FDNA1–TRA1–QDNA2 duplex produced the best fluorescence enhancement

and a relatively low melting point; thus, QDNA2 was selected for further experiments. We also found that for this signaling duplex, the theophylline-induced fluorescence increase progressed rapidly at both 37°C and 45°C, and reached the maximal enhancement after 3 minutes (Figure 2-2c). In contrast, at 25°C, both the rate of signal increase and the maximal signal were considerably poorer. Since the signaling performance was at its best at 37°C, this temperature was chosen for the remaining experiments.

### 2.5.2 Sensing capability of the theophylline reporter

The FDNA1–QDNA2–TRA1 reporter was found to be highly specific for theophylline; the addition of theobromine and caffeine (two structural derivatives of theophylline) did not generate significant signal output (Figure 2-3a). This observation is consistent with the previous report that the theophylline-binding aptamer exhibits much higher affinity for theophylline than for theobromine and caffeine.<sup>[9a]</sup>

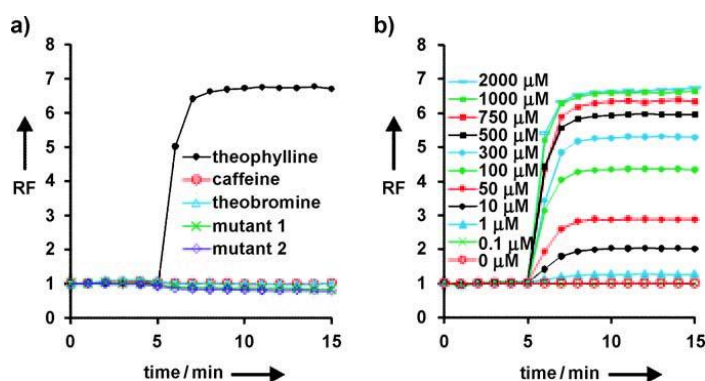


**Figure 2-3.** Specificity and sensitivity of the theophylline reporter. **a)** Specificity test. The signaling duplex was incubated at 37°C for 5 min before addition of 1 mM theophylline (black), caffeine (red), or theobromine (light blue). Two mutant aptamers

(green: mutant 1; purple: mutant 2) were also tested with addition of 1 mM theophylline. **b)** Signal response of the theophylline reporter to theophylline concentrations.

Two mutant aptamers with altered nucleotides critical to target recognition<sup>[9a]</sup> were also examined. In mutant 1, G<sub>41</sub> and A<sub>60</sub> were mutated to A<sub>41</sub> and U<sub>60</sub>; in mutant 2, A<sub>40</sub>G<sub>41</sub> were replaced with G<sub>40</sub>A<sub>41</sub>. The signaling duplexes from both mutants did not produce signal increase upon theophylline addition (Figure 2-3a). This observation verifies the importance of the specified nucleotides for theophylline binding and further validates the specificity data obtained for this reporter. To assess the sensitivity of the theophylline reporter, the relative fluorescence was determined at various concentrations of theophylline (Figure 2-3b). The detection limit was found to be 1  $\mu$ M and the dynamic detection window was between 1–1000  $\mu$ M (Figure 2-3b; the relative fluorescence observed at 20 min versus the theophylline concentrations can be found in Figure S2-3 in Appendix 1, Supporting Information).

### ***2.5.3 Creation of an aptamer reporter for TPP***

We then turned our attention to the TPP-binding RNA aptamer, which is part of natural riboswitches that regulate gene expression in response to intracellular TPP concentrations.<sup>[12]</sup> This aptamer has been the subject of extensive structural and functional analyses.<sup>[14]</sup> We chose to examine this aptamer for the structure-switching design mainly because it is much larger than the theophylline aptamer (87 vs. 33 nucleotides (nt)) and structurally more complex (Figure S2-1 in Appendix 1, Supporting Information).

The design of the TPP reporter was based on the information acquired with the theophylline reporter. Briefly, the 20-nt FDNA1 was retained as the FDNA and 16-nt

QDNA5 was used as the new QDNA (Figure 2-4a and Figure S2-1 in Appendix 1, Supporting Information). The following features were designed into the extended TPP RNA aptamer (TPPRA): G<sub>1</sub>G<sub>2</sub> for high transcription efficiency, C<sub>3</sub>–A<sub>22</sub> for FDNA1 binding, U<sub>23</sub> for optimal F–Q distance, C<sub>24</sub>–G<sub>39</sub> for QDNA binding, and C<sub>33</sub>–G<sub>119</sub> for TPP recognition. Similar to the theophylline reporter, it was determined that the optimal QDNA length was 16 nt and sensing was most optimal at 37°C.

#### ***2.5.4 Sensing capability of the TPP reporter***

The TPP reporter produced a signal enhancement of around fourfold upon addition of 1 mM TPP. At this concentration, the reporter reached maximal enhancement after approximately 5 min. At lower concentrations (10 nM– 100 µM), however, the rate of signal increase was reduced (Figure 2-4b). This reporter exhibited a linear dynamic range between 1–1000 µM when the signaling rate was plotted against TPP concentration, although the detection limit can reach 10 nM (Figure 2-4c). The slightly reduced maximal signal enhancement at 1000 µM in comparison to 100 µM may be caused by the fluorescence quenching of TPP at this concentration. The TPP reporter also showed high specificity for TPP: only a subtle signal was seen with thiamine monophosphate (TMP) and thiamine, and no signal increase was observed with oxythiamine (Figure 2-4d). These observations are consistent with previous results.<sup>[14b,e]</sup>

One mutant aptamer (sequence shown in Figure S2-4 in Appendix 1, Supporting Information) was also examined, and did not produce signal enhancement upon TPP addition (Figure 2-4d).

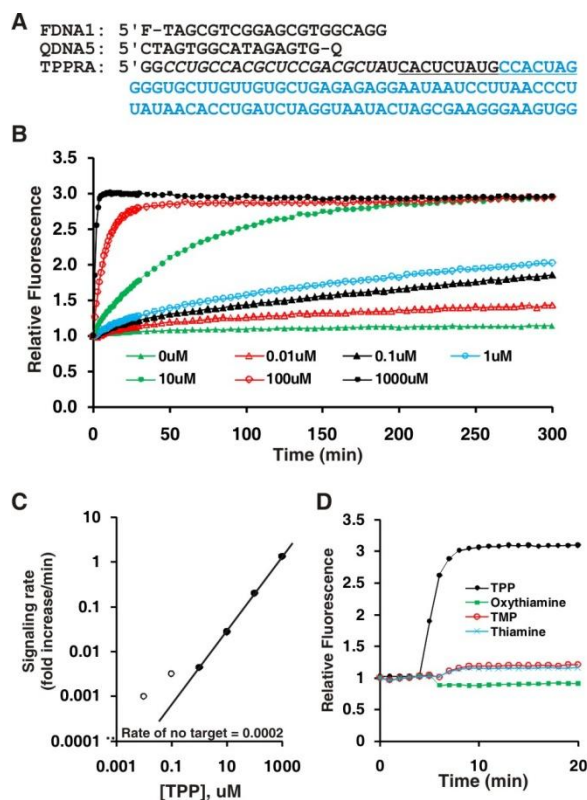


**Figure 2-4.** Structure-switching reporter for TPP. **a**) Sequences of FDNA and QDNA, and the extended RNA aptamer for TPP (TPPRA). **b**) Target-induced fluorescence increase of the reporter where the TPP concentration was varied between 0–1000  $\mu\text{M}$ . **c**) Signaling rate versus TPP concentration (the method for deriving signaling rate (fraction increase/min) is provided in the Supporting Information) Bk rate=background rate, produced by the signaling duplex in the absence of TPP. **d**) Specificity test. The TPP signaling duplex was incubated for 10 min before 100  $\mu\text{M}$  TPP (black), TMP (green), thiamine (red), or oxythiamine (light blue) was introduced (all 100  $\mu\text{M}$ ). One mutant aptamer (gray) was also tested with the addition of 100  $\mu\text{M}$  TPP.

A key difference between theophylline and TPP reporters is the signal increase speed in relation to the target concentration. For the theophylline reporter, the signal increase was rapid (reaching the maximal signal after approximately 5 min) at all responsive target concentrations (Figure 2-3b). In contrast, the signaling rate of the TPP reporter was significantly dependent on the target concentration (Figure 2-4b):

approximate times required to reach the maximal signal were 5 min for 1 mM TPP, 15 min for 0.1 mM TPP, 120 min for 10  $\mu$ M TPP, and much longer times for lower concentrations. We speculate that this natural aptamer may have been evolved to have the necessary ability to respond accurately to the level of TPP in cells. Since the TPP aptamer is proposed to function in cells as TPP-responsive genetic OFF switch (to terminate the transcription of downstream genes that code for proteins involved in TPP biosynthesis),<sup>[12c]</sup> it would be most desirable for cells to have an aptamer that shows exquisite response to the cellular TPP level: very quick response when the TPP concentration is very high (thus no need for more TPP biosynthetic proteins) and progressively reduced response at lower levels of TPP (to reach an optimal biosynthetic proteins/TPP ratio).

## 2.6 Conclusions

In summary, we have demonstrated an approach that can be generally applied for the design of fluorescent reporters from RNA aptamers. Our method is based on a three-component system made of two chromophore-labeled DNA oligonucleotides obtained from chemical synthesis and an aptamer-containing RNA strand produced by in vitro transcription. Since the chemical synthesis of RNA is less efficient than that of DNA, and RNA is more prone to degradation, the production of RNA aptamers by in vitro transcription is an attractive option. The strategy to tag the aptamer with a fluorophore-labeled DNA oligonucleotide by duplex formation also circumvents the need of chemical synthesis of modified RNA and alleviates the probe degradation during storage, which would produce higher background fluorescence.

Three adjustments were made in the design of structure-switching reporters for RNA aptamers when compared to the design for DNA aptamers. Firstly, the number of base pairs in the duplex between FDNA and the extended aptamer sequence was increased from 15 to 20, as we observed that 15 base pair DNA/RNA duplex had a higher background signal and smaller signal enhancement upon target addition (Figure S2-2 in Appendix 1, Supporting Information). Secondly, the optimal length of QDNA (which produce the most desirable balance of background signal, fluorescence enhancement, and signaling rate) was found to be 16 nt for the RNA reporters and 12 nt for the DNA reporters.<sup>[4]</sup> This modification was made based on the observation that the reporters constructed with QDNA of reduced length had higher background signal and reduced signal enhancement. Thirdly, with the increased size of QDNA, we increased the size of the extension domain from 5 nt in the DNA reporters to 9 nt in the RNA reporters (the extension domain consists of nucleotides that participate in the binding of QDNA but not in the binding of the target).

We examined two model aptamers with different origins, sizes, and affinities. The theophylline-binding RNA aptamer was obtained in a SELEX experiment, is 33 nt long and has a dissociation constant  $K_d$  of 0.1  $\mu\text{M}$ .<sup>[9a]</sup> The TPP aptamer is found in cells, is considerably larger (87 nt) and has a  $K_d$  value of 0.85 nM.<sup>[12c]</sup> The successful conversion of the two very different RNA aptamers into structure-switching reporters using the same design demonstrates the general utility of the method. Furthermore, to the best of our knowledge, our work is the first reported attempt of exploring a naturally occurring aptamer for the design of a fluorescent biosensor for bioanalytical applications.

The designed structure-switching reporters retained the binding specificity of the original aptamer. For example, the original theophylline aptamer can distinguish theophylline (cognate target) from caffeine and theobromine that have very similar chemical structures.<sup>[9a]</sup> As shown in Figure 2-3a, the structure-switching reporter displayed the same specificity. Similar observations were made with the TPP reporter (Figure 2-4d).

The detection limit of the theophylline reporter was found to be 1  $\mu\text{M}$ , which is 10 times higher than the  $K_d$  value of the original aptamer. Similarly, the detection limit of the TPP reporter was 10 nM, which is also 10 times higher than the  $K_d$  value of the original aptamer. The fact that structure-switching reporters did not produce better detection sensitivity may have two possible explanations. Firstly, the use of a complementary sequence (i.e., QDNA) to partially block the binding site of an aptamer has reduced its affinity for its target because in this modified system, the target needs to compete with QDNA for binding to the aptamer. Secondly, since the starting signaling duplex itself also exhibits some level of fluorescence, the small signal increase induced by the target at very low concentrations can easily be obscured within the background signal associated with large excess of unswitched duplex. These two inherent problems imply that it may be difficult to achieve extremely high sensitivity with structure-switching fluorescent aptamer reporters, particularly in the real-time sensing mode (i.e., detection without a separation step). Similar observations have also been reported for structure-switching fluorescent reporters based on DNA aptamers.<sup>[4]</sup> To achieve better sensitivity, alternative methods that can offer reduced background signal should be considered. One such

method is electrochemical sensing,<sup>[15]</sup> which has already been applied to achieve improved detection sensitivity with structure-switching DNA aptamers.<sup>[7d,e]</sup>

## 2.7 Acknowledgements

This work was supported by research grants from the Natural Sciences and Engineering Research Council of Canada (NSERC) and partially by MOST (grant 2008DFA30370).

## 2.8 References

- [1] a) S. Klussmann, *The Aptamer Handbook*, Wiley-VCH, Weinheim, 2006; b) Y. Li, Y. Lu, *Functional Nucleic Acids for Analytical Applications*, Springer, New York, 2009; M. Mascini, *Aptamers in Bioanalysis*, Wiley, New York, 2009.
- [2] a) N. K. Navani, Y. Li, *Curr. Opin. Chem. Biol.* 2006, 10, 272; b) J. Liu, Z. Cao, Y. Lu, *Chem. Rev.* 2009, 109, 1948; c) W. Mok, Y. Li, *Sensors* 2008, 8, 7050.
- [3] a) R. Nutiu, Y. Li, *Chem. Eur. J.* 2004, 10, 1868; b) R. Nutiu, Y. Li, *Methods* 2005, 37, 16.
- [4] R. Nutiu, Y. Li, *J. Am. Chem. Soc.* 2003, 125, 4771.
- [5] a) R. Nutiu, Y. Li, *Angew. Chem.* 2005, 117, 1085; *Angew. Chem. Int. Ed.* 2005, 44, 1061; b) J. Liu, Y. Lu, *Angew. Chem.* 2006, 118, 96; *Angew. Chem. Int. Ed.* 2006, 45, 90; c) E. L. Null, Y. Lu, *Analyst* 2010, 135, 419; d) L. Yang, C. W. Fung, E. J. Cho, A. D. Ellington, *Anal. Chem.* 2007, 79, 3320.
- [6] a) R. Nutiu, J. M. Yu, Y. Li, *ChemBioChem* 2004, 5, 1139; b) N. H. Elowe, R. Nutiu, A. Allali-Hassani, J. D. Cechetto, D.W. Hughes, Y. Li, E. D. Brown, *Angew. Chem.* 2006, 118, 5776; *Angew. Chem. Int. Ed.* 2006, 45, 5648; c) R. Nutiu, Y. Li, *Angew. Chem.* 2005, 117, 5600; *Angew. Chem. Int. Ed.* 2005, 44, 5464; d) N. Rupcich, R. Nutiu, Y. Li, J. D. Brennan, *Anal. Chem.* 2005, 77, 4300; e) N. Rupcich, R. Nutiu, Y. Li, J. D. Brennan, *Angew. Chem.* 2006, 118, 3373; *Angew. Chem. Int. Ed.* 2006, 45, 3295.
- [7] a) J. Liu, Y. Lu, *J. Am. Chem. Soc.* 2007, 129, 8634; b) W. Zhao, W. Chiuman, M. A. Brook, Y. Li, *ChemBioChem* 2007, 8, 727; c) Z. Zhu, C. Wu, H. Liu, Y. Zou, X. Zhang, H. Kang, C. J. Yang, W. Tan, *Angew. Chem.* 2010, 122, 1070; *Angew. Chem. Int. Ed.* 2010, 49, 1052; d) Z. S. Wu, M. M. Guo, S. B. Zhang, C. R. Chen, J. H. Jiang, G. L. Shen, R. Q. Yu, *Anal. Chem.* 2007, 79, 2933; e) Y. Du, B. Li, F. Wang, S. Dong, *Biosens. Bioelectron.* 2009, 24, 1979; f) M. Levy, S. F. Cater, A. D. Ellington, *ChemBioChem* 2005, 6, 2163; g) M. Zayats, Y. Huang, R. Gill, C. A. Ma, I. Willner, *J. Am. Chem. Soc.*

2006, 128, 13666; h) J. Elbaz, B. Shlyahovsky, D. Li, I. Willner, *ChemBioChem* 2008, 9, 232; i) Z. S. Wu, H. Zhou, S. Zhang, G. Shen, R. Yu, *Anal. Chem.* 2010, 82, 2221.

[8] a) C. Tuerk, L. Gold, *Science* 1990, 249, 505; b) A. D. Ellington, J. W. Szostak, *Nature* 1990, 346, 818.

[9] a) R. D. Jenison, S. C. Gill, A. Pardi, B. Polisky, *Science* 1994, 263, 1425; b) A. Geiger, P. Burgstaller, H. von der Eltz, A. Roeder, M. Famulok, *Nucleic Acids Res.* 1996, 24, 1029; c) D. S. Wilson, J.W. Szostak, *Annu. Rev. Biochem.* 1999, 68, 611; T. Hermann, D. J. Patel, *Science* 2000, 287, 820.

[10] a) A. Roth, R. R. Breaker, *Annu. Rev. Biochem.* 2009, 78, 305; b) B. J. Tucker, R. R. Breaker, *Curr. Opin. Struct. Biol.* 2005, 15, 342; c) M. Mandal, R. R. Breaker, *Nat. Rev. Mol. Cell Biol.* 2004, 5, 451.

[11] a) R. Yamamoto, T. Baba, P. K. Kumar, *Genes Cells* 2000, 5, 389; b) A. Tsourkas, M. A. Behlke, G. Bao, *Nucleic Acids Res.* 2003, 31, 5168; c) T. Hasegawa, M. Hagihara, M. Fukuda, T. Morii, *Nucleosides Nucleotides Nucleic Acids* 2007, 26, 1277.

[12] a) M. T. Cheah, A. Wachter, N. Sudarsan, R. R. Breaker, *Nature* 2007, 447, 497; b) A. Serganov, A. Polonskaia, A. T. Phan, R. R. Breaker, D. J. Patel, *Nature* 2006, 441, 1167; c) R. Welz, R. R. Breaker, *RNA* 2007, 13, 573; d) M. T. Croft, M. Moulin, M. E. Webb, A. G. Smith, *Proc. Natl. Acad. Sci. USA* 2007, 104, 20770.

[13] a) V. Sharma, Y. Nomura, Y. Yokobayashi, *J. Am. Chem. Soc.* 2008, 130, 16310; b) G. A. Soukup, R. R. Breaker, *Proc. Natl. Acad. Sci. USA* 1999, 96, 3584; c) M. N. Stojanovic, D. M. Kolpashchikov, *J. Am. Chem. Soc.* 2004, 126, 9266; d) B. Suess, B. Fink, C. Berens, R. Stentz, W. Hillen, *Nucleic Acids Res.* 2004, 32, 1610; e) S. Topp, J. P. Gallivan, *J. Am. Chem. Soc.* 2007, 129, 6807; f) C. C. Fowler, E. D. Brown, Y. Li, *ChemBioChem* 2008, 9, 1906; g) A. Ogawa, M. Maeda, *Bioorg. Med. Chem. Lett.* 2008, 18, 6517; h) E. E. Ferapontova, E. M. Olsen, K. V. Gothelf, *J. Am. Chem. Soc.* 2008, 130, 4256.

[14] a) S. Thore, M. Leibundgut, N. Ban, *Science* 2006, 312, 1208; b) J. Noeske, C. Richter, E. Stirnal, H. Schwalbe, J. Wohnert, *ChemBioChem* 2006, 7, 1451; c) G. Mayer, M. S. Raddatz, J. D. Grunwald, M. Famulok, *Angew. Chem.* 2007, 119, 563; *Angew. Chem. Int. Ed.* 2007, 46, 557; d) J. Miranda-Rios, *Structure* 2007, 15, 259; e) M. Wieland, A. Benz, B. Klauser, J. S. Hartig, *Angew. Chem.* 2009, 121, 2753; *Angew. Chem. Int. Ed.* 2009, 48, 2715; f) N. Muranaka, K. Abe, Y. Yokobayashi, *ChemBioChem* 2009, 10, 2375.

[15] a) I. Willner, M. Zayats, *Angew. Chem.* 2007, 119, 6528; *Angew. Chem. Int. Ed.* 2007, 46, 6408; b) A. K. Cheng, D. Sen, H. Z. Yu, *Bioelectrochemistry* 2009, 77, 1.

## CHAPTER 3

# QUALITY CONTROL CERTIFICATION OF RNA APTAMER-BASED DETECTION

### 3.1 Author's Preface

To provide assurance against concerns of RNA aptamer instability and degradation during analysis, the second research project describes the first aptamer-based sensing strategy capable of monitoring quality control. Base on the structure-switching design, this novel sensing strategy can distinguish between true-positive and false-positive signals. By using this strategy to pin-point defective samples, remedy methods to correct a false-positive signal are also demonstrated in this chapter.

This work has been published and provisionally patented. This chapter appears in its published format (see full citation below). I am the first author of this publication. I took the leading role for project design, and data analysis. I conducted all experiments to demonstrate false-positive signal reporting, as well as the correction of false-positive signals. With my supervision, Chung Kit Lai performed assays to assess sensitivity and specificity of the sensing systems. I wrote the manuscript with assistance from Dr. Yingfu Li. Supplementary information is found in Appendix 1.

Lau PS, Lai CK, Li Y (2013) Quality control certification of RNA aptamer-based detection. *Chembiochem* 14: 987-992.

Lau PS, Lai CK, Li Y. Provisional U. S. Patent (61/658,650) Issued June 14, 2012.  
Structure-Switching RNA Aptamer Reporters with a Quality Control Element.

### 3.2 Abstract

Aptamers are single-stranded DNA or RNA molecules with a defined tertiary structure for molecular recognition. Numerous RNA aptamers with excellent binding affinity and specificity have been reported; they constitute an attractive reservoir of molecular recognition elements for biosensor development. However, RNA is relatively unstable owing to spontaneous hydrolysis and nuclease degradation. Thus, RNA aptamer-based biosensors are prone to producing false-positive signals. Here, we present an RNA aptamer biosensor design strategy that utilises an internal control to distinguish target binding from false-positive signals. The sequence of a chosen RNA aptamer is expanded so that it can form three consecutive short RNA–DNA duplexes with 1) a quencher-labelled DNA strand ( $Q_1$ DNA), 2) a dual-fluorophore-labelled DNA strand ( $F_1$ DNA $F_2$ ) and 3) another quencher-labelled DNA strand ( $Q_2$ DNA). The addition of a target releases  $Q_2$ DNA from the duplex assembly, and produces the expected positive signal from  $F_2$ . However, the authenticity of target recognition is validated only if no signal is generated from  $F_1$ . We have successfully engineered two fluorescent reporters by using an RNA aptamer that binds thrombin and one that binds theophylline. Both reporters show the expected binding affinity and specificity, and are capable of reporting system malfunction when treated with nucleases and chemical denaturants. This strategy provides a simple and reliable way to ensure high-quality detection when RNA aptamers are employed as molecular-recognition elements.

### 3.3 Introduction

RNA is a functionally versatile biopolymer from which numerous molecular recognition elements, known as aptamers, have been derived in different ways. Nature, for instance, has employed a host of RNA aptamers to construct riboswitches to regulate gene expression.<sup>[1]</sup> With the development of the in vitro selection technique, a large battery of artificial RNA aptamers have been isolated from random-sequence RNA libraries to recognise wide-ranging targets.<sup>[2]</sup> Many naturally occurring and artificially developed RNA aptamers exhibit excellent binding affinity and specificity, thus making them attractive for biosensor development.<sup>[3]</sup> However, reports on exploring RNA aptamers for biosensing applications are relatively limited, largely owing to the poor chemical stability of RNA and its susceptibility to RNase degradation. To harness RNA aptamers as sensing elements, we previously developed a general approach to create structure-switching reporters from RNA aptamers.<sup>[4]</sup> More recently, we have shown that entrapment in sol-gel-derived materials conferred protection from nuclease degradation on these RNA-based reporters.<sup>[5]</sup> Nucleotide chemical modifications, spiegelmers and locked nucleic acids (LNAs) are other established methods of RNA protection.<sup>[6]</sup>

Working with RNA aptamer-based biosensors requires appropriate experimental controls to ensure the validity of the detection results. Although external experiments can be implemented to assess RNA integrity,<sup>[7]</sup> a biosensing strategy that incorporates a simple internal control for continuous monitoring of RNA quality would be highly beneficial. Many biosensing designs, such as structure-switching reporters, require the formation of DNA–DNA or RNA–DNA duplexes as critical structural elements.<sup>[4]</sup>

Unintentional structural denaturation, however, can occur from a variety of factors, such as altered pH and suboptimal ion strength. RNA is also prone to spontaneous transesterification,<sup>[8]</sup> and degradation by ubiquitous RNases.<sup>[6]</sup> Therefore, having a simple internal control that can detect system malfunction would ensure the reliability and reproducibility of RNA aptamer-based sensing.

Herein, we present an aptamer biosensor design strategy that exploits an internal control as a quality control (QC) element to distinguish target binding from false-positive signals in real time. The sensing system consists of a multifunctional RNA (mRNA) with three sequence domains (Figure 3-1A): the first forms a duplex with a quencher-labelled DNA strand ( $Q_1$ DNA), the second forms a duplex with a dual-fluorophore labelled DNA strand ( $F_1$ DNA $F_2$ ), and the third is an RNA aptamer sequence capable of forming a duplex with another quencher-labelled DNA strand ( $Q_2$ DNA). The addition of target releases  $Q_2$ DNA from the duplex assembly, and produces an expected signal from  $F_2$  (Figure 3-1B). Incorporation of the  $Q_1F_1$  pair allows true-positive signals to be distinguished from false positives that can arise from unexpected system malfunctions, such as the destruction of the DNA/RNA assembly by nucleases (Figure 3-1C). According to this strategy, we have successfully engineered two fluorescent reporters by using an RNA aptamer that binds thrombin and one that binds theophylline.

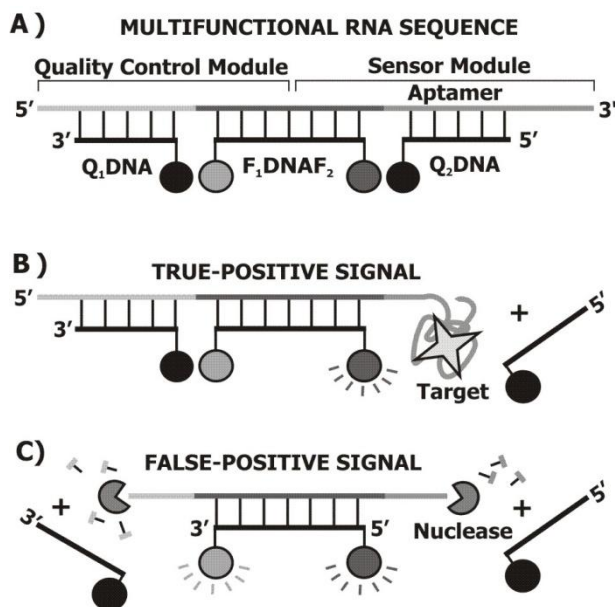


**Figure 3-1.** Structure-switching RNA aptamers with a quality control element. **A)** Duplex assembly between a multifunctional RNA with Q<sub>1</sub>DNA, F<sub>1</sub>DNAF<sub>2</sub>, and Q<sub>2</sub>DNA. **B)** True-positive signal. Addition of the target (star) results in target-aptamer complex formation and the departure of Q<sub>2</sub>DNA, which is accompanied by signal generation from F<sub>2</sub>. **C)** False-positive signal. System destruction, for example, by a nuclease, would lead to signal production from both F<sub>1</sub> and F<sub>2</sub>.

### 3.4 Materials and Methods

**3.4.1 Materials.** All DNA oligonucleotides were synthesized using automated DNA synthesis (Integrated DNA Technologies, Coralville, IA). F<sub>1</sub> and F<sub>2</sub> of F<sub>1</sub>DNAF<sub>2</sub> are 3'-fluorescein and 5'-TYE665, respectively; F<sub>2</sub> was introduced using TYE665 phosphoramidite while F<sub>1</sub> was introduced using fluorescein derivatized controlled pore glass (CPG). Q<sub>1</sub>DNA contains a 5'-Iowa Black FQ dark quencher introduced using Iowa Black FQ phosphoramidite. Q<sub>2</sub>DNA contains a 3'-Iowa Black RQ dark quencher introduced using Iowa Black RQ derivatized CPG. Unmodified oligonucleotides were purified by 10% denaturing PAGE, and modified DNAs were purified by HPLC before use. Human  $\alpha$ -thrombin, and human prothrombin were obtained from Haematological

Technologies (Essex Jct., VT). Unless otherwise noted, all other materials were purchased from Sigma (Oakville, Canada), and used without further purification.

**3.4.2 Polymerase Chain Reaction.** The synthetic DNA template for the thrombin reporter has the sequence of 5'-GAATT CTAAT ACGAC TCACT ATAGG GAGAC ACGTC GTGCG TACTC CTGCC ACGCT CCGAC GCTAG CTGAT CACTC GAAGT CCGGA TCGAA GTTAG TAGGC GGA-3'. It was amplified by PCR using primers 5'-GAATT CTAAT ACGAC TCACT ATA-3' (forward) and 5'-TCCGC TCACT AACTT C-3' (reverse). The theophylline reporter has the sequence of 5'-GAATT CTAAT ACGAC TCACT ATAGG GAGAC ACGTC GTGCG TACTC CTGCC ACGCT CCGAC GCTAG CTGAT CACTC GAAGG GCGAT ACCAG CCGAA AGGCC CTTGG CAGCG TCCAA CACAT CG-3' and was amplified using primers 5'-GAATT CTAAT ACGAC TCACT ATA-3' (forward) and 5'-CGATG TGTTG GACGC-3' (reverse). PCR was conducted in Tris-HCl [pH 9.0] (75 mM), MgCl<sub>2</sub> (2 mM), KCl (50 mM), (NH<sub>4</sub>)<sub>2</sub>SO<sub>4</sub> (20 mM), primers (0.5 μM of each), DNA template (3 nM), dNTPs (0.5 mM of each), and Taq DNA polymerase (5 units, Biotools, Madrid, Spain). Thermal cycling steps were: 94°C for 1 min, 20 cycles of 94°C-42°C-72°C (30 sec for each temperature), and finally 72°C for 8 min.

**3.4.3 RNA transcription.** The transcription reaction was conducted at 37°C for 3 h in 150 μL of Tris-HCl [pH 7.9] (40 mM), MgCl<sub>2</sub> (6 mM) DTT (10 mM), NaCl (10 mM), spermidine (2 mM), PCR amplified DNA (25 pmol), NTPs (2.5 mM of each), RiboLock Ribonuclease Inhibitor (1.07 units/μL), and T7 RNA polymerase (1.33 units/μL, Fermentas, Burlington, Canada). The transcription mixture was then treated with DNase I

(3 units, Fermentas) in the presence of  $\text{CaCl}_2$  (0.2 mM) at 37°C for 15 min. The transcribed RNA was subsequently purified by 10% denaturing PAGE, and quantified by absorbance at 260 nm.

**3.4.4 Fluorescence measurements.** The signalling mixture contained  $\text{F}_1\text{DNAF}_2$  (40 nM), extended RNA aptamer (80 nM),  $\text{Q}_1\text{DNA}$  (120 nM), and  $\text{Q}_2\text{DNA}$  (120 nM) in a binding buffer (50  $\mu\text{L}$  total volume) corresponding to each aptamer. Thrombin buffer: Tris-HCl [pH 7.7] (50 mM), NaCl (100 mM), DTT (1 mM), and  $\text{MgCl}_2$  (1 mM). Theophylline buffer: Tris-HCl [pH 7.5] (50 mM),  $\text{MgCl}_2$  (20 mM). The mixture was first heated at 65°C for 2 min, then cooled at room temperature for 10 min, and stored at 4°C until analysis. Fluorescence measurements were taken at an excitation/emission of 645/665 and 495/520 nm every min at 37°C (unless stated otherwise) on Cary Eclipse (Varian). Target-sensing assays were conducted by adding thrombin, theophylline or their structural analogs to signalling mixtures. For degradation assays, the following were introduced: i) RNase A (0.1  $\mu\text{g}/\mu\text{L}$ , Fermentas), ii) DNase I (0.06 units/ $\mu\text{L}$ , Fermentas) plus  $\text{CaCl}_2$  (0.1 mM), iii) NaOH (50 mM) in Tris-HCl [pH 7.5] (50 mM) plus NaCl (300 mM), or iv) no addition (negative control). To test the effects of human serum on the theophylline reporter, the following were added to each signalling mixture: i) serum (5  $\mu\text{L}$ ), ii) filtered serum (10 K filtration column, Sartorius Stedium Biotech), iii) theophylline (60 mM) in serum, iv) filtered theophylline (60 mM) in serum, v) filtered theophylline (60 mM), or vi) no addition (negative control). To test the effects of human serum on the thrombin reporter, the following were added to each signalling mixture: i) serum (1  $\mu\text{L}$ ), ii) RiboLock RNase Inhibitor (4.8 units/ $\mu\text{L}$ ) plus thrombin (3  $\mu\text{M}$ ) in

serum, iii) no addition (negative control). Relative fluorescence (RF) was calculated using  $F/F_0$ , where  $F_0$  and  $F$  are the fluorescence intensity before and after addition of target/degrading agent, respectively. To obtain the thermal denaturation profiles, each signalling mixture was incubated at 65°C for 5 min in the fluorimeter before temperature was decreased to 20°C at a rate of 1°C/min.

### **3.5 Results and Discussion**

#### ***3.5.1 Construction of an aptamer reporter for thrombin***

As the first demonstration, we chose an RNA aptamer that recognises human  $\alpha$ -thrombin,<sup>[9]</sup> a serine protease that plays a critical role in the regulation of thrombosis, and haemostasis.<sup>[10]</sup> The DNA sequence encoding both the QC and aptamer elements was chemically synthesised, and amplified through polymerase chain reaction (PCR) with necessary primers to produce a double-stranded DNA template, which was then used for in vitro transcription to generate the required  $\text{mRNA}_{\text{throm}}$  (its sequence is given in Figure 3-2A, along with those of the relevant chromophore-containing DNA molecules).  $\text{mRNA}_{\text{throm}}$  was designed to form a 20 bp duplex with  $\text{Q}_1\text{DNA}$ , and a 25 bp duplex with  $\text{F}_1\text{DNAF}_2$ .

To determine the optimum length of  $\text{Q}_2\text{DNA}$  for the third duplex, which is critical to the sensing performance of the system, we examined thermal-denaturation profiles of the duplex assemblies with  $\text{Q}_2\text{DNAs}$  containing 13–16 nt (Figure S3-1A; found in Appendix 1, Supplementary Information). As the 13-nt  $\text{Q}_2\text{DNA}$  ( $\text{Q}_2\text{DNA}_{13}$ ) produced the best signal enhancement with a relatively low melting point (which should facilitate the

displacement of Q<sub>2</sub>DNA by thrombin), this molecule was chosen for further study. Note that we incorporated several non-aptameric nucleotides (underlined letters) immediately upstream of the aptamer domain (boldfaced letters). This feature, which was established in our previous studies,<sup>[4]</sup> allows the formation of a stable Q<sub>2</sub>DNA–mfRNA duplex without sequestering many nucleotides in the aptamer domain that are involved in target recognition (Figure 3-2A).

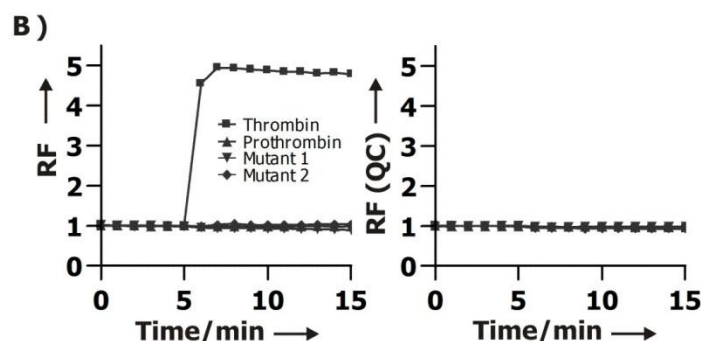


**Figure 3-2.** A thrombin reporter. **A)** The sequences of mfRNA, Q<sub>1</sub>DNA, F<sub>1</sub>DNAF<sub>2</sub> and Q<sub>2</sub>DNA used. **B)** Specificity test. The signaling duplex was incubated for 5 min before addition of thrombin or prothrombin (3 μM). Mutants 1 and 2: modified mfRNAs with mutations in the aptamer domain; both were tested with thrombin. RF: relative fluorescence, calculated as F<sub>t</sub>/F<sub>0</sub>, fluorescence intensity at time t and time 0. RF from F<sub>2</sub> (sensor module), and F<sub>1</sub> (QC module) are presented on the left and right, respectively. The data are the average of three independent experiments.

### 3.5.2 Sensing performance of the thrombin reporter

The aptamer reporter produced an approximately fivefold increase in intensity at 665 nm upon the addition of thrombin (Figure 3-2B, left); the fluorescence of TYE665 as

F<sub>2</sub> was indicative of Q<sub>2</sub>DNA departure from the duplex assembly. The high level signal enhancement from F<sub>2</sub> confirms that the reporter is capable of thrombin detection. Two experiments were conducted to verify specific molecular recognition between the aptamer and thrombin. First, prothrombin, a precursor of thrombin that has no affinity for the original RNA aptamer,<sup>[9]</sup> was tested. No signal enhancement was observed at F<sub>2</sub> (Figure 3-2B, left). Second, two mutated versions of mRNA sequences, in which selective nucleotides critical for thrombin recognition were altered (Figure S3-2A, Appendix 1, Supplementary Information), were examined. Neither mutant was able to register a signal increase at F<sub>2</sub> (Figure 3-2B, left). To assess the sensitivity of the reporter, the relative fluorescence from F<sub>2</sub> was determined at various concentrations of thrombin (Figure S3-3A, left, Appendix 1, Supplementary Information). The detection limit was found to be 0.01 μM, and the dynamic detection window was between 0.01–3 μM.

### ***3.5.3 Functionality test of the QC element***

Two scenarios are expected of the QC element with regard to signal generation: when the reporter is fully functional, no signal change from F<sub>1</sub> should be observed; however, the observation of notable fluorescence changes from both F<sub>1</sub> and F<sub>2</sub> indicates system malfunction. No intensity increase was observed at 520 nm (Figure 3-2B, right and Figure S3-3A; fluorescence from fluorescein as F<sub>1</sub> in the QC element) in the presence of the intended target, thrombin. However, when the system was treated with RNase A, DNase I and NaOH, notable signal enhancement for both F<sub>2</sub> (Figure 3-3A), and F<sub>1</sub> (Figure 3-3B) was observed. These results validate the complete function of the thrombin reporter.

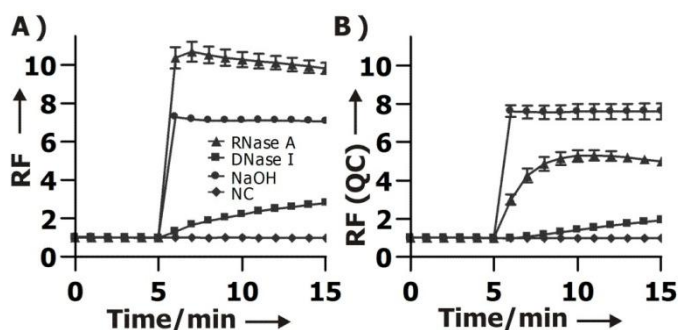


**Figure 3-3.** False-positive signal reporting. The signaling duplex was incubated for 5 min, before the addition of RNase A, DNase I, and NaOH. NC: negative control (no denaturant added). Relative fluorescence (RF) was measured for **A)** F<sub>2</sub> and **B)** F<sub>1</sub>. Data are the average of two independent experiments.

### 3.5.4 Construction of an aptamer reporter for theophylline

To demonstrate the generality of the approach, we designed a second reporter by using the well-characterised anti-theophylline RNA aptamer.<sup>[3d,4b]</sup> We directly incorporated many design features shown to be effective for the thrombin reporter into the construction of the theophylline reporter. As shown in Figure 3-4A, the theophylline reporter used the same Q<sub>1</sub>DNA and F<sub>1</sub>DNAF<sub>2</sub>. The mfRNA sequence (mfRNA<sub>theo</sub>) possessed the same non-aptameric nucleotides upstream of the aptamer domain (underlined letters), and only differed in the actual aptamer sequence (boldfaced letters). To determine the optimal Q<sub>2</sub>DNA length, we examined the thermal denaturation profiles of four different Q<sub>2</sub>DNA sequences (13–16 nt) in duplex with mfRNA<sub>theo</sub>, F<sub>1</sub>DNAF<sub>2</sub> and Q<sub>1</sub>DNA (Figure S3-1B). As for the thrombin reporter, the optimum length of Q<sub>2</sub>DNA for the theophylline system was determined to be 13 nt (Q<sub>2</sub>DNA13; best signal enhancement with relatively low melting point), and this sequence was selected for further experiments.

### ***3.5.5 Sensing capability of the theophylline reporter***

Consisting of  $\text{mRNA}_{\text{theo}}\text{-Q}_1\text{DNA-F}_1\text{DNAF}_2\text{-Q}_2\text{DNA}$ , the theophylline reporter generated an approximately sixfold signal enhancement at 665 nm upon addition of theophylline (Figure 3-4B, left). This  $F_2$  signal was verified to be target-specific, as addition of the closely related structural derivatives caffeine or theobromine (Figure 3-4B, left) generated no signal at  $F_2$ . Likewise, the  $F_2$  signal increase from theophylline addition was also demonstrated to be aptamer sequence-specific, as mutations of critical recognition nucleotides in the mRNA sequence (Figure S3-2B) abolished the binding activity, as shown by the absence of  $F_2$  signal for mutants 1 and 2 (Figure 3-4B, left). After evaluation of the sensitivity of the reporter (Figure S3-3B, left), the detection limit was determined to be 1  $\mu\text{M}$ , and the dynamic detection window was between 1-1000  $\mu\text{M}$ .

### ***3.5.6 Test of QC element function within the theophylline reporter***

No  $F_1$  fluorescent increase was observed at 520 nm in assessment of the specificity and sensitivity of the theophylline reporter (Figure 3-4B, right and Figure S3-3B, right); this verifies the ability of the QC element to detect true-positive signals. To test for false-positive signalling, we evaluated the performance of the theophylline reporter in human serum, a medium routinely used in medical testing, and a known source of nucleases. The addition of serum produced signal enhancement for  $F_2$ , as well as  $F_1$  (Figure 3-4C), thus signifying separation of the fluorophores from their respective quenchers. This observation was confirmed to be the result of nuclease degradation, as filtration of the serum on a 10 kDa molecular weight cut-off column before addition to the reporter removed nucleases on the basis of molecular size and eliminated both  $F_2$  and

**A)**  $\text{mRNA}_{\text{theo}}$ : 5'GGGAGACACGUCGUGCGUACUCCUGCCACGCUCCGACG  
 CUAGCUGAUCACUCGAAGGGCGAUACCAGCCGAAAGGCCCUUGG  
**CAGCGUCCAACACAUCG3'**  
**Q<sub>1</sub>DNA:** 5'Q<sub>1</sub>-GTACGCACGACGTGTCTCCC3'  
**F<sub>1</sub>DNAF<sub>2</sub>:** 5'F<sub>2</sub>-TCAGCTAGCGTCGGAGCGTGGCAGG-F<sub>1</sub>3'  
**Q<sub>2</sub>DNA13:** 5'CGCCCTCGAGTG-Q<sub>2</sub>3'

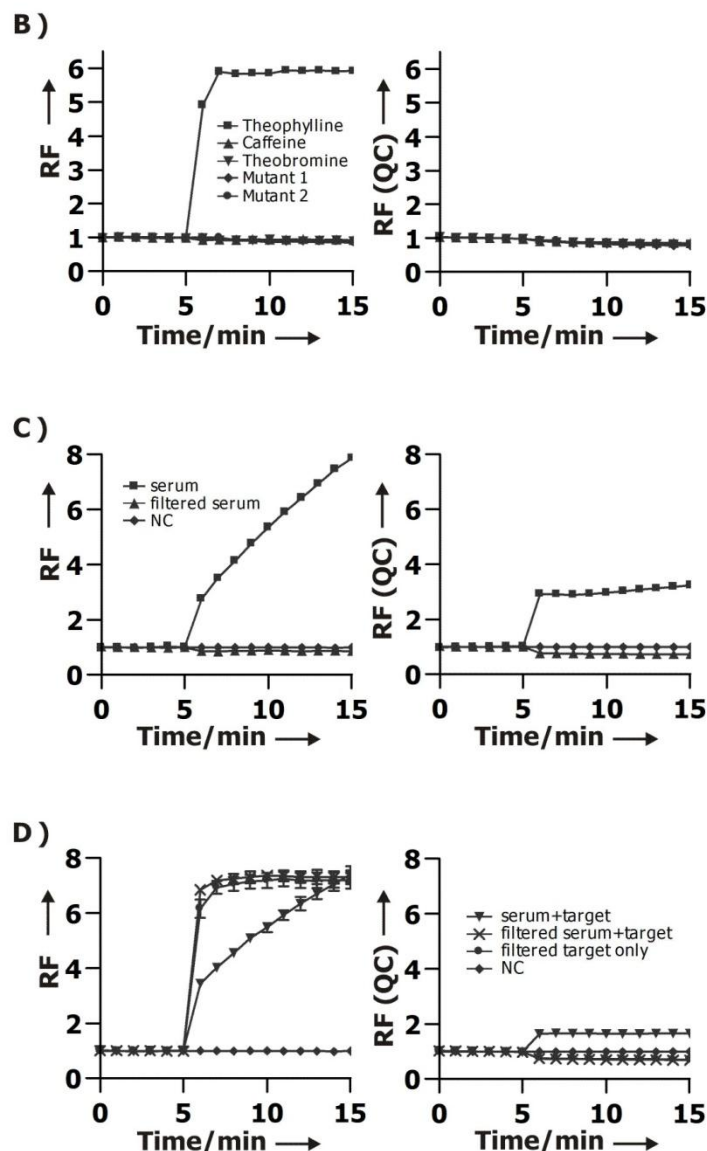


**Figure 3-4.** A theophylline reporter. **A)** The sequences of mRNA, Q<sub>1</sub>DNA, F<sub>1</sub>DNAF<sub>2</sub> and Q<sub>2</sub>DNA used. **B)** Specificity test. The signaling duplex was incubated for 5 min before addition of 1 mM theophylline, caffeine or theobromine. Mutants 1 and 2: modified mRNAs with mutations in the aptamer domain; both were tested with theophylline. RF from F<sub>2</sub> (sensor module), and F<sub>1</sub> (QC module) are presented on the left and right, respectively (same layout for subsequent panels). **C)** and **D)** Test in human serum. Comparing effects produced by the addition of unfiltered and filtered human serum doped with theophylline.

F<sub>1</sub> signals (Figure 3-4C). Together, these results validate the complete function of the theophylline reporter. Notably, a small signal decrease in F<sub>1</sub> and F<sub>2</sub> was produced upon the addition of filtered serum. Given the complex components found in serum, smaller molecules (peptides, hormones, small molecules, electrolytes, etc.) can still pass through the filter, and cause slight fluctuations in fluorescence due to molecular crowding of the fluorophores.<sup>[11]</sup>

### ***3.5.7 Elimination of false-positive signals guided by QC element***

We have already established that the QC element was able to detect the degradation effects of serum in the theophylline reporter (Figure 3-4C). False-positive signalling was also exhibited when testing the effects of serum and theophylline together (as would be the case in clinical blood testing for drugs and other substances). Here, we found that any theophylline-binding effects were “masked” by the F<sub>2</sub> and F<sub>1</sub> signals produced by serum degradation (Figure 3-4D). To correct this detection error, we removed contaminating nucleases by membrane column filtration, while retaining theophylline. By filtering serum doped with theophylline before addition, we were able to accurately detect theophylline (F<sub>2</sub> signal enhancement from aptamer-sensing module; Figure 3-4D, left), without any system malfunction (absence of F<sub>1</sub> signal from QC element; Figure 3-4D, right). Furthermore, we found that, after filtration, serum did not alter the signalling ability of the reporter, as both the filtered serum plus target sample (Figure 3-4D, left), and the filtered target-only sample (Figure 3-4D, left) produced the same magnitude of F<sub>2</sub> signal.

The thrombin reporter was also able to detect the degradation effects of serum, as high  $F_2$  and  $F_1$  signals were generated (Figure S3-4). However, given that thrombin possesses a molecular weight in the same range as those of most nucleases, simple column-filtration of the protein–serum mixture would not be a feasible remedy method for the detection of protein targets. In this case, adding RiboLock RNase inhibitor to the target–serum mixture successfully inactivated most nucleases, and the  $F_1$  signal was substantially reduced compared to that of the serum sample without treatment with nuclease inhibitor (Figure S3-4, right). The likely reason why not all the  $F_1$  signal was abolished is the capability of RiboLock to inhibit common nucleases, but not all. Further studies could benefit from the use of a cocktail of common nuclease inhibitors to inactivate a wider range of nucleases in complex samples.

### **3.6 Conclusions**

In summary, we have demonstrated a new general approach to creating RNA aptamer-based biosensors that exploit an internal quality control element to distinguish target binding from false-positive signals. The sensing strategy is based on a multifunctional RNA sequence that forms a duplex with one dual-fluorophore-modified oligonucleotide and two quencher modified DNA oligonucleotides, which function in coordination to form the QC element and sensor module. To the best of our knowledge, this is the first example of an aptamer-based sensor that is capable of monitoring the quality of detection.

The QC element was able to report true-positive signals for both reporters (production of an  $F_2$  signal and lack of an  $F_1$  signal) and also reliably reported system malfunction when treated with known chemical denaturants and nucleases (production of both  $F_1$  and  $F_2$  signals). These results demonstrate the utility of the QC element and showcase the generality of the design strategy. In testing the human serum samples doped with theophylline, we discovered that simple filtration of the drug–serum mixture prior to addition to the theophylline reporter removed all contaminating nucleases, but retained the drug target for detection. This approach is likely to be applicable for the detection of other small-molecule targets in serum. However, for the detection of protein targets, which have molecular weights in the same range as most nucleases, simple filtration would not be a feasible method. One possible solution that we have demonstrated is to treat protein–serum mixtures with common nuclease inhibitors. Hence, incorporation of a QC element will be useful to help identify remedy methods to eliminate false-positive signals.

Generating aptamers that are intrinsically resistant to degradation would be an attractive option to avoid the need for remedy methods altogether. Chemical modification of nucleotides can prolong the lifetime of RNA aptamers for several days,<sup>[6]</sup> and sol–gel entrapment of RNA structure-switching reporters has demonstrated long-term chemical stability of up to one month.<sup>[5]</sup> However, generating modified RNA libraries for SELEX remains expensive, and some modified nucleotide building blocks are not commercially available. Furthermore, some modifications can only be incorporated into aptamers post-SELEX, and this can alter aptamer binding properties. This is especially the case for

naturally occurring RNA aptamers, which offer a plethora of possibilities for biosensor development, yet still remain relatively underexplored. To utilise these aptamer species for biosensing applications, having a QC element can ensure the validity of the results obtained and provide greater user confidence.

Structure-switching reporters have been expanded to detect many small-molecule and protein targets,<sup>[12]</sup> and applied in many secondary applications, such as enzymatic reaction monitoring and inhibitor screening,<sup>[13]</sup> designing nanodevices and solid-phase assays,<sup>[14]</sup> and in vivo sensing.<sup>[15]</sup> Additionally, the fluorescence detection platform has been expanded to include other signal-transduction methods such as electrochemical, and colourimetric detection.<sup>[16]</sup> It is conceivable that aptamer reporters with a QC element could be useful for many of the aforementioned purposes, as well as for other future applications in which high-quality detection is needed.

### **3.7 Acknowledgements**

This work was supported by research grants from the Natural Sciences and Engineering Research Council of Canada (NSERC), and the Canadian Food Inspection Agency (CFIA).

### 3.8 References

- [1] a) A. Roth, R. R. Breaker, *Annu. Rev. Biochem.* 2009, 78, 305–334; b) T. E. Edwards, D. J. Klein, A. R. Ferré-D'Amaré, *Curr. Opin. Struct. Biol.* 2007, 17, 273–279.
- [2] a) A. D. Ellington, J. W. Szostak, *Nature* 1990, 346, 818–822; b) C. Tuerk, L. Gold, *Science* 1990, 249, 505–510.
- [3] a) N. K. Navani, Y. Li, *Curr. Opin. Chem. Biol.* 2006, 10, 272–281; b) M. Famulok, G. Mayer, *Acc. Chem. Res.* 2011, 44, 1349–1358; c) J. X. Wang, E. R. Lee, D. R. Morales, J. Lim, R. R. Breaker, *Mol. Cell* 2008, 29, 691–702; d) R. D. Jenison, S. C. Gill, A. Pardi, B. Polisky, *Science* 1994, 263, 1425–1429.
- [4] a) R. Nutiu, Y. Li, *J. Am. Chem. Soc.* 2003, 125, 4771–4778; b) P. S. Lau, B. K. Coombes, Y. Li, *Angew. Chem.* 2010, 122, 8110–8114; *Angew. Chem. Int. Ed.* 2010, 49, 7938–7942.
- [5] C. Carrasquilla, P. S. Lau, Y. Li, J. D. Brennan, *J. Am. Chem. Soc.* 2012, 134, 10998–11005.
- [6] a) D. Jellinek, L. S. Green, C. Bell, C. K. Lynott, N. Gill, C. Vargeese, G. Kirschenheuter, D. P. McGee, P. Abesinghe, W. A. Pieken, R. Shapiro, D. B. Rifkin, D. Moscatelli, N. Janjic, *Biochemistry* 1995, 34, 11363–11372; b) Y. Lin, Q. Qiu, S. C. Gill, S. D. Jayasena, *Nucleic Acids Res.* 1994, 22, 5229–5234; c) S. Klussmann, A. Nolte, R. Bald, V. A. Erdmann, J. P. Furste, *Nat. Biotechnol.* 1996, 14, 1112–1115; d) A. Nolte, S. Klussmann, R. Bald, V. A. Erdmann, J. P. Furste, *Nat. Biotechnol.* 1996, 14, 1116–1119; e) R. Kumar, S. K. Singh, A. A. Koshkin, V. K. Rajwanshi, M. Meldgaard, J. Wengel, *Bioorg. Med. Chem. Lett.* 1998, 8, 2219–2222.
- [7] a) H. Lehrach, D. Diamond, J. M. Wozney, H. Boedtke, *Biochemistry* 1977, 16, 4743–4751; b) K. L. Manchester, *Biotechniques* 1995, 19, 208–210; c) O. Mueller, K. Hahnenberger, M. Dittmann, H. Yee, R. Dubrow, R. Nagle, D. Ilsley, *Electrophoresis* 2000, 21, 128–134.
- [8] Y. Li, R. R. Breaker, *J. Am. Chem. Soc.* 1999, 121, 5364–5372.
- [9] M. F. Kubik, A. W. Stephens, D. Schneider, R. A. Marlar, D. Tasset, *Nucleic Acids Res.* 1994, 22, 2619–2626.
- [10] J. W. Fenton II, *Ann. N. Y. Acad. Sci.* 1981, 370, 468–495.
- [11] J. D. Fowlkes, C. P. Collier, *Lab Chip* 2013, 13, 877–885.
- [12] a) R. Nutiu, Y. Li, *Angew. Chem.* 2005, 117, 1085–1089; *Angew. Chem. Int. Ed.* 2005, 44, 1061–1065; b) J. Liu, D. Mazumdar, Y. Lu, *Angew. Chem.* 2006, 118, 8123–8127; *Angew. Chem. Int. Ed.* 2006, 45, 7955–7959; c) E. L. Null, Y. Lu, *Analyst* 2010,

135, 419–422; d) L. Yang, C. W. Fung, E. J. Cho, A. D. Ellington, *Anal. Chem.* 2007, 79, 3320–3329.

[13] a) R. Nutiu, J. M. Yu, Y. Li, *ChemBioChem* 2004, 5, 1139–1144; b) N. H. Elowe, R. Nutiu, A. Allali-Hassani, J. D. Cechetto, D. W. Hughes, Y. Li, E. D. Brown, *Angew. Chem.* 2006, 118, 5776–5780; *Angew. Chem. Int. Ed.* 2006, 45, 5648–5652.

[14] a) R. Nutiu, Y. Li, *Angew. Chem.* 2005, 117, 5600–5603; *Angew. Chem. Int. Ed.* 2005, 44, 5464–5467; b) N. Rupcich, R. Nutiu, Y. Li, J. D. Brennan, *Anal. Chem.* 2005, 77, 4300–4307; c) N. Rupcich, R. Nutiu, Y. Li, J. D. Brennan, *Angew. Chem.* 2006, 118, 3373–3377; *Angew. Chem. Int. Ed.* 2006, 45, 3295–3299.

[15] D. Zheng, D. S. Seferos, D. A. Giljohann, P. C. Patel, C. A. Mirkin, *Nano Lett.* 2009, 9, 3258–3261.

[16] a) J. Liu, Y. Lu, *J. Am. Chem. Soc.* 2007, 129, 8634–8643; b) W. Zhao, W. Chiuman, M. A. Brook, Y. Li, *ChemBioChem* 2007, 8, 727–731; c) Z. Zhu, C. Wu, H. Liu, Y. Zou, X. Zhang, H. Kang, C. J. Yang, W. Tan, *Angew. Chem.* 2010, 122, 1070–1074; *Angew. Chem. Int. Ed.* 2010, 49, 1052–1056; d) Z. S. Wu, M. M. Guo, S. B. Zhang, C. R. Chen, J. H. Jiang, G. L. Shen, R. Q. Yu, *Anal. Chem.* 2007, 79, 2933–2939; e) M. Levy, S. F. Cater, A. D. Ellington, *ChemBioChem* 2005, 6, 2163–2166; f) M. Zayats, Y. Huang, R. Gill, C. A. Ma, I. Willner, *J. Am. Chem. Soc.* 2006, 128, 13666–13667.

## CHAPTER 4

### A GENERAL STRATEGY TO CREATE RNA APTAMER SENSORS USING REGULATED GRAPHENE OXIDE ADSORPTION

#### 4.1 Author's Preface

In the third research project, the versatility of the structure-switching approach using RNA aptamers is demonstrated by adapting the design for sensor development on graphene material. Furthermore, this strategy involves a novel method to regulate RNA aptamer adsorption on graphene oxide, which immensely broadens applicability of the sensing design to accommodate aptamers of various lengths.

The work presented in this chapter has been submitted for publication. I will be co-first author (\*) for this manuscript. For this work, I conceived the project idea, and was principally responsible for experimental design and data interpretation. With my guidance, Jinping Song performed the experiments. I wrote the entire manuscript. Meng Liu provided the graphene oxide material. Dr. Yingfu Li, Dr. Chuan Dong and Dr. Shaomin Shuang provided helpful guidance and suggestions. Supplementary information is found in Appendix 1.

Song J\*, Lau PS\*, Liu M, Shuang S, Dong C, Li Y (submitted) A general strategy to create RNA aptamer sensors using regulated graphene oxide adsorption.

## 4.2 Abstract

Aptamers are single-stranded DNA or RNA molecules that can fold into a defined tertiary structure to bind a designated target. Aptamers have been used for sensor development in combination with graphene oxide (GO), a nanomaterial with properties including fluorescence quenching, and selective adsorption of single-stranded nucleic acids. However, previous sensor designs based on aptamer-GO adsorption have not demonstrated wide applicability. Many RNA aptamers possess superior sensing properties, and provide many opportunities for further exploration. Herein, we present a novel sensing strategy based on “regulated” GO adsorption that can accommodate various RNA aptamers. First, the RNA aptamer hybridizes to a fluorophore-modified, complementary DNA strand (FDNA). Adsorption of FDNA-RNA aptamer duplex to GO then results in fluorescence quenching due to close proximity of the fluorophore to GO. The addition of a complementary, “blocking” DNA strand (BDNA) that hybridizes to the 3'-end of the aptamer, weakens aptamer-GO interaction, and enables higher fluorescent signal generation upon the addition of target, as the sensing system becomes completely separated from GO. Using this strategy, we have engineered two novel RNA aptamer-based sensors, which require BDNA for increased signal generation. Our findings can be applied towards different aptamers, and adapted to enhance generality of existing sensing applications.

## 4.3 Introduction

Aptamers are single-stranded DNA or RNA molecules that fold into a defined tertiary structure to bind a designated target.<sup>[1]</sup> These unique molecular probes have been

widely implemented for sensor development, particularly using fluorescence due to ease in aptamer labeling, and availability of detection instruments.<sup>[2]</sup>

Exploration of RNA aptamers for sensor development has begun to emerge in recent years. Through bioinformatics and biochemical testing, new RNA aptamers continue to be discovered as part of riboswitches, or systems that regulate gene expression in diverse organisms.<sup>[3]</sup> Additionally, many RNA aptamers continue to be artificially developed through the process of systematic evolution of ligands by exponential enrichment (SELEX).<sup>[4]</sup> To make use of the abundance of RNA aptamers for sensor development, we have previously demonstrated a fluorescent “structure-switching” strategy that is widely applicable to various RNA aptamers.<sup>[5]</sup> Furthermore, since RNA is known to be chemically instable, and prone to nuclease degradation, several RNA aptamer protection methods have been well-established including chemical nucleotide modifications,<sup>[6]</sup> and Spiegelmers.<sup>[7]</sup> More recently, we have demonstrated that sol-gel entrapment can also confer protection towards structure-switching RNA aptamers.<sup>[8]</sup> Additionally, we have also previously developed a method to monitor the quality control of detection from structure-switching RNA aptamers to safeguard against false-positive signals that can arise from degradation.<sup>[9]</sup>

A common theme among all of these developments is the general applicability of each design to accommodate different RNA aptamers. Well-constructed design generality can extend applicability beyond merely proof-of-concept examples. Furthermore, general design applicability can greatly facilitate the overall progression of sensor development. As discussed above, the broad concept of structure-switching for example, has been

effectively adapted and optimized to meet the specific requirements of several different applications. Continued efforts to establish effective general applicability towards emerging sensing technologies may further expand the utility of RNA aptamers for future sensor development.

One notable emerging nanomaterial is graphene. Since its discovery in 2004,<sup>[10]</sup> graphene has made tremendous contributions for sensing.<sup>[11]</sup> Made up of a single-layer lattice of hexagonal carbon, graphene possess many useful properties including high surface area, mechanical strength, conductivity, biocompatibility, fluorescence quenching ability, and amenability to functionalization.<sup>[11b,12]</sup>

In several reported studies, the oxidized form of graphene, graphene oxide (GO) has been applied as a fluorescence quencher in fluorescence resonance energy transfer (FRET)-based detection using aptamers.<sup>[12c,13]</sup> Typically, these designs make use of the ability of GO to preferentially bind the aptamer in its free, single-stranded state rather than the state where the aptamer is target-bound. Hence, adsorption of a fluorescently labelled aptamer to GO, results in fluorescence quenching through FRET. The addition of target however, results in structure-switching of the aptamer to form the aptamer-target complex. The subsequent disruption of FRET generates a high fluorescent signal.

This strategy of GO functionalization through non-covalent adsorption of the aptamer possesses many advantages compared to covalent strategies including the preservation of intrinsic GO properties, and the simplicity of functionalization without the need of any coupling reagents.<sup>[11a]</sup> However, this strategy may not be widely applicable to

many aptamers, particularly longer sequences. The binding interaction of single-stranded nucleic acids to GO typically becomes greater with increasing sequence length.<sup>[14]</sup> For this reason, the relatively stronger GO adsorption from longer aptamers is likely to out-compete the formation of target-aptamer complex, especially when dealing with low-affinity aptamers. While previously reported studies have successfully implemented this strategy for sensing, it must be noted that the aptamers used were relatively short (< 40 nt in length),<sup>[12c,13b-e]</sup> and very few studies have pertained to RNA aptamers.<sup>[13f-g]</sup>

Adaptability of the GO adsorption method towards longer aptamers would immensely enhance its utility. For example, RNA aptamers derived from riboswitches, are typically longer aptamers (>100 nt),<sup>[15]</sup> and have not yet been explored for graphene-based sensing. Many of these natural aptamers possess superior target-binding specificity and affinity,<sup>[4a,16]</sup> and represent a class of aptamers that may be highly beneficial for sensor development.

Herein, we present a generalizable sensing strategy based on regulated GO adsorption that can accommodate RNA aptamers of various lengths. In our design, the 5'-end of an extended RNA aptamer is first hybridized to a complementary DNA strand that is modified with fluorophore (FDNA) (Figure 4-1, reaction a). Adsorption of this FDNA-RNA aptamer duplex to GO results in fluorescence quenching due to the close proximity of the fluorophore to GO. The addition of a complementary, “blocking” DNA strand (BDNA) that hybridizes to the 3'-end of the aptamer, weakens aptamer-GO interaction (Figure 4-1, reaction b), and enables higher fluorescent signal generation upon the

addition of target, as the sensing system becomes completely separated from GO due to structure-switching (Figure 4-1, reaction c). Using this strategy, we have successfully engineered two novel sensors based on RNA aptamers that recognize theophylline, and thiamine pyrophosphate (TPP), respectively.

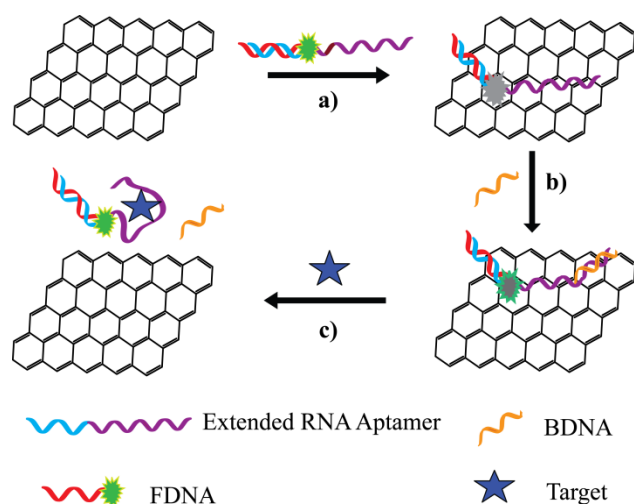


**Figure 4-1.** RNA aptamer sensors based on regulated graphene oxide (GO) adsorption. GO adsorption of duplex assembly between FDNA and Extended RNA Aptamer (reaction a), results in fluorescence quenching. Addition of BDNA (reaction b), leads to duplex formation with part of the aptamer, and weakening of GO absorption to produce moderate fluorescence. The addition of target (reaction c) results in complete separation of the sensing system from GO, and high fluorescence is generated.

#### 4.4 Materials and Methods

**4.4.1 Materials.** All DNA oligonucleotides were synthesized using automated DNA synthesis (Integrated DNA Technologies, Coralville, IA) following the standard phosphoramidite chemistry. FDNA modified with 5'-fluorescein was introduced using 5'-fluorescein phosphoramidite. All DNA oligonucleotides were purified by 10% denaturing PAGE before use. FDNA was purified by HPLC. Graphene oxide was obtained from the

Dalian University of Technology (Dalian, China) and was synthesized according to a modified Hummers method.<sup>[17]</sup> Unless otherwise noted, all other materials were purchased from Sigma (Oakville, Canada) and used without further purification.

**4.4.2 Polymerase Chain Reaction.** The theophylline DNA template with the sequence of 5'-GAATT CTAAT ACGAC TCACT ATAGG CCTGC CACGC TCCGA CGCTA TGGCG ATACC AGCCG AAAGG CCCTT GGCAG CGTC-3' was amplified by PCR using 5'-GAATT CTAAT CGAC TCACT ATA-3' and 5'-GACGC TGCCA AGG-3' as forward and reverse primers. The TPP DNA template with the sequence of 5'-GAATT CTAAT ACGAC TCACT ATAGG CCTGC CACGC TCCGA CGCTA TCCAC TAGGG GTGCT-3' and 5'-TGTTG TGCTG AGAGA GGAAT AATCC TTAAC CCTTA TAACA CCTGA TCTAG GTAAT ACTAG CGAAG GGAAG TGG-3' was obtained through T4 polynucleotide kinase (PNK)-mediated ligation of DNA template fragments. Ligation reaction was conducted according to manufacturer's protocol (Thermo Scientific, Canada). TPP template fragments with sequences of 5'-GAATT CTAAT ACGAC TCACT ATAGG CCTGC CACGC TCCGA CGCTA TCCAC TAGGG GTGCT-3' and 5'-TGTTG TGCTG AGAGA GGAAT AATCC TTAAC CCTTA TAACA CCTGA TCTAG GTAAT ACTAG CGAAG GGAAG TGG-3' were ligated together using a ligation template sequence of 5'-CAGCA CAACA AGCAC CCCTA-3'. The final ligated TPP DNA template was then purified by 10% denaturing PAGE and amplified through PCR using 5'-GAATT CTAAT CGAC TCACT ATA-3' (forward primer) and 5'-CCACT TCCCT TCGCT AGTAT-3' (reverse primer). PCR was carried out in Tris·HCl (pH 9.0,

75 mM), MgCl<sub>2</sub> (2 mM), KCl (50 mM), (NH<sub>4</sub>)<sub>2</sub>SO<sub>4</sub> (20 mM), primers (0.5 μM of each), DNA template (3 nM), dNTPs (0.5 mM of each) and Taq DNA polymerase (5 units, Biotools, Madrid, Spain). Thermal cycling steps were 94°C for 1 min, 18 cycles of 94°C–45°C–72°C (30 sec for each temperature), and finally 72°C for 8 min.

**4.4.3 RNA transcription.** The transcription reaction was conducted at 37°C for 2.5 hr in Tris-HCl (150 μL, 40 mM, pH 7.9), MgCl<sub>2</sub> (6 mM), dithiothreitol (DTT, 10 mM), NaCl (10 mM), spermidine (2 mM), PCR amplified DNA (25 pmol), NTPs (2.5 mM of each), RiboLock ribonuclease inhibitor (1.07 units/μL) and T7 RNA polymerase (1.33 units/μL, Thermo Scientific, Canada). The transcription mixture was then treated with DNase I (3 units, Thermo Scientific) in the presence of CaCl<sub>2</sub> (0.2 mM) at 37°C for 15 min. The transcribed RNA was subsequently purified by 10% denaturing PAGE, and quantified by absorbance at 260 nm.

**4.4.4 Fluorescence measurements.** For FDNA-RNA aptamer duplex assembly, a mixture of FDNA (200 nM) and RNA aptamer (200 nM), in a reaction buffer (50 μL total volume) of Tris-HCl (25 mM, pH 7.5) and MgCl<sub>2</sub> (10 mM) was first heated at 65°C for 2 min, then cooled at room temperature for 10 min, and finally cooled at 4°C for 10 min. GO (20 μL from 100 μg/mL stock) was then mixed into the FDNA-RNA aptamer mixture, and an aliquot (50 μL) was taken for analysis. All fluorescence readings were measured at 37°C (unless stated otherwise) on Cary Eclipse spectrophotometer (Varian) with an  $\lambda_{\text{ex}}/\lambda_{\text{em}}$  of 490/520 nm. Aliquots of FDNA-RNA aptamer-GO were incubated at 37°C for 30-60 min to reach stable background fluorescence and then the following were introduced: i) BDNA only, ii) target only or iii) BDNA and then target/structural

analogue. For assays measuring fluorescence in real time, relative fluorescence (RF) was calculated by using  $F/F_0$ , where  $F_0$  and  $F$  are the fluorescence intensity before and after the addition of BDNA/target, respectively. For assays measuring fluorescence spectra, fluorescence readings of test samples were recorded after 1 hr incubation at 37°C. For thermal denaturation profiles, each test sample was incubated at 20°C for 5 min in the fluorimeter before the temperature was increased to 65°C at a rate of 1°C/min.

## 4.5 Results and Discussion

### 4.5.1 Creation of an aptamer reporter for theophylline

For the first demonstration, we chose the well-characterized theophylline RNA aptamer, a relatively short aptamer of 33 nt.<sup>[4a,5b]</sup> The DNA sequence that encodes both the FDNA-binding site and aptamer domain was chemically synthesized and amplified through polymerase chain reaction (PCR) using the necessary primers to produce a double-stranded DNA template. The PCR product was then used for in vitro transcription to generate the extended RNA aptamer. The sequence is presented in Figure 4-2A (aptamer domain in blue), along with relevant DNA sequences. The extended RNA aptamer was designed to form a duplex with an FDNA of 20 nt, which we have previously demonstrated to be a sufficient length for generating relatively low background and high target-induced signal enhancement.<sup>[5b]</sup>

In our preliminary analysis, we optimized the experimental conditions necessary for target detection using the classic method of GO adsorption. We systematically tested each relevant factor by assessing the theophylline-sensing ability of the FDNA-RNA

aptamer duplex adsorbed to GO. By assessing concentrations of divalent metal ion (Figure S4-1A), FDNA (Figure S4-1B) and GO (Figure S4-1C), as well as temperature (Figures S4-1D and S4-1E), we determined the optimal conditions to minimize background fluorescence, and generate the highest fluorescent signal enhancement possible using this design. The maximum fold enhancement was found to be ~5-fold.

To further enhance signaling ability, we designed various lengths of BDNA (8-12 nt) to hybridize to the 3'-end of the theophylline aptamer (Figure 4-2A). For all BDNA lengths, we found that the addition of theophylline and BDNA together significantly enhanced fluorescent signal, even after subtraction of BDNA background (black and red data sets respectively, Figure 4-2B), as compared to the addition of BDNA or target only (gray and striped data sets respectively, Figure 4-2B). Particularly, BDNA length of 10 nt (BDNA10) generated the highest signal enhancement and was chosen for further analysis (Figure 4-2B).

To investigate the mechanism of BDNA for signal enhancement, we tested the effect of various BDNA10 concentrations on the FDNA-RNA aptamer-GO system. In samples treated with BDNA10 alone, we discovered that increasing BDNA10 concentration, expectedly led to increasing background signal, which signifies increasing FDNA-RNA aptamer dissociation from GO (gray data set, Figure 4-3A). The ability of BDNA10 to weaken FDNA-RNA aptamer interaction with GO was also confirmed in our thermal denaturation analysis (Figure 4-3B). In this assay, the control sample of FDNA-RNA aptamer-GO produced the expected low fluorescence at all temperatures signifying

adsorption of FDNA-RNA aptamer to GO (black data set, Figure 4-3B). However, the addition of BDNA10 to FDNA-RNA aptamer-GO resulted in relatively high fluorescence at lower testing temperatures, and a gradual decrease in fluorescence with increasing temperature. These results confirm that when the temperature is lower than the melting temperature of BDNA10 ( $T_m = 41^\circ\text{C}$ , predicted by IDT Oligo Analyzer), BDNA10 can hybridize to FDNA-RNA aptamer and weaken GO adsorption to generate moderate fluorescence (red data set, Figure 4-3B). In contrast, at higher temperatures, BDNA10 remains unhybridized and FDNA-RNA aptamer can strongly absorb to GO for fluorescence quenching (red data set, Figure 4-3B). Notably, a small gradual decrease in fluorescence was found from low to high temperatures for both samples. This may be due to the well established effect of temperature on fluorophore emission,<sup>[18]</sup> as well as GO solubility.<sup>[19]</sup> In further testing, we found that the addition of a fixed concentration of theophylline along with increasing BDNA10 concentration (black data set, Figure 4-3A) resulted in increased overall signal enhancement (red data set, Figure 4-3A), as compared to the addition of either theophylline or BDNA10 alone (striped data set, and gray data set, Figure 4-3A). The optimal BDNA10 concentration was determined to be 400 nM since the highest signal enhancement was generated: ~17-fold raw fluorescent value before subtraction of signal produced by BDNA10 (black data set, Figure 4-3A), ~14-fold finalized value after subtraction of BDNA10 signal (red data set, Figure 4-3A), which are respectively 12- and 9-fold higher than the addition of theophylline alone (striped data set, Figure 4-3A). Overall, the mechanism of the sensing system is summarized in Figure 4-3C, whereby FDNA-RNA aptamer duplex is initially absorbed onto GO to produce low

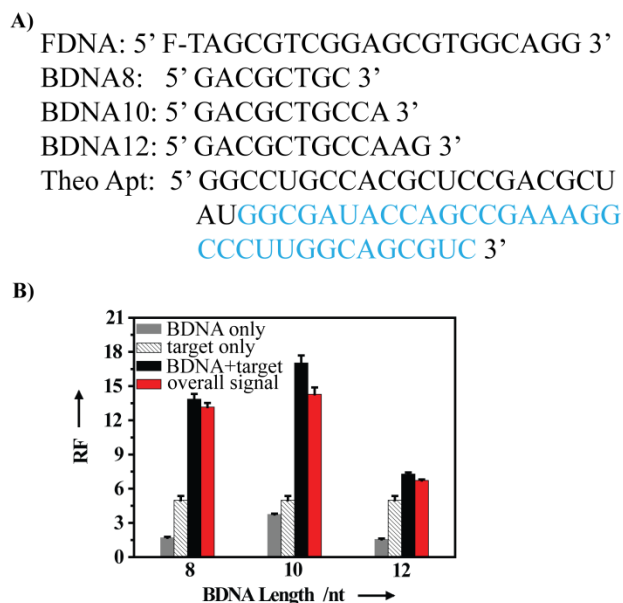


**Figure 4-2.** Creation of the theophylline reporter. **A)** Sequences tested for the reporter (aptamer domain shown in blue). **B)** Optimization of BDNA length (nucleotides, nt). FDNA-RNA Aptamer-GO was incubated for 30 min, then BDNA (gray, 400 nM), theophylline target (striped, 800  $\mu$ M), or a combination of BDNA+target (black) was added. Relative fluorescence (RF) was plotted after 1 hr.  $RF = F_t/F_0$ , fluorescence intensity at time  $t$  and 0. Calculation of overall signal enhancement (shown in red) = [BDNA+target]-BDNA. The data are an average of two independent experiments.

fluorescence (FDNA-RNA Apt-GO). The addition of BDNA forms a duplex with the 3' end of the aptamer and weakens aptamer interaction with GO to generate moderate fluorescence (FDNA-RNA Apt-BDNA ••• GO). The addition of target in the final step, results in the formation of FDNA-RNA Apt-Target complex, and dissociation of BDNA. Complete separation of the sensing system from GO leads to high fluorescence signal generation. In combination, the addition of target and BDNA together can shift the equilibrium to form FDNA-RNA Apt-Target complex better than either target or BDNA alone.

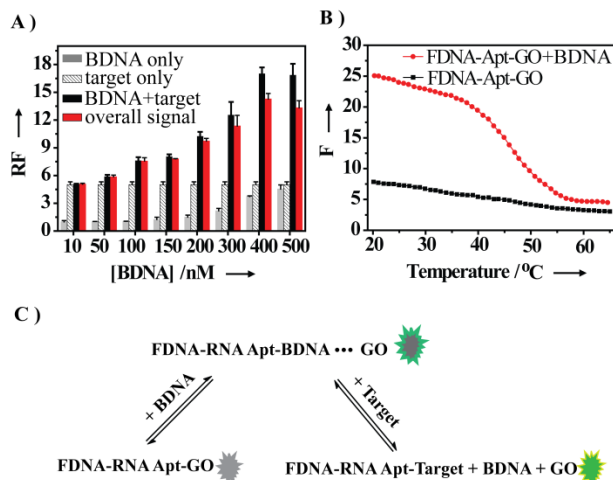


**Figure 4-3.** BDNA mechanism for signal enhancement. **A)** Testing the effect of increasing BDNA concentration. FDNA-RNA Aptamer-GO was incubated for 30 min, then BDNA (gray, 10-500 nM), theophylline target (striped, 800  $\mu$ M), or a combination of BDNA+target (black) was added. RF was plotted after 1 hr. Overall signal enhancement shown in red. **B)** Thermal denaturation profiles of FDNA-RNA Aptamer-GO system with the addition of BDNA (red), or without BDNA (black). All data are an average of two independent experiments. **C)** Summary of sensing scheme.

#### 4.5.2 Sensing capability of theophylline reporter

The FDNA-aptamer-GO-BDNA10 system was found to be highly specific for theophylline detection. The addition of BDNA10 along with structural derivatives theobromine or caffeine generated relatively low fluorescent signals, which were comparable to the sample treated with BDNA10 alone (Figure 4-4A). Similarly, mutation of aptamer nucleotides known to be critical for theophylline recognition abolished binding activity, as a low fluorescent signal was produced (Figure 4-4A and sequence found in Figure S4-2A). To determine the sensitivity of the system, fluorescent signal was measured at various theophylline concentrations. The detection limit was found to be 0.5  $\mu$ M, and the dynamic detection window was between 0.5 - 2000  $\mu$ M (Figure 4-4B). The

relative fluorescence observed at 1 hr versus theophylline concentration is found in Figures 4-4C and 4-4D.

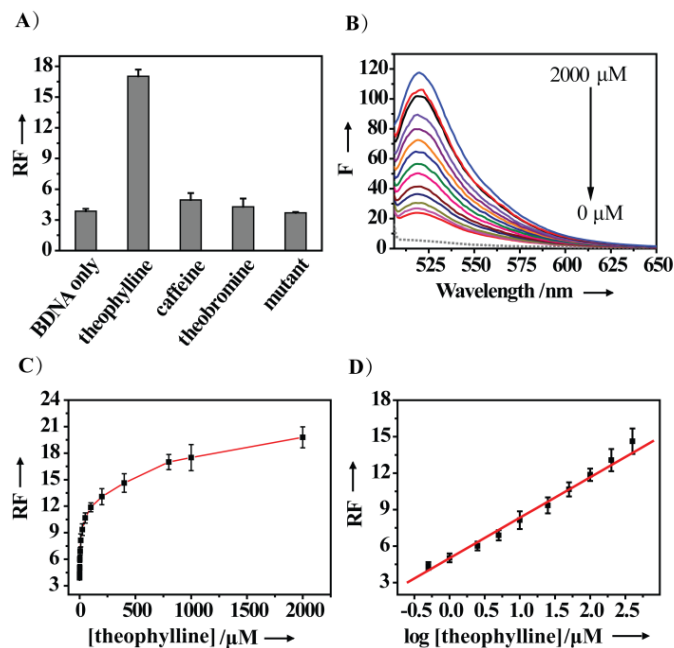


**Figure 4-4.** Sensing capability of the theophylline reporter. **A)** Specificity test. FDNA-RNA Aptamer-GO was incubated for 30 min, then BDNA (400 nM) was added, and finally theophylline (800 μM), caffeine (800 μM), theobromine (800 μM) or no addition (BDNA only) was introduced. Mutant aptamer was tested with theophylline. RF was plotted after 1 hr. **B)** Fluorescence spectra of FDNA-RNA Aptamer-GO (dotted line), and after the addition of BDNA10 (400 nM) along with theophylline (0, 0.5, 1, 2.5, 5, 10, 25, 50, 100, 200, 400, 800, 1000, and 2000 μM). **C)** Signal response of the reporter to theophylline concentration. **D)** Signal response to logarithm of theophylline concentration. The data are an average of two independent experiments.

#### 4.5.3 Creation of an aptamer reporter for TPP

To demonstrate that our novel sensing strategy is generalizable and can accommodate longer RNA aptamers, we chose the TPP aptamer as the second example. The TPP aptamer is 87 nt in length, and derived from a well-characterized riboswitch that is found in diverse organisms.<sup>[5b,20]</sup> The design of the TPP reporter was mostly based on

our findings from the theophylline reporter and used the same 20-nt FDNA sequence (all sequences presented in Figure 4-5A, aptamer domain in blue), as well as the optimized conditions for sensing (Figure S4-1). The only difference was the BDNA sequence required. By testing various BDNA lengths (10 to 15 nt), the BDNA length of 13 nt (BDNA13) was found to be optimal since the highest overall signal enhancement of ~3-fold was produced (red data set, Figure 4-5B), which is 2× higher than the enhancement from TPP addition alone (striped data set, Figure 4-5B).

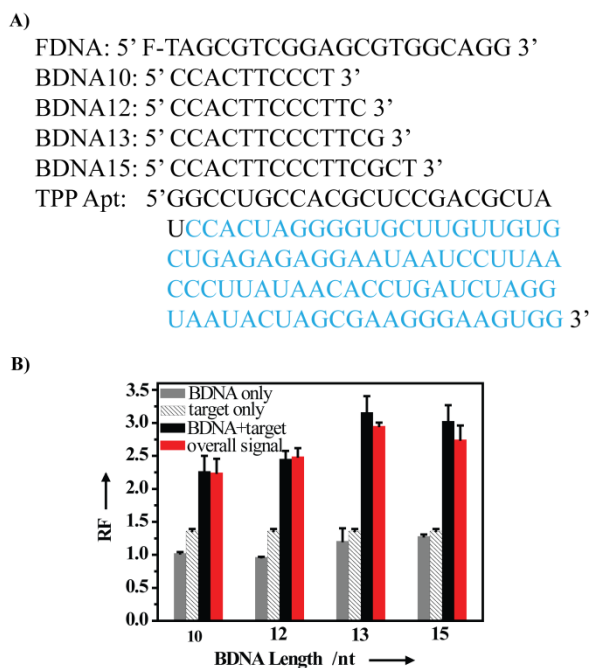


**Figure 4-5.** Creation of the TPP reporter. **A)** Sequences tested for the reporter (aptamer domain shown in blue). **B)** Optimization of BDNA length (nt). FDNA-RNA Aptamer-GO was incubated for 1 hr, then BDNA (gray, 400 nM), TPP target (striped, 100  $\mu$ M), or a combination of BDNA+target (black) was added. RF was plotted after 1 hr. Overall signal enhancement shown in red. The data are an average of two independent experiments.

#### 4.5.4 Sensing capability of TPP reporter

The TPP reporter could also detect TPP specifically, as the addition of structural derivatives thiamine monophosphate (TMP), thiamine, or oxythiamine generated low fluorescent levels, which were comparable to the sample treated with BDNA13 only (Figure 4-6A). Likewise, mutation of aptamer nucleotides that are known to be critical for TPP recognition, also abolished target binding as low fluorescence was generated (Figure 4-6A and sequence found in Figure S4-2B). The detection limit was determined to be 0.01  $\mu\text{M}$ , and the dynamic detection window was between 0.01 - 100  $\mu\text{M}$  (Figure 4-6B). The relative fluorescence observed at 1 hr versus TPP concentration is found in Figure 4-6 (panels C and D).

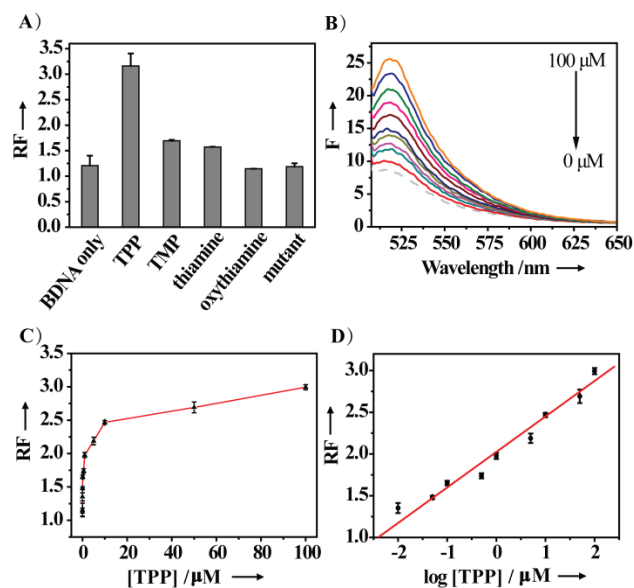


**Figure 4-6.** Sensing capability of the TPP reporter. **A)** Specificity test. FDNA-RNA Aptamer-GO was incubated for 1 hr, then BDNA13 (400 nM) was added, and finally TPP (100  $\mu\text{M}$ ), TMP (100  $\mu\text{M}$ ), thiamine (100  $\mu\text{M}$ ), oxythiamine (100  $\mu\text{M}$ ) or no addition (BDNA only) was introduced. Mutant aptamer was tested with TPP. RF was plotted after 1 hr. **B)** Fluorescence spectra of FDNA-RNA Aptamer-GO (dotted line), and after the addition of BDNA13 (400 nM) along with TPP (0, 0.01, 0.05, 0.1, 0.5, 1, 5, 10, 50, and

100  $\mu\text{M}$ ). **C)** Signal response of the reporter to TPP concentration. **D)** Signal response to logarithm of TPP concentration. The data are an average of two independent experiments.

## 4.6 Conclusions

In summary, we have demonstrated a generalizable strategy to create fluorescent sensors based on regulated GO adsorption that can accommodate RNA aptamers of various lengths. The sensing strategy makes use of the fluorescence quenching property of GO when it comes in contact with an FDNA-labelled RNA aptamer. The introduction of a BDNA sequence that forms a duplex with the 3' end of the aptamer provides a novel way to weaken aptamer-GO interaction. In effect, the addition of BDNA and target together can facilitate separation of the sensing system from GO and provide greater signal enhancement, compared to the existing, classical method of GO adsorption.

Using this strategy, sensors were created for both the relatively shorter theophylline aptamer, as well as the relatively longer TPP aptamer. Both reporters retained binding specificity and sensitivity that are characteristic of the original aptamers,<sup>[4a,20]</sup> and these results are consistent with previous studies.<sup>[5b,9]</sup>

For both reporters, BDNA incorporation substantially increased overall signal enhancement compared to the addition of target alone. The theophylline reporter produced an overall 14-fold signal enhancement, which is 9-fold greater enhancement than the addition of theophylline alone (Figure 4-3A). Similarly, the TPP reporter produced a 3-fold signal enhancement, which is 2 $\times$  greater than the addition of TPP alone

(Figure 4-5B). Notably, overall BDNA-mediated signal enhancement for the theophylline reporter is higher than for the TPP reporter. We speculate that FDNA-RNA Aptamer adsorption to GO is stronger for TPP aptamer than for the theophylline aptamer due to longer sequence length.<sup>[14]</sup> As a result, the overall signal enhancement for the TPP reporter is reduced possibly because more copies of FDNA-RNA aptamer are unable to switch off from GO, even after the addition of BDNA. To obtain higher signal enhancement particularly when using longer aptamers, implementation of fluorescent signal amplification strategies may be beneficial to generate higher fluorescence per aptamer-target binding interaction, or to facilitate a greater overall number of aptamer-target binding interactions. Several of these amplification strategies have already been demonstrated for graphene-based sensing using relatively short, model DNA aptamers.<sup>[13c,21]</sup> Future application of our generalizable strategy of regulated GO adsorption may lead to further exploration of less characterized aptamers. Furthermore, adaptation of this strategy towards previously reported studies using classic GO adsorption, may enhance the generality of these methods, which have been implemented for important applications such as the detection of multiple targets,<sup>[13f,22]</sup> and live cell analysis.<sup>[12c]</sup>

#### **4.7 Acknowledgements**

This work was supported by research grants from the Natural Sciences and Engineering Research Council of Canada (NSERC), and the Canadian Food Inspection Agency (CFIA).

## 4.8 References

- [1] a) A. D. Ellington, J. W. Szostak, *Nature* **1990**, *346*, 818; b) C. Tuerk, L. Gold, *Science* **1990**, *249*, 505.
- [2] a) R. Nutiu, Y. Li, *Chemistry* **2004**, *10*, 1868; b) R. Nutiu, Y. Li, *Methods* **2005**, *37*, 16.
- [3] a) A. Roth, R. R. Breaker, *Annu. Rev. Biochem.* **2009**, *78*, 305; b) B. J. Tucker, R. R. Breaker, *Curr. Opin. Struct. Biol.* **2005**, *15*, 342; c) M. Mandal, R. R. Breaker, *Nature Rev. Mol. Cell Biol.* **2004**, *5*, 451.
- [4] a) R. D. Jenison, S. C. Gill, A. Pardi, B. Polisky, *Science* **1994**, *263*, 1425; b) A. Geiger, P. Burgstaller, H. von der Eltz, A. Roeder, M. Famulok, *Nucleic Acids Res.* **1996**, *24*, 1029; c) D. S. Wilson, J. W. Szostak, *Annu. Rev. Biochem.* **1999**, *68*, 611.
- [5] a) R. Nutiu, Y. Li, *J. Am. Chem. Soc.* **2003**, *125*, 4771; b) P. S. Lau, B. K. Coombes, Y. Li, *Angew. Chem. Int. Ed.* **2010**, *49*, 7938.
- [6] a) D. Jellinek, L. S. Green, C. Bell, C. K. Lynott, N. Gill, C. Vargeese, G. Kirschenheuter, D. P. McGee, P. Abesinghe, W. A. Pieken, R. Shapiro, D. B. Rifkin, D. Moscatelli, N. Jankić, *Biochemistry* **1995**, *34*, 11363; b) Y. Lin, Q. Qiu, S. C. Gill, S. D. Jayasena, *Nucleic Acids Res.* **1994**, *22*, 5229; c) R. Kumar, S. K. Singh, A. A. Koshkin, V. K. Rajwanshi, M. Meldgaard, J. Wengel, *Bioorg. Med. Chem. Lett.* **1998**, *8*, 2219.
- [7] a) S. Klussmann, A. Nolte, R. Bald, V. A. Erdmann, J. P. Furste, *Nature Biotechnol.* **1996**, *14*, 1112; b) A. Nolte, S. Klussmann, R. Bald, V. A. Erdmann, J. P. Furste, *Nature Biotechnol.* **1996**, *14*, 1116.
- [8] C. Carrasquilla, P. S. Lau, Y. Li, J. D. Brennan, *J. Am. Chem. Soc.* **2012**, *134*, 10998.
- [9] P. S. Lau, C. K. Lai, Y. Li, *Chembiochem* **2013**, *14*, 987.
- [10] K. S. Novoselov, A. K. Geim, S. V. Morozov, D. Jiang, Y. Zhang, S. V. Dubonos, I. V. Grigorieva, A. A. Firsov, *Science* **2004**, *306*, 666.
- [11] a) Y. Liu, X. Dong, P. Chen, *Chem. Soc. Rev.* **2012**, *41*, 2283; b) P. S. Sharma, F. D'Souza, W. Kutner, *Top. Curr. Chem.* **2013**.
- [12] a) A. K. Geim, *Science* **2009**, *324*, 1530; b) Q. O. Zeng, J. S. Cheng, L. H. Tang, X. F. Liu, Y. Z. Liu, J. H. Li, J. H. Jiang, *Adv. Funct. Mater.* **2010**, *20*, 3366; c) Y. Wang, Z. Li, D. Hu, C. T. Lin, J. Li, Y. Lin, *J. Am. Chem. Soc.* **2010**, *132*, 9274; d) Y. Wang, J. Lu, L. Tang, H. Chang, J. Li, *Anal. Chem.* **2009**, *81*, 9710; e) Y. Wang, Y. M. Li, L. H. Tang, J. Lu, J. H. Li, *Electrochem. Commun.* **2009**, *11*, 889.
- [13] a) C. H. Lu, H. H. Yang, C. L. Zhu, X. Chen, G. N. Chen, *Angew. Chem. Int. Ed.* **2009**, *48*, 4785; b) H. Chang, L. Tang, Y. Wang, J. Jiang, J. Li, *Anal. Chem.* **2010**, *82*, 2341; c) Y. Pu, Z. Zhu, D. Han, H. Liu, J. Liu, J. Liao, K. Zhang, W. Tan, *Analyst* **2011**, *136*, 4138; d) Y. He, Z. G. Wang, H. W. Tang, D. W. Pang, *Biosens. Bioelectron.* **2011**, *29*, 76; e) L. Sheng, J. Ren, Y. Miao, J. Wang, E. Wang, *Biosens. Bioelectron.* **2011**, *26*, 3494; f) Y. Wang, Z. Li, T. J. Weber, D.

- Hu, C. T. Lin, J. Li, Y. Lin, *Anal. Chem.* **2013**, *85*, 6775; g) L. Cui, Z. Chen, Z. Zhu, X. Lin, X. Chen, C. J. Yang, *Anal. Chem.* **2013**, *85*, 2269.
- [14] a) S. Manohar, A. R. Mantz, K. E. Bancroft, C. Y. Hui, A. Jagota, D. V. Vezenov, *Nano Lett.* **2008**, *8*, 4365; b) S. J. Sowerby, C. A. Cohn, W. M. Heckl, N. G. Holm, *Proc. Natl. Acad. Sci. U. S. A.* **2001**, *98*, 820; c) S. J. Sowerby, C. M. Morth, N. G. Holm, *Astrobiology* **2001**, *1*, 481.
- [15] R. R. Breaker, in *The RNA World* (Eds.: R. F. Gesteland, T. R. Cech, J. F. Atkins), Cold Spring Harbor Laboratory Press, Cold Spring Harbor, New York, **2006**, pp. 89-107.
- [16] a) N. K. Navani, Y. Li, *Curr. Opin. Chem. Biol.* **2006**, *10*, 272; b) M. Famulok, G. Mayer, *Acc. Chem. Res.* **2011**, *44*, 1349; c) J. X. Wang, E. R. Lee, D. R. Morales, J. Lim, R. R. Breaker, *Mol. Cell* **2008**, *29*, 691.
- [17] M. Liu, Q. Zhang, H. Zhao, S. Chen, H. Yu, Y. Zhang, X. Quan, *Chem. Comm.* **2011**, *47*, 4084.
- [18] a) C. E. Estrada-Perez, Y. A. Hassan, S. C. Tan, *Rev. Sci. Instrum.* **2011**, *82*; b) X. L. Guan, X. Y. Liu, Z. X. Su, P. Liu, *React. Funct. Polym.* **2006**, *66*, 1227.
- [19] a) Y. Zhou, Q. L. Bao, L. A. L. Tang, Y. L. Zhong, K. P. Loh, *Chem. Mat.* **2009**, *21*, 2950; b) Y. W. Zhu, M. D. Stoller, W. W. Cai, A. Velamakanni, R. D. Piner, D. Chen, R. S. Ruoff, *ACS Nano* **2010**, *4*, 1227.
- [20] R. Welz, R. R. Breaker, *RNA* **2007**, *13*, 573.
- [21] a) C. Chen, J. Zhao, J. Jiang, R. Yu, *Talanta* **2012**, *101*, 357; b) P. Hu, C. Zhu, L. Jin, S. Dong, *Biosens. Bioelectron.* **2012**, *34*, 83; c) K. Hu, J. Liu, J. Chen, Y. Huang, S. Zhao, J. Tian, G. Zhang, *Biosens. Bioelectron.* **2013**, *42*, 598; d) J. Liu, C. Wang, Y. Jiang, Y. Hu, J. Li, S. Yang, Y. Li, R. Yang, W. Tan, C. Z. Huang, *Anal. Chem.* **2013**, *85*, 1424.
- [22] L. Wang, J. Zhu, L. Han, L. Jin, C. Zhu, E. Wang, S. Dong, *ACS Nano* **2012**, *6*, 6659.

## CHAPTER 5

### SECONDARY APPLICATION #1: STABILIZING STRUCTURE-SWITCHING SIGNALING RNA APTAMERS BY ENTRAPMENT IN SOL-GEL DERIVED MATERIALS FOR SOLID-PHASE ASSAYS

#### 5.1 Author's Preface

In the preceding chapters, we have already established general and versatile structure-switching strategies that demonstrate the ability of RNA aptamers to function as molecular recognition elements for sensor development. Our findings set up the basis for further exploration of RNA aptamer-based detection. Collaborations with other research groups have begun to explore secondary applications of structure-switching RNA aptamers. The remaining chapters of this thesis discuss these projects.

In collaboration with Dr. John Brennan's group, the first secondary application demonstrates successful entrapment of structure-switching RNA aptamers in sol-gel materials for solid-assay development. Importantly, this work demonstrates that sol-gel entrapment provides a general method to protect RNA aptamers against nucleases, and chemical instability.

This chapter has been published, and appears in its original format (see full citation below). As a co-author of this publication, I provided my expertise on structure-switching RNA aptamers by performing experiments to create the solution-based reporters, interpreting data, and preparing the manuscript. Carmen Carrasquilla performed

experiments pertaining to sol-gel entrapment, and took the principle role for project design, and manuscript writing. Dr. John Brennan and Dr. Yingfu Li provided guidance and helpful suggestions. Due to thesis space restrictions, full experimental details and supplementary information can be found online.

Carrasquilla C, Lau PS, Li Y, Brennan JD (2012) Stabilizing structure-switching signaling RNA aptamers by entrapment in sol-gel derived materials for solid-phase assays. *J Am Chem Soc* 134: 10998-11005.

## **5.2 Abstract**

Structure-switching, fluorescence-signaling DNA and RNA aptamers have been reported as highly versatile molecular recognition elements for biosensor development. While structure-switching DNA aptamers have been utilized for solid-phase sensing, equivalent RNA aptamers have yet to be successfully utilized in solid-phase sensors due to their lack of chemical stability and susceptibility to nuclease attack. In this study, we examined entrapment into sol-gel derived organic-inorganic composite materials as a platform for immobilization of structure-switching fluorescence-signaling RNA aptamer reporters, using both the synthetic theophylline- and naturally occurring thiamine pyrophosphate-binding RNA aptamers as test cases. Structure-switching versions of both aptamers were entrapped into a series of sol-gel derived composites, ranging from highly polar silica to hydrophobic methylsilsesquioxane-based materials, and the target-binding and signaling capabilities of these immobilized aptamers were assessed relative to solution. Both immobilized aptamers demonstrated sensitivity and selectivity similar to

that of free aptamers when entrapped in a composite material derived from 40% (v/v) methyltrimethoxysilane/tetramethoxysilane. This material also conferred protection from nuclease degradation and imparted long-term chemical stability to the RNA reporter systems. Given the versatility of sol-gel entrapment for development of biosensors, microarrays, bioaffinity columns and other devices, this entrapment method should provide a useful platform for numerous solid-phase RNA aptamer-based devices.

### 5.3 Introduction

Aptamers are single-stranded nucleic acids commonly generated through *in vitro* selection that can function as receptors for small molecules, proteins or even cells, due to their ability to fold into distinct three-dimensional structures<sup>1-3</sup> that possess specificity and affinity for their target ligands comparable to, if not surpassing, that of antibodies.<sup>4</sup> These features, combined with their chemical stability and ease of modification, have seen DNA aptamers emerge as promising biological recognition elements in analytical and diagnostic applications.<sup>5-9</sup> However, the limited range of analytes for DNA aptamers (with only 12 small-molecule and 9 protein targets as of 2009)<sup>10</sup> and the lack of known naturally-evolved DNA aptamers limit their potential for widespread use in sensing applications.

RNA aptamers, by contrast, can fold into more complex structures in order to provide a greater diversity of potential analytes as demonstrated by over 90 unique RNA aptamers for various small-molecule and protein targets.<sup>10-12</sup> Moreover, RNA aptamers have recently been derived from natural sources (i.e. riboswitches).<sup>13-15</sup> However, reports on

the use of RNA-based aptamers in solution or solid-phase biosensing applications are still relatively limited, mostly due to their inherent chemical instability<sup>16-18</sup> and susceptibility to nuclease attack,<sup>19</sup> combined with their lack of intrinsic signal-development capabilities. Several studies have focused on increasing the stability of functional RNA, usually by substituting the highly reactive hydroxyl group at the 2'-position of nucleotides containing pyrimidines, to make them nuclease-resistant.<sup>20-24</sup> However, chemical modification of RNA aptamers may alter their selectivity and binding affinity<sup>25</sup> without a significant increase in stability if the aptamer is purine rich. Studies involving *in vitro* selections using a combinatorial library with modified bases<sup>26</sup> or Spiegelmers<sup>27-29</sup> (mirror-image nucleotides) have generated families of aptamers with distinctly dissimilar minimal sequences compared to conventional RNA aptamers, providing completely different molecules and making these methods of limited use for unmodified RNA aptamers that are naturally-occurring or have already been selected in the past twenty years.

Recently, the Li group addressed the signaling ability of RNA aptamers by developing a structure-switching/fluorescence-signaling approach similar to that described previously for DNA aptamers.<sup>30</sup> The synthetic theophylline-binding aptamer (33 nt, 100 nM  $K_d$ )<sup>31</sup> and the naturally-occurring thiamine pyrophosphate (TPP)-binding aptamer (87 nt, 0.85 nM  $K_d$ )<sup>32</sup> were converted to reporter systems by designing complementary fluorophore-labeled DNA (FDNA) and quencher-labeled DNA (QDNA) strands to assemble a tripartite signalling duplex such that a conformational change from a RNA/DNA duplex to a RNA/target complex was coupled to a fluorescence-dequenching mechanism, generating a fluorescence signal upon target binding (secondary

structures found in online Supporting Information, Figure S1). While the structure-switching reporters retained the same specificity as the original aptamers, the affinities of both aptamers were observed to be 10-fold poorer than the original  $K_d$  values (1  $\mu\text{M}$  and 0.1  $\mu\text{M}$ , respectively), with maximal signal enhancements of ~6-fold and 3.5-fold for the theophylline-binding and TPP-binding aptamer, respectively.<sup>33</sup>

To extend the utility of signalling RNA aptamers for diagnostic applications, it is generally necessary to immobilize these species onto or within a suitable surface while maintaining chemical stability and structure-switching abilities.<sup>34</sup> At this time, very few studies have examined immobilized RNA aptamers for solid-phase biosensing devices,<sup>35-41</sup> and none have examined the immobilization of structure-switching signaling RNA aptamers. In this report, we investigate the use of a low temperature sol-gel process for entrapment of structure-switching RNA aptamers into porous silica and organosilane materials.<sup>42,43</sup> This simple immobilization process has been shown to be “biofriendly” and applicable to the entrapment of a variety of viable biomolecules,<sup>44-49</sup> including structure-switching DNA aptamers<sup>50</sup> and DNA enzymes,<sup>51</sup> suggesting that the method should be useful for the development of solid-phase RNA aptamer biosensors. However, the entrapment of functional RNA aptamers requires a material that can stabilize these labile molecules against degradation by both intramolecular transesterification and external nuclease attack. Therefore, structure-switching variants of both an *in vitro* selected RNA aptamer and a naturally-occurring aptamer were entrapped in a variety of sol-gel processed composite materials (polar, anionic, cationic, hydrophobic) and the leaching, stability, resistance to nuclease attack and signaling capabilities were evaluated

relative to these species in solution. The data clearly show that the optimal materials for entrapment of RNA aptamers are very different from those that stabilize proteins, and demonstrate the versatility of the sol-gel immobilization method to expand solid-phase sensing through the utilization of relatively unexplored RNA aptamer species.

## **5.4 Results and Discussion**

**5.4.1 Characterization of sol-gel derived materials.** Sol-gel derived materials were prepared from two previously reported biofriendly precursors (sodium silicate (SS) and diglyceryl silane (DGS) with and without 3-aminopropyltriethoxysilane (APTES) (to produce a cationic surface), along with tetramethylorthosilicate (TMOS) derived composites containing up to 80% methyltrimethoxysilane (MTMS) to produce a gradient of polarity, and methylsilsesquioxane (MSQ) materials derived from pure MTMS to examine whether aptamers could be entrapped into highly hydrophobic materials. Prior to performing studies focused on the leaching of tripartite RNA aptamers from the various sol-gel materials, the polarity (as judged by contact angle) and morphology of all materials were assessed. Table S1 (online Supporting Information) showed that all silica-based materials, with or without added APTES, had contact angles in the range of 16-28 degrees, indicative of highly polar, hydrophilic materials. Addition of MTMS caused a non-linear increase in contact angle, with only moderate increases in contact angle up to 40% MTMS (49 degrees), followed by a large increase in contact angle to 91 degrees at 60% MTMS and 120 degrees for MSQ, indicative of a highly hydrophobic material. The morphology of the materials was also highly dependent on composition, with high surface areas and nanometer scale pores, indicative of mesoporous materials, being observed up

to 60% MTMS, followed by a sudden change to low surface area macroporous materials at 80% MTMS and above (see scanning electron microscopy images of all materials in online Supporting Information, Table S2). These data show that the switchover from predominantly silica to predominantly MSQ-based materials resulted in a loss of mesopores and a tendency toward phase separation to generate macropores.<sup>42</sup>

**5.4.2 Leaching of aptamers from sol-gel derived materials.** The extent of leaching of the entrapped aptamer was evaluated for each material, as indicated in Figure 5-1. Leaching ranged from a low of ~5% in SS materials to ~30% in materials containing up to 80% MTMS, and then increased to 60-80% in pure MSQ materials, depending on the aptamer, demonstrating the general trend of increased leaching with increased hydrophobicity and increased pore size. Leaching was generally higher for the anti-TPP aptamer relative to the anti-theophylline aptamer, and typically occurred predominantly during the first washing step. The very large extent leaching in pure MSQ materials is likely reflective of the lack of mesopores, which would be expected to retain the small aptamers while macropores would not. The MSQ materials also are unlikely to be able to template around the RNA aptamers to aid in retention, as has been reported for some proteins entrapped in silica.<sup>51</sup>

The overall degree of leaching is relatively high compared proteins, but is similar to that of DNA aptamers entrapped in polar silica monoliths.<sup>50</sup> This previous study found that the attachment of a bulky streptavidin protein to biotinylated DNA, used to enlarge the molecular complex, did not improve leaching within error. Use of streptavidin would also be incompatible with the use of hydrophobic composites, and thus this strategy was

not examined in this study. Since fluorescence intensity measurements are used to determine the amount of leaching, the FDNA cannot be distinguished from the FDNA-aptamer complex. However, given that the FDNA is essential for signaling target binding in the tripartite design, measuring leaching of these short 20-nt oligonucleotide components is of equal importance for this reporter system.

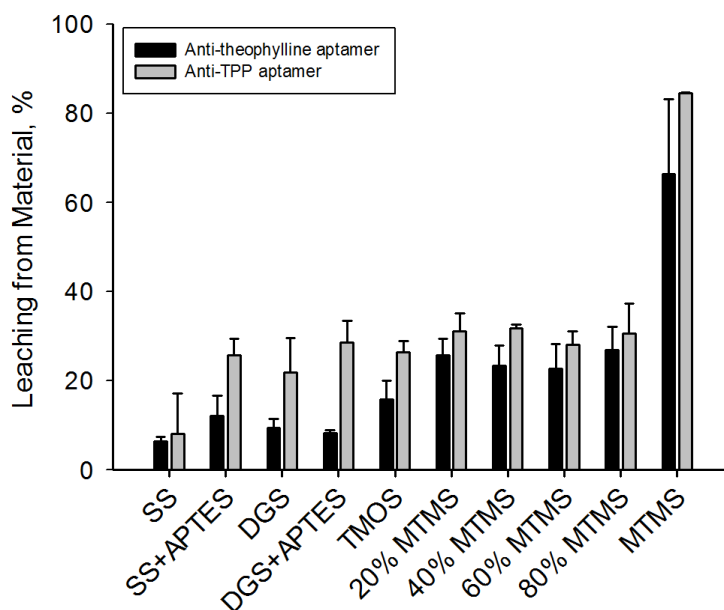


**Figure 5-1.** Leaching of the anti-theophylline and anti-TPP RNA aptamer reporter constructs from various sol-gel derived materials.

**5.4.3 Signal generation from entrapped RNA aptamer reporters.** A key requirement for entrapped structure-switching signaling aptamers is the ability to undergo conformational changes upon binding of ligands and to subsequently release the QDNA strand to elicit a fluorescence response. Experiments were performed to assess the degree of signal enhancement upon target binding for each RNA aptamer entrapped in the full series of sol-gel derived materials. All materials were first washed to remove leachable aptamers,

followed by addition of either 1 mM theophylline or 100  $\mu$ M TPP to the appropriate RNA reporter system. Figure 5-2 shows relative fluorescence enhancement and rate of signal development for each of the RNA aptamers when in solution and entrapped in the various sol-gel derived materials. Consistent with the previous findings,<sup>33</sup> full signal development required a longer time for the anti-TPP aptamer relative to the anti-theophylline aptamer, even in solution. When entrapped, both aptamer reporter systems were able to structure-switch and produce a fluorescence signal in all materials, however, the signal enhancements and rates of signal development were highly dependent on the type of sol-gel derived material used for entrapment.

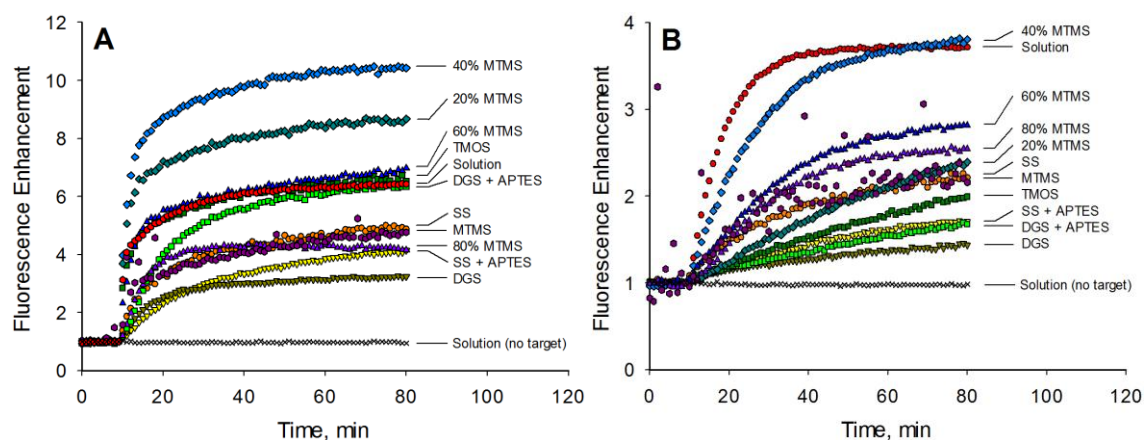


**Figure 5-2.** Fluorescence signaling ability of RNA aptamer reporters in solution and in various sol-gel derived materials. Target-induced response of the **A)** theophylline-binding aptamer and **B)** TPP-binding aptamer upon exposure to 1 mM theophylline and 100  $\mu$ M TPP, respectively, after 10 min baseline incubation.

Composite materials derived from mixtures of MTMS and TMOS always produced higher signal enhancements than polar silica materials (SS, DGS) or nonpolar MSQ materials. Previous studies have shown that only a small fraction ( $\sim$ 10%) of biomolecules

entrapped in polar materials are inaccessible to external analytes,<sup>50,52</sup> thus the loss of signal in polar materials likely reflects electrostatic aptamer backbone silica interactions that prevented structure switching of the aptamer. The high silica content of polar materials may also be detrimental to the chemical stability of RNA by promoting hydrolysis reactions, which cause cleavage of the phosphodiester linkages to degrade the aptamer.<sup>16</sup> DGS derived materials demonstrated the lowest enhancement for both aptamers, which is not surprising since it has been suggested that glycerol modifies electrostatic interactions between polynucleotides<sup>53</sup> and destabilizes double-stranded DNA.<sup>54</sup> Thus, this byproduct of DGS condensation, though proven as a stabilizer of proteins, appears to destabilize the doublestranded structure required for the intact RNA aptamer reporter complex, causing higher background fluorescence and a poorer signal enhancement. Interestingly, both reporters showed decreased signal enhancements when entrapped in SS+APTES (compared to SS materials) while the addition of APTES to DGS improved the signal generation, particularly for the antitheophylline aptamer. The inconsistent results related to the addition of APTES are not fully understood, but suggest that this species may be located in different environments in SS relative to DGS derived materials, or that the strength of its electrostatic effects differ in materials with varied porosity and pore size, as suggested by previous studies entrapping DNA in cationic hydrogels.<sup>55</sup> The low signal enhancement and high variability in pure MSQ materials is most likely due to the significant leaching of the reporters from this particular matrix. The best overall performance for both aptamers (highest signal enhancement and fastest signal development) was observed using an organic–inorganic hybrid material composed of

40% MTMS and 60% TMOS (v/v), suggesting that this material had the best balance of polarity and surface charge that minimized analyte- and/or RNA-surface interactions while retaining enough conformational flexibility to allow for structure-switching and signaling to occur. When compared to the signal enhancement obtained in solution, the entrapped theophylline-binding RNA generated a greater enhancement, up to 10-fold as compared to 6-fold in solution. The signal enhancement of the TPP-binding aptamer was comparable to that of the solution, with almost a 4-fold enhancement. The high signal enhancements observed for both aptamers using this material may also be due to alterations in the local pH of the microenvironment around the aptamers (see below) or restriction of RNA backbone mobility caused by entrapment in the pores of a partially hydrophobic composite matrix.

The physical restriction of RNA mobility appears to stabilize the secondary structure of the entrapped RNA aptamers, promoting FDNA/QDNA hybridization for a lower background signal and preventing sampling of in-line geometries that induce intramolecular cleavage.<sup>18</sup> These effects would be more evident using the smaller theophylline-binding aptamer, which has a larger amount of its sequence hybridized to DNA and a shorter flexible single-stranded region that is less likely to sample conformations susceptible to spontaneous cleavage, producing the significant improvement in signaling that was observed for this particular aptamer.

**5.4.4 Sensitivity and selectivity of entrapped RNA aptamer reporters.** Figures 5-3A and 5-3B show the target concentration-dependent signal enhancements of the anti-theophylline and anti-TPP aptamers, respectively, when entrapped in the 40% MTMS

material and in solution. The anti-theophylline RNA reporter demonstrated a similar detection limit and dynamic range to that reported in solution (1-1000  $\mu\text{M}$ ) while the anti-TPP aptamer had a detection limit of 1  $\mu\text{M}$ , which was 10-fold worse than the value in solution, and an upper concentration range of 100  $\mu\text{M}$ , which was similar to the value in solution.<sup>33</sup> The poorer detection limit may be due to the exclusion of the anionic TPP from the hydrophobic matrix, which would require a higher external concentration to reach a sufficient internal concentration to produce signalling. Interestingly, the use of initial rate data provided a broader dynamic range for TPP sensing while maintaining the detection limit of 1  $\mu\text{M}$  (Figure 5-3B, inset).

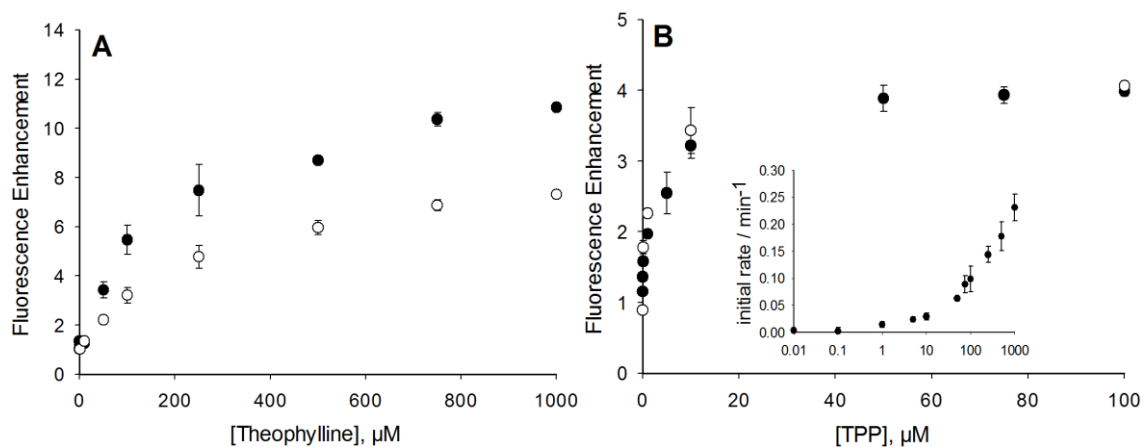


**Figure 5-3.** Sensitivity of the sol-gel entrapped RNA aptamer reporters. Response curve of the **A)** theophylline-binding aptamer to increasing theophylline concentrations and **B)** TPP-binding aptamer to increasing TPP concentrations, either entrapped in the 40% MTMS material (●) or in solution (○). Inset B): Change in initial signaling rate of the entrapped TPP-binding aptamer when exposed to increasing TPP concentrations.

The selectivity of entrapped RNA reporters was assessed using molecules that were chemically similar to their targets. These included caffeine and theobromine for the theophylline-binding aptamer and thiamine monophosphate (TMP), thiamine and

oxythiamine for the TPP-binding aptamer. Mutant versions of each RNA aptamer were also entrapped and subjected to either theophylline or TPP at concentrations of 1 mM and 100  $\mu$ M, respectively. Selectivity was maintained for both entrapped aptamer reporters, with little to no change in responses when using structural derivatives of targets or mutant constructs (online Supporting Information, Figure S2).

**5.4.5 RNA aptamer sensitivity to ribonucleases.** Previous studies have shown that entrapping DNA aptamers within a polyacrylamide hydrogel<sup>56</sup> or silica matrix<sup>50</sup> can provide a steric barrier to digestive enzymes, such as DNase I. To assess the protective effects of entrapment in MTMS/TMOS composites on the RNA reporters, the stability of free (solution) and entrapped aptamers toward digestion by two different ribonucleases was compared. RNase A was chosen since it is abundant in biological fluids and is pyrimidine-specific,<sup>57</sup> while RNase H is known to degrade the RNA from RNA/DNA hybrids<sup>58</sup> such as the tripartite reporter complex in this work. Degradation by either ribonuclease can be monitored by an increase in fluorescence as the distance between the fluorescein and dabcyll moieties increases due to release of the QDNA, FDNA or both from the digested RNA aptamer strand. As shown in Figure 5-4, the addition of RNase A or RNase H to either RNA aptamer reporter in solution resulted in an increase in fluorescence of greater than 20-fold and 4-fold, respectively. In the case of the aptamers entrapped in the 40% MTMS sol-gel derived material, less than 4-fold and 2-fold fluorescence enhancements were observed upon addition of RNase A or RNase H, respectively. These results indicate that both ribonucleases are unable to enter the material and access the entrapped RNA aptamers, producing 80% less digestion with

RNase A and 70% less digestion when using RNase H. The small amount of degradation is likely due to the digestion of aptamer molecules that reside very close to the surface of the small silica disks (less than 1 mm thickness). These thin monoliths have a much higher surface area-to-volume ratio than typical large bulk monoliths, but are more representative of a biosensor design that uses thin films to minimize target diffusion time. Overall, these results indicate that the majority of the entrapped RNA was not accessible to the RNase enzymes and thus was well-protected from digestion when entrapped in the mesoporous matrix.

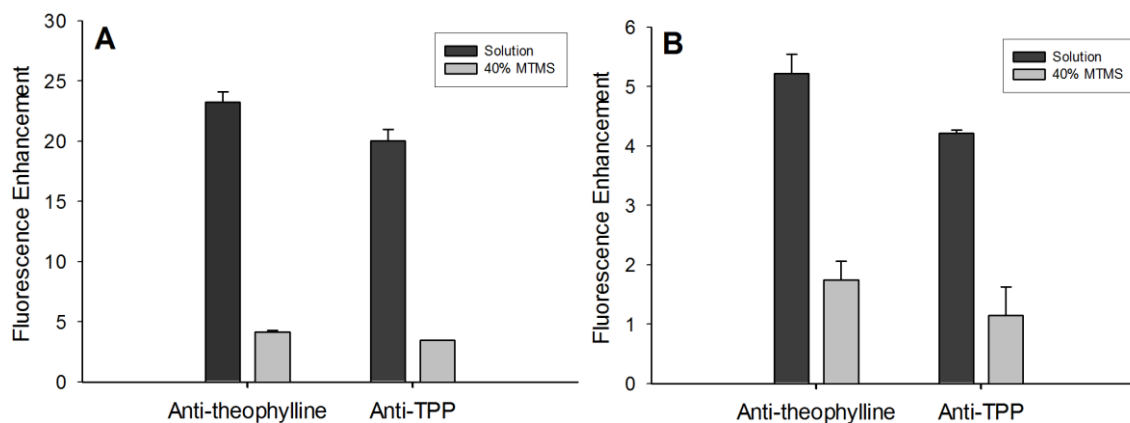


**Figure 5-4.** Changes in emission intensity of RNA aptamer reporters upon exposure to RNase A or RNase H. Fluorescence measurements 2 hrs after addition of 3 units of **A)** RNase A or **B)** RNase H to the theophylline-binding and TPP-binding reporter constructs in solution or entrapped within the sol-gel derived material.

**5.4.6 Effects of long-term storage on RNA aptamer activity.** The long-term stability of the RNA reporters was examined when entrapped in the 40% MTMS material and compared to RNA reporters in solution. Figure 5-5 demonstrates that when in solution, the activity of the theophylline-binding aptamer after 1 week is similar to the level in a

freshly prepared solution, while that of the 1 week old TPP-binding aptamer is almost half the original activity. This is consistent with the hypothesis that the larger anti-TPP aptamer undergoes greater intrinsic cleavage due to in-line nucleophilic attack. However, after 1 month of storage in solution, both RNA aptamer reporters show relatively low signal enhancements upon target addition with about 2-fold increase for the anti-theophylline aptamer and 1.5-fold enhancement with the anti-TPP aptamer. This loss in signal is due to higher fluorescence backgrounds as the RNA is degraded over time, causing release of the fluorescent moiety from its close interaction with the quencher prior to introduction of the target.

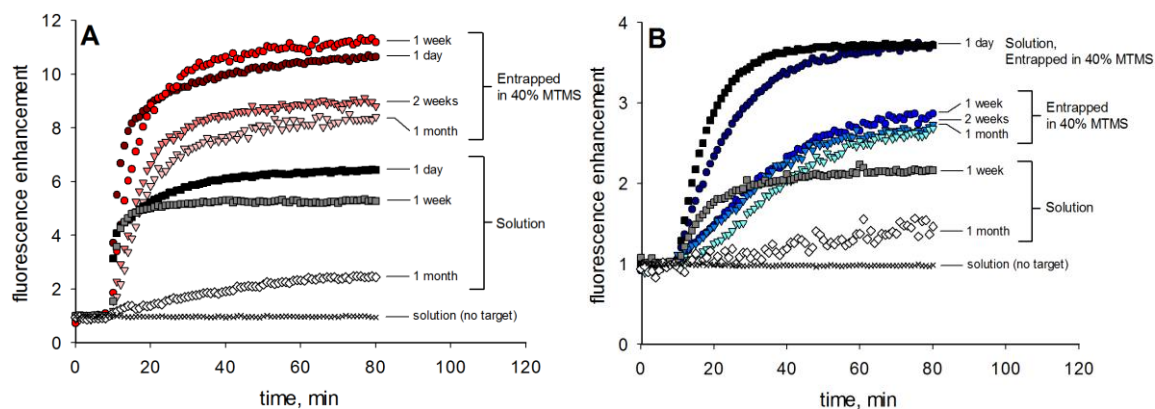


**Figure 5-5.** Structure-switching and signaling ability of RNA aptamer reporters after different storage time. Target-induced fluorescence signaling ability of solution-based or entrapped RNA aptamer reporters after increasing storage time at 4 °C of the **A)** theophylline-binding aptamer using 1mM theophylline and **B)** TPP-binding aptamer using 100  $\mu$ M TPP, after 10 min baseline incubation.

When the aptamers were entrapped in the 40% MTMS/60% TMOS derived material and then stored up to 1 month, the signal enhancements were maintained above 8-fold and 2.5-fold for the theophylline-binding and TPP-binding aptamers, respectively. The observed loss of activity (~20–30%) likely reflects continued evolution of the

sol–gel matrix, which could lead to pore shrinkage and subsequent restriction of dynamic motion or restriction of access of analytes to the entrapped RNA<sup>42,59</sup> (currently under investigation). Initial fluorescence levels of all aged materials (1 week to 1 month) were slightly lower than those of newly prepared composites, indicating that the entrapped aptamers were not being degraded upon storage, although further leaching of surface-proximal RNA during the longer storage periods may have contributed to the observed loss in activity (fluorescence intensity values provided in Table S3 of Online Supporting Information). The ability to remove leached FDNA or degraded aptamer as a means of lowering background signals highlights another benefit of entrapment over solutionbased studies. In general, although the signal enhancements of both aptamers are slightly reduced over the first 1–2 weeks, the signaling ability is maintained over an extended storage time, highlighting the ability of the matrix to protect the RNA aptamers from both intrinsic chemical instability and external enzymatic degradation, and leading to a more robust solidphase sensor.

The origin of the enhanced chemical stability is not fully understood at this time. However, it is well-known that under neutral or alkaline pH conditions (in the presence of alkali metals and alkali-earth metals), the dominant pathway for RNA chemical degradation is the internal phosphoester transfer reaction via an SN2 mechanism wherein the 2'-oxygen attacks the adjacent phosphorus center.<sup>16</sup> The protonation state of the 2'-oxygen largely dictates this rate of transesterification, which is enhanced by specific base catalysis through deprotonation of the 2'-hydroxyl group to the more nucleophilic 2'-oxyanion group.<sup>17</sup> Thus, in solution, exposure to hydroxide ions increases the fraction of

these reactive 2'-oxyanion groups to promote RNA cleavage. However, when entrapped in a relatively hydrophobic sol-gel derived matrix, the RNA species interacts with only a few hydroxide ions present in the thin solution layer between the biomolecule and the material surface,<sup>60</sup> effectively decreasing the hydroxide-dependent degradation rate. Moreover, previous studies<sup>61</sup> have shown that the apparent pKa of pH sensitive dyes increases when entrapped in organic-inorganic composites, demonstrating that the effective pH within the composites is less basic than in the surrounding solution (i.e., a probe with a pKa of 6.0 in solution has an apparent pKa of 8.3 in materials composed of MTES/TEOS). Additional studies are currently underway to further examine the specific effects of entrapment in inorganic materials that chemically stabilize RNA.

## 5.5 Conclusions

A simple and general approach for improving the stability of RNA aptamers is demonstrated based on their entrapment in a sol-gel derived composite material. Two different RNA aptamer reporters retained maximum sensitivity and selectivity when entrapped in an organic-inorganic composite material prepared by cohydrolysis and condensation of 40% MTMS and 60% TMOS (v/v). Since the RNA reporter system was entrapped in the pores of the sol-gel derived matrix, it was relatively well protected from nuclease degradation and, perhaps more importantly, the composite material also reduced the extent of in-line chemical degradation, providing the longterm stability required of a robust biosensor. As such, this immobilization scheme expands the use of functional

nucleic acids from the limited number of DNA aptamers to the much broader range of relatively unexplored RNA aptamer species.

Importantly, sol-gel derived materials possess significant versatility in that they are amenable to many configurations, including microarrays, bioaffinity columns or thin-film coatings for interfacing to various analytical devices.<sup>43,62</sup> Although the current study focuses on fluorescence signaling in monolithic materials, the use of the sol-gel method for biomolecular entrapment has been utilized in both colorimetric and electrochemical sensors<sup>63</sup> and thus presents a broadly applicable platform for preparing solid-phase RNA aptamer sensors. Such biosensors may find wide appeal in environmental and clinical analysis, particularly for the detection of small metabolites, an area where elicitation of monoclonal antibodies is difficult.

## 5.6 References

- (1) Wilson, D. S.; Szostak, J. W. *Annu. Rev. Biochem.* **1999**, *68*, 611-647.
- (2) Ellington, A. D.; Szostak, J. W. *Nature* **1990**, *346*, 818-822.
- (3) Tuerk, C.; Gold, L. *Science* **1990**, *249*, 505-510.
- (4) Jayasena, S. D. *Clin. Chem.* **1999**, *45*, 1628-1650.
- (5) Clark, S. L.; Remcho, V. T. *Electrophoresis* **2002**, *23*, 1335-1340.
- (6) Hamula, C. L. A.; Guthrie, J. W.; Zhang, H.; Li, X.-F.; Le, X. C. *TrAC-Trends Anal. Chem.* **2006**, *25*, 681-691.
- (7) Song, S. P.; Wang, L. H.; Li, J.; Zhao, J. L.; Fan, C. H. *TrAC-Trends Anal. Chem.* **2008**, *27*, 108-117.
- (8) Sefah, K.; Phillips, J. A.; Xiong, X.; Meng, L.; Van Simaey, D.; Chen, H.; Martin, J.; Tan, W. *Analyst* **2009**, *134*, 1765-1775.
- (9) Liu, J.; Cao, Z.; Lu, Y. *Chem. Rev.* **2009**, *109*, 1948-1998.
- (10) Silverman, S. K. In *Functional Nucleic Acids for Analytical Applications*; Li, Y., Yi, L., Eds.; Springer New York: 2009, p 47-108.
- (11) Klug, S. J.; Famulok, M. *Mol. Biol. Rep.* **1994**, *20*, 97-107.
- (12) Marshall, K. A.; Ellington, A. D. *Methods Enzymol.* **2000**, *318*, 193-214.
- (13) Winkler, W. C.; Breaker, R. R. *ChemBiochem* **2003**, *4*, 1024-1032.
- (14) Mandal, M.; Breaker, R. R. *Nat. Rev. Mol. Cell Biol.* **2004**, *5*, 451-463.
- (15) Montange, R. K.; Batey, R. T. *Annu. Rev. Biophys.* **2008**, *37*, 117-133.

- (16) Oivanen, M.; Kuusela, S.; Lonnberg, H. *Chem. Rev.* **1998**, *98*, 961-990.
- (17) Li, Y.; Breaker, R. R. *J. Am. Chem. Soc.* **1999**, *121*, 5364-5372.
- (18) Soukup, G. A.; Breaker, R. R. *RNA* **1999**, *5*, 1308-1325.
- (19) Famulok, M.; Mayer, G.; Blind, M. *Acc. Chem. Res.* **2000**, *33*, 591-599.
- (20) Pieken, W. A.; Olsen, D. B.; Benseler, F.; Aurup, H.; Eckstein, F. *Science* **1991**, *253*, 314-317.
- (21) Cummins, L. L.; Owens, S. R.; Risen, L. M.; Lesnik, E. A.; Freier, S. M.; McGee, D.; Guinosso, C. J.; Cook, P. D. *Nucleic Acids Res.* **1995**, *23*, 2019-2024.
- (22) Kubik, M. F.; Bell, C.; Fitzwater, T.; Watson, S. R.; Tasset, D. M. *J. Immunol.* **1997**, *159*, 259-267.
- (23) Kujau, M. J.; Wolfl, S. *Nucleic Acids Res.* **1998**, *26*, 1851-1853.
- (24) Kusser, W. *J. Biotechnol.* **2000**, *74*, 27-38.
- (25) Jellinek, D.; Green, L. S.; Bell, C.; Lynott, C. K.; Gill, N.; Vargeese, C.; Kirschenheuter, G.; McGee, D. P.; Abesinghe, P.; Pieken, W. A. *Biochemistry* **1995**, *34*, 11363-11372.
- (26) Burmeister, P. E.; Lewis, S. D.; Silva, R. F.; Preiss, J. R.; Horwitz, L. R.; Pendergrast, P. S.; McCauley, T. G.; Kurz, J. C.; Epstein, D. M.; Wilson, C.; Keefe, A. D. *Chem. Biol.* **2005**, *12*, 25-33.
- (27) Klussmann, S.; Nolte, A.; Bald, R.; Erdmann, V. A.; Furste, J. P. *Nat. Biotechnol.* **1996**, *14*, 1112-1115.
- (28) Leva, S.; Lichte, A.; Burmeister, J.; Muhn, P.; Jahnke, B.; Fesser, D.; Erfurth, J.; Burgstaller, P.; Klussmann, S. *Chem. Biol.* **2002**, *9*, 351-359.
- (29) Eulberg, D.; Klussmann, S. *ChemBioChem* **2003**, *4*, 979-983.
- (30) Nutiu, R.; Li, Y. *J. Am. Chem. Soc.* **2003**, *125*, 4771-4778.
- (31) Jenison, R. D.; Gill, S. C.; Pardi, A.; Polisky, B. *Science* **1994**, *263*, 1425-1429.
- (32) Welz, R.; Breaker, R. R. *RNA* **2007**, *13*, 573-582.
- (33) Lau, P. S.; Coombes, B. K.; Li, Y. *Angew. Chem. Int. Ed.* **2010**, *49*, 7938-7942.
- (34) Potyrailo, R. A.; Conrad, R. C.; Ellington, A. D.; Hieftje, G. M. *Anal. Chem.* **1998**, *70*, 3419-3425.
- (35) Clark, S. L.; Remcho, V. T. *Anal. Chem.* **2003**, *75*, 5692-5696.
- (36) McCauley, T. G.; Hamaguchi, N.; Stanton, M. *Anal. Biochem.* **2003**, *319*, 244-250.
- (37) Minunni, M.; Tombelli, S.; Gullotto, A.; Luzi, E.; Mascini, M. *Biosens. Bioelectron.* **2004**, *20*, 1149-1156.
- (38) Cho, E. J.; Collett, J. R.; Szafranska, A. E.; Ellington, A. D. *Anal. Chim. Acta* **2006**, *564*, 82-90.
- (39) Min, K.; Cho, M.; Han, S. Y.; Shim, Y. B.; Ku, J.; Ban, C. *Biosens. Bioelectron.* **2008**, *23*, 1819-1824.
- (40) Lee, H. S.; Kim, K. S.; Kim, C. J.; Hahn, S. K.; Jo, M. H. *Biosens. Bioelectron.* **2009**, *24*, 1801-1805.
- (41) Ferapontova, E. E.; Olsen, E. M.; Gothelf, K. V. *J. Am. Chem. Soc.* **2008**, *130*, 4256-4258.
- (42) Brinker, C. J.; Scherer, G. W. *Sol-Gel Science*; Academic Press: New York, 1990.
- (43) Brennan, J. D. *Acc. Chem. Res.* **2007**, *40*, 827-835.

- (44) O'Driscoll, K. F. *Methods Enzymol.* **1976**, *44*, 169-183.
- (45) Avnir, D.; Braun, S.; Lev, O.; Ottolenghi, M. *Chem. Mater.* **1994**, *6*, 1605-1614.
- (46) Braun, S.; Rappoport, S.; Zusman, R.; Avnir, D.; Ottolenghi, M. *Mater. Let.* **1990**, *10*, 1- 5.
- (47) Bhatia, R. B.; Brinker, C. J.; Gupta, A. K.; Singh, A. K. *Chem. Mater.* **2000**, *12*, 2434- 2441.
- (48) Jin, W.; Brennan, J. D. *Anal. Chim. Acta* **2002**, *461*, 1-36.
- (49) Pierre, A. C. *Biocatal. Biotransform.* **2004**, *22*, 145-170.
- (50) Rupcich, N.; Nutiu, R.; Li, Y.; Brennan, J. D. *Anal. Chem.* **2005**, *77*, 4300-4307.
- (51) Shen, Y. T.; Mackey, G.; Rupcich, N.; Gloster, D.; Chiuman, W.; Li, Y. F.; Brennan, J. D. *Anal. Chem.* **2007**, *79*, 3494-3503.
- (52) Sui, X.; Cruz-Aguado, J. A.; Chen, Y.; Zhang, Z.; Brook, M. A.; Brennan, J. D. *Chem. Mater.* **2005**, *17*, 1174-1182.
- (53) Del Vecchio, P.; Esposito, D.; Ricchi, L.; Barone, G. *Int. J. Biol. Macromol.* **1999**, *24*, 361-369.
- (54) Bonner, G.; Klibanov, A. M. *Biotechnol. Bioeng.* **2000**, *68*, 339-344.
- (55) Joseph, K. A.; Dave, N.; Liu, J. *ACS Appl. Mater. Interfaces* **2011**, *3*, 733-739.
- (56) Dave, N.; Chan, M. Y.; Huang, P.-J. J.; Smith, B. D.; Liu, J. *J. Am. Chem. Soc.* **2010**, *132*, 12668-12673.
- (57) Raines, R. T. *Chem. Rev.* **1998**, *98*, 1045-1066.
- (58) Donis-Keller, H. *Nucleic Acids Res.* **1979**, *7*, 179-192.
- (59) Keeling-Tucker, T.; Brennan, J. D. *Chem. Mater.* **2001**, *13*, 3331-3350.
- (60) Frenkel-Mullerad, H.; Avnir, D. *J. Am. Chem. Soc.* **2005**, *127*, 8077-8081.
- (61) Gulcev, M. D.; Goring, G. L. G.; Rakic, M.; Brennan, J. D. *Anal. Chim. Acta* **2002**, *457*, 47-59.
- (62) Monton, M. R. N.; Forsberg, E. M.; Brennan, J. D. *Chem. Mater.* **2011**, *24*, 796-811.
- (63) Avnir, D.; Coradin, T.; Lev, O.; Livage, J. *J. Mater. Chem.* **2006**, *16*, 1013-1030.
- (64) Brook, M. A.; Chen, Y.; Guo, K.; Zhang, Z.; Brennan, J. D. *J. Mater. Chem.* **2004**, *14*, 1469-1479.
- (65) Brook, M. A.; Chen, Y.; Guo, K.; Zhang, Z.; Jin, W.; Deisingh, A.; Cruz-Aguado, J.; Brennan, J. D. *J. Sol-Gel Sci. Technol.* **2004**, *31*, 343-348.
- (66) Carrasquilla, C.; Li, Y.; Brennan, J. D. *Anal. Chem.* **2011**, *83*, 957-965.
- (67) Besanger, T. R.; Hodgson, R. J.; Guillon, D.; Brennan, J. D. *Anal. Chim. Acta* **2006**, *561*, 107-118.

## CHAPTER 6

### SECONDARY APPLICATION #2: SYNTHESIS AND EVALUATION OF GLUCOSAMINE-6-PHOSPHATE ANALOGUES AS ACTIVATORS OF GLMS RIBOSWITCH

#### 6.1 Author's Preface

In collaboration with Dr. Xin-Shan Ye's group, the *glmS* ribozyme, a natural structure-switching RNA aptamer found in numerous Gram-positive bacteria has been further explored as a potential drug target for antibiotic development. Chemical synthesis of different metabolite analogues has resulted in one particular analogue that may be a potential lead for drug design.

This chapter has been published, and appears in its original format (see full citation below). As a co-author of this publication, I provided my expertise on structure-switching RNA aptamers by performing experiments to test the effect of the synthetic analogues on *glmS* ribozyme, interpreting data, and preparing the manuscript. Guan-Nan Wang performed experiments to organically synthesize the analogues, and took the principle role for project design, and manuscript writing. Dr. Xin-Shan Ye and Dr. Yingfu Li provided guidance and helpful suggestions. Due to thesis space restrictions, full experimental details and supplementary information can be found online.

Wang GN, Lau PS, Li Y, Ye XS (2012) Synthesis of evaluation of glucosamine-6-phosphate analogues as activators of *glmS* riboswitch. *Tetrahedron* 68: 9405-9412.

## 6.2 Abstract:

The *glmS* riboswitch is a ribozyme found in numerous Gram-positive bacteria and responds to the cellular concentrations of glucosamine 6-phosphate (GlcN6P). Given the importance of GlcN6P for cell wall biosynthesis, the *glmS* riboswitch has become a new drug target for the development of antibiotics. Herein, we describe the efficient synthesis of three GlcN6P analogues and their evaluation on inducing self-cleavage of the *glmS* riboswitch from *B. subtilis*. Our results provide valuable information for further elucidation of the structure-activity relationships and drug design for *glmS* riboswitch antibiotics.

## 6.3 Introduction

Riboswitches are structural mRNA domains that regulate gene expression in response to the intracellular concentration of specific metabolites. They control essential genes in many pathogenic bacteria, thus representing an intriguing class of RNA target for the development of antibiotics and chemical-biological tools.<sup>1-3</sup> Notably, the *glmS* riboswitch, which is located upstream of the gene encoding glucosamine-6-phosphate synthase (GlmS) in numerous Gram-positive bacteria, is unique in that it is the first example of a natural ribozyme that is also a riboswitch.<sup>4</sup> As part of gene regulation, it binds to its small molecule metabolite, glucosamine-6-phosphate (GlcN6P), which triggers self-cleavage targeting its own mRNA.<sup>5,6</sup> Functionally, the *glmS* ribozyme controls the amount of GlmS to regulate cellular production of GlcN6P,<sup>4,7</sup> which is an essential metabolite for the biosynthesis of bacterial cell walls and fungal cell wall

chitin.<sup>8-11</sup> Given the importance of GlcN6P, inhibition of the metabolite is lethal to microorganisms. Consequently, the *glmS* riboswitch is emerging as a new drug target, and small molecules that mimic GlcN6P to trigger riboswitch activity have the potential to become antibiotics.

Although substantial structural and mechanistic information of the *glmS* riboswitch have been disclosed over recent years,<sup>5,6,12-15</sup> few small molecule agonists and antagonists have been developed.<sup>16,17</sup> Activators that have comparable or superior activity than natural GlcN6P are in great demand for a better understanding of the riboswitch and pave the way to the discovery of effective antibiotics. In this research, three GlcN6P analogues have been designed and synthesized (Figure 6-1). Carba-sugar **1** was designed to address the role of the oxygen atom in pyranose ring for riboswitch activation. Compounds **2** and **3** were designed to add an extra hydroxyl group at the C-6 position with the consideration of providing extra binding sites around the pocket. Instead of 6-phosphate, the 6-phosphonate was introduced to the 6-position. It is known that the P–C bond makes compounds resistant to enzymatic hydrolysis<sup>18,19</sup> and has conformational preferences different from those in phosphates.<sup>20</sup> These analogues were subsequently investigated for their ability to induce self-cleavage of the *glmS* riboswitch from *B. subtilis*.

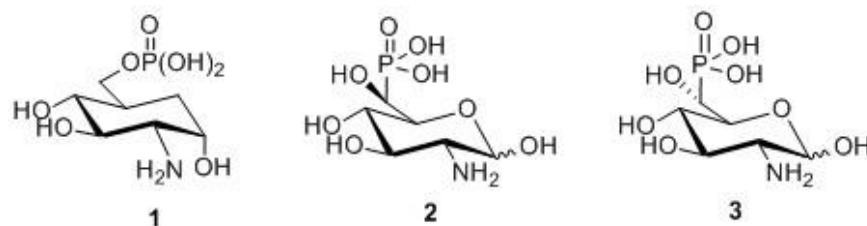
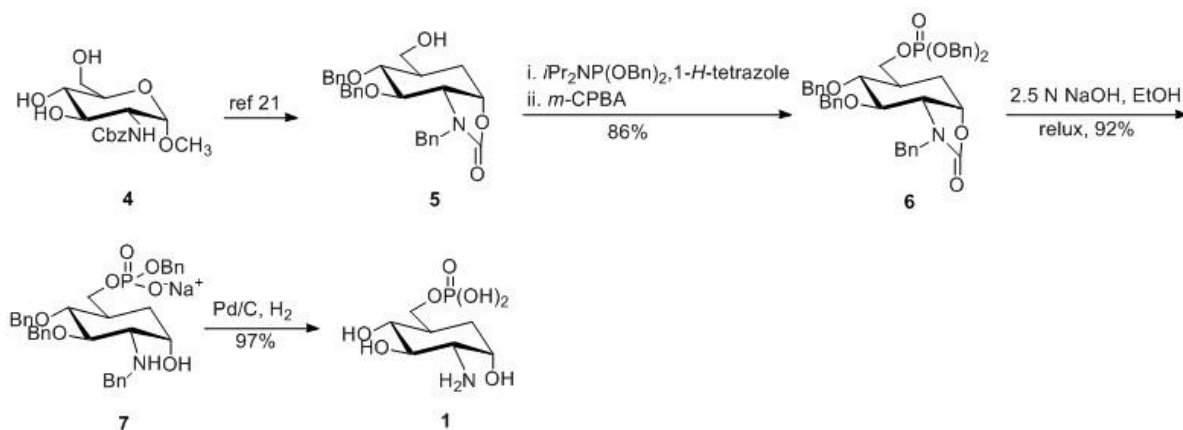


**Figure 6-1.** The structures of three GlcN6P analogues

## 6.4 Results and Discussion

The synthesis of carba-sugar **1** is shown in Scheme 6-1. Carbocyclic compound **5** was prepared from methyl glucopyranoside **4** according to the procedures described by Barton *et al.*<sup>21</sup> Compound **5** was treated with dibenzyl *N,N*-diisopropylphosphoramidite, followed by oxidation with *meta*-chloroperoxybenzoic acid (*m*-CPBA) to give the fully protected phosphate **6** in 86% isolated yield. The chemical shift of compound **6** in <sup>31</sup>P NMR spectroscopy is at  $\delta$  3.14, indicating the formation of phosphate.<sup>22</sup> Subsequently, basic opening of the oxazolidinone in **6** also resulted in the removal of one of the benzyl groups on phosphate, yielding compound **7**. Catalytic hydrogenolysis of **7** provided the phosphorylated carba-sugar **1** smoothly.

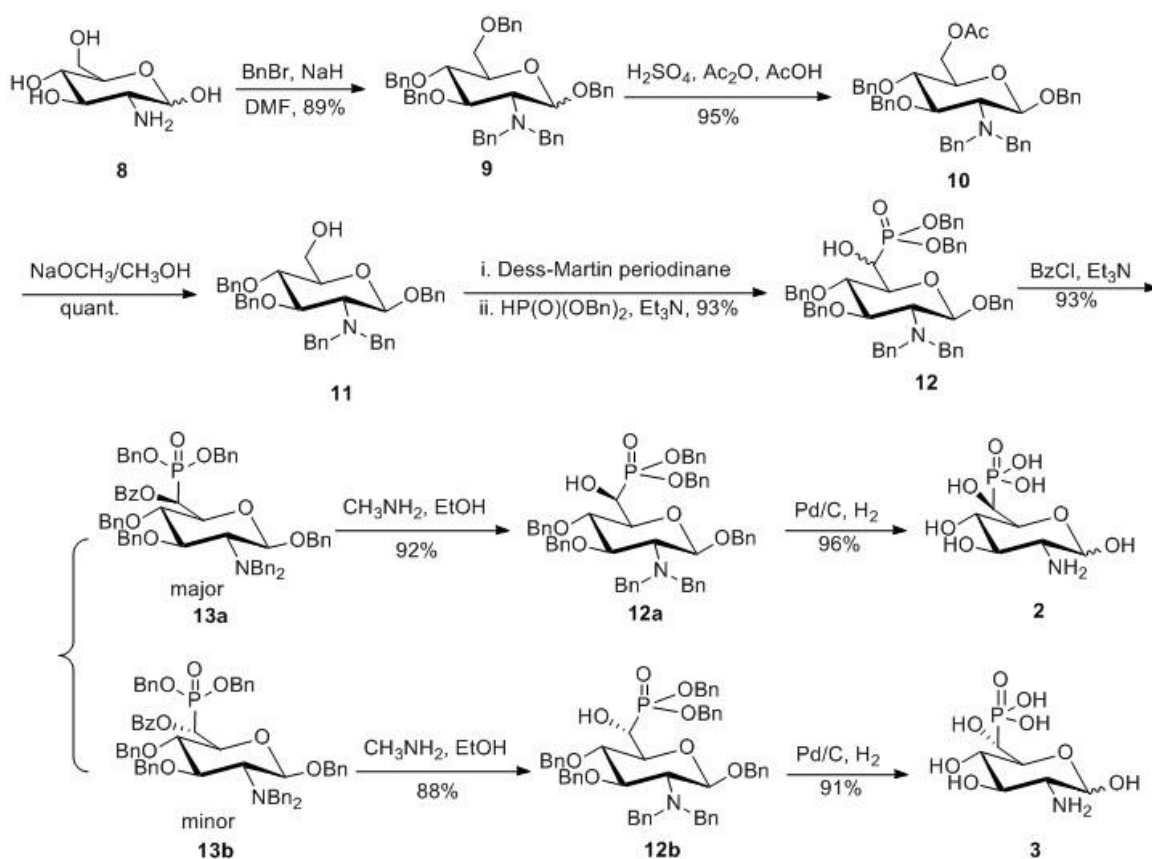


**Scheme 6-1.** Synthesis of carba-sugar **1**

The synthesis of compounds **2** and **3** started from glucosamine **8**. As shown in Scheme 6-2, perbenzylation of **8** provided compound **9**, and selective acetolysis of **9** afforded the 6-acetylated compound **10** in good yield. It was reported that the anomeric

position is usually acetylated prior to the 6-position in substrates such as perbenzylated glucose, galactose and mannose.<sup>23,24</sup> However, in the case of compound **9**, the dibenzylated amino group protected the anomeric position from acetolysis. Removal of the acetyl group in **10** led to compound **11**, which was oxidized by Dess-Martin periodinane followed by the Pudovik reaction<sup>25,26</sup> with dibenzyl phosphonate and triethylamine to yield the  $\alpha$ -hydroxyphosphonate **12** in 93% isolated yield as an inseparable mixture of diastereoisomers (3:1). The separation of two diastereoisomers was achieved after benzylation of the nascent hydroxyl groups. Deprotection of the benzoyl groups with methylamine solution, which was followed by deprotection of the benzyl groups using catalytic hydrogenolysis, afforded the target compounds **2** and **3** in good yields, respectively.

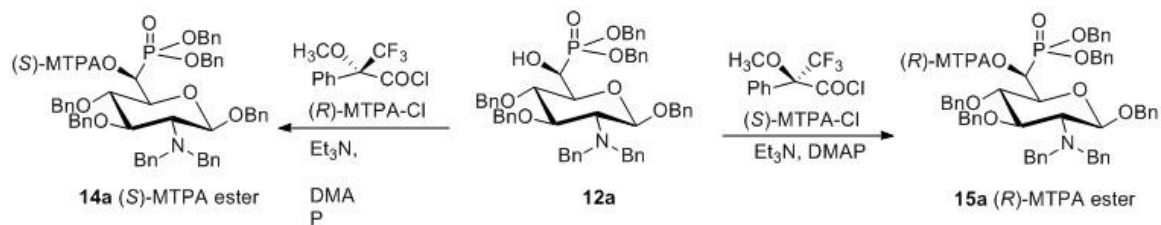
The absolute configurations of diastereoisomers **12a** and **12b** were assigned by the Mosher method (also known as Mosher ester analysis).<sup>27-29</sup> As displayed in Scheme 6-3, each of the diastereomeric *S*- and *R*- MTPA esters of major diastereomer **12a** was prepared from (*R*)-MTPA-Cl and (*S*)-MTPA-Cl, respectively (*S*- Mosher acid chloride gives rise to the *R*- Mosher ester due to relative priority: CF<sub>3</sub> is lower than COCl but higher than COOR). The H-5 proton signal of each diastereomeric Mosher ester was assigned by <sup>1</sup>H-<sup>1</sup>H COSY experiments. The chemical shift of H-5 in *S*-MTPA ester is  $\delta_S = 3.925$ , while the chemical shift of H-5 in *R*-MTPA ester is  $\delta_R = 3.851$ . That is, the  $\Delta\delta^{SR} = \delta_S - \delta_R = 3.925 - 3.851 = 0.074$  was positive. According to the Mosher empirical rule, the absolute configuration of the 6-position in compound **12a** was *S*-. This could be explained by the MTPA plane figures (Figure 6-2).



**Scheme 6-2.** Synthesis of GlcN6P analogues **2** and **3**

The H-5 of *R*-MTPA ester, in which H-5 and phenyl group reside are on the same side of the MTPA plane, is relatively more shielded (upfield in its spectrum) than H-5 in the *S*-MTPA ester due to the magnetic shielding effect of phenyl group. Correspondingly, the minor diastereomer was assigned as *R*-configuration. To further confirm the assignment of the absolute configurations of **12a** and **12b**, the *S*-MTPA esters (**14a** and **14b**) generated from both diastereoisomers **12a** and **12b** were compared (Figure 6-3).<sup>27,30</sup> The <sup>1</sup>H NMR analysis of both products showed that the H-5 proton of the major diastereomer

**14a** was downfield ( $\delta = 3.93$  ppm) relative to that of the minor diastereomer **14b** ( $\delta = 3.56$  ppm). These confirmed the configuration of major product **12a** is *S* and the configuration of minor product **12b** is *R*.



**Scheme 6-3.** Synthesis of *R*- and *S*- Mosher esters from compound **12a**

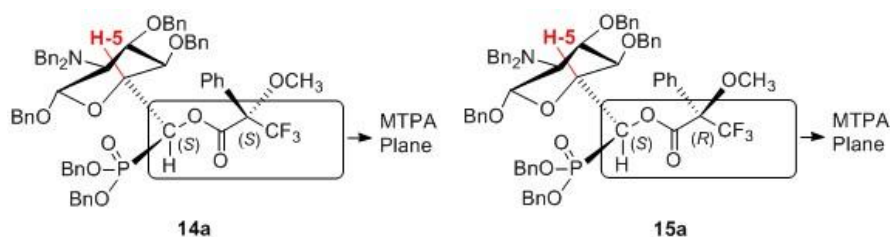


**Figure 6-2.** The MTPA plane of *S*- and *R*-MTPA esters

The Pudovik reaction, one of the most versatile methods for construction of C-P bonds, involves the addition of organophosphorus compounds to unsaturated bonds. With the potential to synthesize biologically important  $\alpha$ -hydroxyphosphonic acids derivatives,<sup>31-33</sup> this reaction has received more and more attention to make the process highly enantioselective.<sup>34,35</sup> The examples presented herein showed the versatility of the Mosher method as a convenient and alternative approach to the assignment of

stereochemistry of Pudovik products especially when the crystallization of products is impossible. It is applicable to either a single enantiomer or a pair of enantiomers.

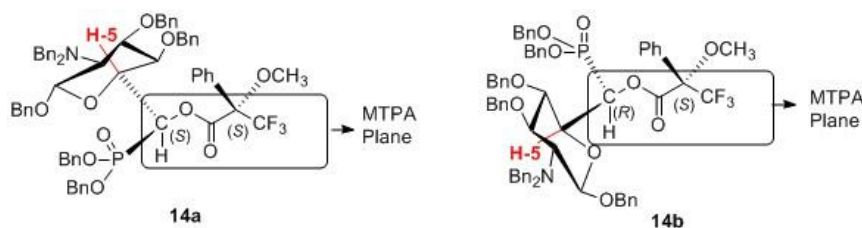


**Figure 6-3.** The MTPA plane of *S*-MTPA esters **14a** and **14b** made from **12a** and **12b**

The synthetic compounds **1**, **2**, and **3** were subsequently investigated for their ability to induce self-cleavage of 5'-<sup>32</sup>P-labeled *glmS* riboswitch from *B. subtilis*. As shown in Table 6-1 and Figure 6-4, carba-sugar **1** showed moderate activation of self-cleavage of *glmS* riboswitch from *B. subtilis*. The percentage of riboswitch self-cleavage induced by compound **1** is around half to that by natural metabolite GlcN6P. At the same time during the preparation of this manuscript, Wittmann and Mayer *et al.* reported their research of carba-sugar **1** on *glmS* riboswitch of vancomycin-resistant *Staphylococcus aureus*.<sup>36</sup> In their study, it was found that the potency of compound **1** for *glmS* riboswitch of *S. aureus* is similar to that of GlcN6P. They also mentioned the activation by compound **1** in the *glmS* riboswitch of *B. subtilis*. The activation achieved by compound **1** in our experiments compared favourably with the data reported by them. It seems that different sources of *glmS* ribozyme might have different sensitivities to GlcN6P analogues. On the other hand, the 6-phosphonate derivatives **2** and **3** did not exhibit activity under the tested assay conditions.

**Table 6-1.** Effect of synthetic compounds on *glmS* riboswitch

Sample	% Cleavage	
	1 min	2 min
No reaction (NR)	-	-
No magnesium (-Mg <sup>2+</sup> )	-	-
GlcN6P	67.50	65.12
1	29.08	38.68
2	0	0.37
3	0	0.29

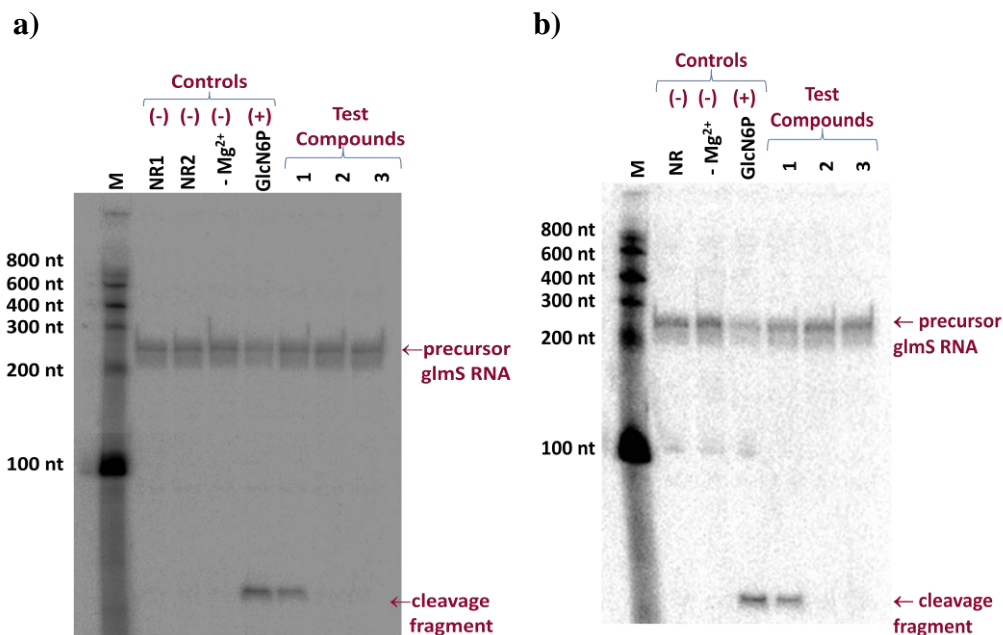


**Figure 6-4.** Cleavage of *glmS* RNA with and without compounds. **a)** Cleavage of *glmS* RNA after 1 min reaction time; **b)** Cleavage of *glmS* RNA after 2 min reaction time. A 200  $\mu$ M concentration of GlcN6P or a test compound was added to 0.5 pmol of 5'-<sup>32</sup>P labelled *glmS* RNA. Samples were incubated in 50 mM of HEPES (pH 7.5), 10 mM of MgCl<sub>2</sub>, 200 mM of KCl at room temperature for a duration of 1 or 2 min. Negative control samples included: i) addition of double-distilled water instead of compound, or ii)

addition of GlcN6P, without  $Mg^{2+}$  in the reaction buffer. RNA products were separated by 10% denaturing polyacrylamide gel electrophoresis (PAGE).

It was determined that the oxygen ring and phosphate group are required for stabilization of the interaction of the riboswitch with GlcN6P rather than being involved in the catalytic reaction.<sup>37,38</sup> The results herein show that the destabilization of the interaction can tolerate carba-sugar to some extent, whereas the 6-phosphate group is critical for interaction.<sup>16,38</sup> The phosphate moiety form the fixed network of  $Mg^{2+}$ -coordinated interactions with the various functional groups of the ligand binding pocket.<sup>15</sup> The electrical properties of  $\alpha$ -hydroxyl-phosphonate are slightly different from 6-phosphate. The change in electrical properties of 6-phosphonate might change the coordination with cations and further change the interaction with the binding pocket.<sup>13</sup> The other factor may rely on the unfilled space within the ligand binding pocket in the absence of the bridging oxygen.

## 6.5 Conclusions

Three GlcN6P analogues have been prepared to investigate their effect on the *glmS* riboswitch. The Pudovik reaction was applied to synthesize the  $\alpha$ -hydroxyphosphonate substrates and the configurations of two diastereomeric products were assigned by the Mosher method. Among the three analogues, carba-sugar **1** induced moderate self-cleavage of the *glmS* riboswitch from *B. subtilis*. The displacement of phosphate in GlcN6P by  $\alpha$ -hydroxyphosphonate led to massive loss of activation. These results highlight the role of the phosphate moiety in contributing to the binding of the *glmS* riboswitch. These insights are useful in further development of chemical agonists or

antagonists for the *glmS* riboswitch. It seems that *glmS* riboswitch exhibits high level of discrimination against many closely related GlcN6P analogues. Our results provide a deeper understanding of the *glmS* riboswitch and further elucidation on the structure-activity relationships of metabolite derivatives.

## 6.6 References

1. Winkler, W.; Nahvi, A.; Breaker, R. R. *Nature* **2002**, *419*, 952-956.
2. Coppins, R. L.; Hall, K. B.; Groisman, E. A. *Curr. Opin. Microbiol.* **2007**, *10*, 176-181.
3. Blount, K. F.; Breaker, R. R. *Nat. Biotechnol.* **2006**, *24*, 1558-1564.
4. Barrick, J. E.; Corbino, K. A.; Winkler, W. C.; Nahvi, A.; Mandal, M.; Collins, J.; Lee, M.; Roth, A.; Sudarsan, N.; Jona, I.; Wickiser, J. K.; Breaker, R. R. *Proc. Natl. Acad. Sci. U. S. A.* **2004**, *101*, 6421-6426.
5. Klein, D. J.; Ferre-D'Amare, A. R. *Science* **2006**, *313*, 1752-1756.
6. Cochrane, J. C.; Lipchock, S. V.; Strobel, S. A. *Chem. Biol.* **2007**, *14*, 97-105.
7. Winkler, W. C.; Nahvi, A.; Roth, A.; Collins, J. A.; Breaker, R. R. *Nature* **2004**, *428*, 281-286.
8. Milewski, S. *Biochim. Biophys. Acta* **2002**, *1597*, 173-192.
9. Wu, H. C.; Wu, T. C. *J. Bacteriol.* **1971**, *105*, 455-466.
10. Sarvas, M. *J. Bacteriol.* **1971**, *105*, 467-471.
11. Freese, E. B.; Cole, R. M.; Klofat, W.; Freese, E. *J. Bacteriol.* **1970**, *101*, 1046-1062.
12. Watson, P. Y.; Fedor, M. J. *Nat. Struct. Mol. Biol.* **2011**, *18*, 359-363.
13. Gong, B.; Klein, D. J.; Ferre-D'Amare, A. R.; Carey, P. R. *J. Am. Chem. Soc.* **2011**, *133*, 14188-14191.
14. Davis, J. H.; Dunican, B. F.; Strobel, S. A. *Biochemistry.* **2011**, *50*, 7236-7242.
15. Brooks, K. M.; Hampel, K. J. *Biochemistr.* **2011**, *50*, 2424-2433.
16. McCarthy, T. J.; Plog, M. A.; Floy, S. A.; Jansen, J. A.; Soukup, J. K.; Soukup, G. A. *Chem. Biol.* **2005**, *12*, 1221-1226.
17. Lim, J.; Grove, B. C.; Roth, A.; Breaker, R. R. *Angew. Chem. Int. Ed.* **2006**, *45*, 6689-6693.
18. Engel, R. *Chem. Rev.* **1977**, *77*, 349-367.
19. Kraszewski, A.; Stawinski, J. *Pure Appl. Chem.* **2007**, *79*, 2217-2227.
20. Thibaudeau, C.; Acharya, P.; Chattopadhyaya, J., Eds. *Stereoelectronic Effects in Nucleosides and Nucleotides and their Structural Implications*; Uppsala University Press, Uppsala, 2005.

21. Barton, D. H. R.; Augydorey, S.; Camara, J.; Dalko, P.; Delaumeny, J. M.; Gero, S. D.; Quicletsire, B.; Stutz, P. *Tetrahedron* **1990**, *46*, 215-230.
22. Ko, K. S.; Zea, C. J.; Pohl, N. L. *J. Am. Chem. Soc.* **2004**, *126*, 13188-13189.
23. Eby, R.; Sondheimer, S. J.; Schuerch, C. *Carbohydr. Res.* **1979**, *73*, 273-276.
24. Wang, G. N.; Twigg, G.; Butters, T. D.; Zhang, S.; Zhang, L.; Zhang, L.-H.; Ye, X.-S. *Org. Biomol. Chem.* **2012**, *10*, 2923-2927.
25. Pudovik, A. N.; Konovalova, I. V. *Synthesis* **1979**, 81-96.
26. Cherkasov, R. A.; Galkin, V. I.; Khabibullina, A. B.; Alkurdi, K. *Phosphorus, Sulfur Silicon Relat. Elem.* **1990**, *49*, 61-64.
27. Dale, J. A.; Mosher, H. S. *J. Am. Chem. Soc.* **1973**, *95*, 512-519.
28. Dale, J. A.; Dull, D. L.; Mosher, H. S. *J. Org. Chem.* **1969**, *34*, 2543-2549.
29. Hoyer, T. R.; Jeffrey, C. S.; Shao, F. *Nat. Protoc.* **2007**, *2*, 2451-2458.
30. Ng, S. S.; Jamison, T. F. *Tetrahedron* **2005**, *61*, 11405-11417.
31. Kolodiazhnyi, O. I. *Tetrahedron: Asymmetry* **2005**, *16*, 3295-3340.
32. Frechette, R. F.; Ackerman, C.; Beers, S.; Look, R.; Moore, J. *Bioorg. Med. Chem. Lett.* **1997**, *7*, 2169-2172.
33. Dellaria Jr., J. F.; Maki, R. G.; Stein, H. H.; Cohen, J.; Whittern, D.; Marsh, K.; Hoffman, D. J.; Plattner, J. J.; Perun, T. J. *J. Med. Chem.* **1990**, *33*, 534-542.
34. Kee, T. P.; Nixon, T. D. In *New Aspects in Phosphorus Chemistry II; Topics in Current Chemistry 223*; Majoral, J.-P. Ed.; Springer-Verlag: Berlin, 2003; pp. 45-65.
35. Abell, J. P.; Yamamoto, H. *J. Am. Chem. Soc.* **2008**, *130*, 10521-10523.
36. Lunse, C. E.; Schmidt, M. S.; Wittmann, V.; Mayer, G. *ACS Chem. Biol.* **2011**, *6*, 675-678.
37. Klein, D. J.; Been, M. D.; Ferre-D'Amare, A. R. *J. Am. Chem. Soc.* **2007**, *129*, 14858-14859.
38. Xin, Y.; Hamelberg, D. *RNA* **2010**, *16*, 2455-2463.

## CHAPTER 7

### DISCUSSION AND FUTURE DIRECTIONS

In summary, the work embodied in this thesis demonstrates the potential of RNA aptamers for sensor development, an area that is still relatively underexplored. Using the design principle of structure-switching, this thesis establishes the advantages of RNA-aptamer based detection, and provides methods to overcome some of the limitations. In the first project, a fluorescent sensing strategy was created that demonstrated to be generally applicable to various RNA aptamers. This work sets the foundation for all subsequent work in this thesis. In the second project, the RNA aptamer-based sensing strategy was adapted to include an internal control that could effectively monitor the quality control of detection. This strategy enabled the distinction of a true-positive signal from a false-positive one, which ultimately provided assurance of high quality detection from RNA aptamers. Remedy methods to correct detection errors were also demonstrated. In the third project, the RNA aptamer-based sensing strategy was adapted for application on graphene material, which further showcases the versatility of the structure-switching design. Furthermore, this novel strategy considerably enhanced the signaling capability of the RNA aptamers tested.

Structure-switching RNA aptamers were also expanded into secondary applications involving collaborations with other research groups. In collaboration with the Brennan group, the fluorescent sensing strategy was directly entrapped in sol-gel derived materials for solid-assay development. Importantly, sol-gel entrapment also demonstrated

to confer protection of RNA aptamers against nucleases, as well as enhance the chemical stability of the aptamers. Additionally, in collaboration with the Ye group, the glmS ribozyme, a natural structure-switching RNA aptamer found in numerous Gram-positive bacteria was further explored as a potential drug target for antibiotic development. One particular GlcN6P analogue was able to induce self-cleavage of the ribozyme, and may be a potential lead for drug design.

While this thesis has made considerable progress to demonstrate the potential of RNA aptamers for sensing purposes, further investigation is important in several areas for the application of RNA aptamers for real-life detection. The remainder of this chapter discusses some of the possibilities for future studies.

As discussed in the earlier introductory chapter, structure-switching reporters using DNA aptamers [22] have already garnered substantial success, including expansion to detect a range of targets [27, 29-38], application in a variety of secondary applications [42, 46, 47, 247-249], and adaptation for use in different signal transduction methods [40, 66, 250-253]. In consideration of the future possibilities of structure-switching RNA aptamers, it is conceivable that a similar trajectory of development may follow. To facilitate this progression, it is necessary to understand the fundamental differences in structure-switching between RNA and DNA aptamers, which much is unknown. For instance, differences in design elements were found to be required for effective structure-switching (discussed in Chapter 2). Compared to the previously reported DNA aptamer reporters, the RNA aptamer reporters required longer FDNA, central extension domain, and QDNA sequences, in order to obtain the optimal balance of low background, and

high signal enhancement. One possible reason why longer design elements are required for RNA aptamer reporters may reflect a weaker stability of the RNA-DNA duplex relative to the DNA-DNA duplex for the sequences specifically used in these designs. These results are compatible with previous studies, which have measured the thermodynamic parameters of RNA-RNA, DNA-DNA and hybrid duplexes to demonstrate that duplex stability is highly sequence dependent [254, 255]. Another possible reason for the differences found in design element requirements, may stem from natural behavioral differences between DNA and RNA sequences. Normally, DNA sequences readily adopt a double-helical structure. In contrast, RNA is naturally found as a single-stranded sequence with the tendency to fold up upon itself to form intricate structures [256]. These structures are stabilized by various intramolecular interactions including standard base-pairing of complementary segments found within the sequence, non-Watson-Crick base-pairing such as the G-U mismatch, and additional hydrogen bonding from the 2'-OH group of ribose sugar that is unique to RNA [256-262]. To overcome the intramolecular folding of RNA, longer design elements may be required to compete favorably to form the FDNA-aptamer-QDNA duplex system. To definitively test the two possibilities mentioned above, a comparison study between RNA and DNA aptamer reporters would be valuable. The FDNA and associated hybridization site on the extended aptamer are ideal testing sites since these elements can be altered, unlike the well-conserved aptamer domain. Furthermore, any effects produced by alterations of these elements can be assessed by directly measuring target-induced structure-switching ability. Different FDNAs that vary in length and sequence can be designed to form an

FDNA-aptamer-QDNA duplex requiring standard and non-standard base-pairing. Assessment of background signal, and signal enhancement for each of these systems could provide insight about optimal sequence composition required for effective sensor engineering. The applicability of these findings may extend beyond solely structure-switching-based designs, and also include any sensing platforms that require RNA-DNA and DNA-DNA duplex formation.

Understanding the fundamental differences in structure-switching between RNA and DNA aptamers is also important for further development of solid-phase assays. Previous studies have shown that while polar materials (SS, DGS) are suitable for entrapment of DNA aptamer reporters [47], more hydrophobic materials (40% (v/v) MTMS/TMOS) are best for entrapment of RNA aptamers (discussed in Chapter 5). To better understand these differences, we are currently collaborating with Christy Hui from the Brennan group to analyze how structural differences between RNA and DNA aptamers affect interaction with sol-gel. We have chosen to focus our investigation on the ATP-binding RNA [263] and DNA [23] aptamers as they are model systems. To enable this comparison, I have successfully created and optimized the ATP-binding RNA aptamer reporter using the generalizable structure-switching design. Christy has determined the optimal sol-gel conditions to entrap both the RNA aptamer reporter, as well as the previously demonstrated DNA aptamer reporter. Future comparative studies between RNA and DNA aptamer reporters will involve determination of detection limit and specificity, as well as characterization of protective properties of sol-gel against nuclease degradation, chemical instability, and structural denaturation. These findings

may provide the general criteria required for effective entrapment of RNA and DNA aptamers in sol-gel, and may accelerate solid-assay development, particularly for the more recently developed RNA reporters.

RNA structure-switching reporters may also play a significant role for in vitro applications relating to diagnostics, environmental testing, and food safety. However, to further advance RNA aptamer reporters, key limitations first need to be addressed. As discussed in Chapter 2, the detection limit of RNA aptamer reporters was found to be 10 times higher than the  $K_d$  of the original aptamers as a result of target competition with QDNA for binding to the aptamer, as well as the inherent background fluorescence. To improve detection limit, signal amplification methods may provide solutions by tagging each aptamer with multiple copies of fluorophore to generate an amplified fluorescent signal for every aptamer-target interaction. Silica nanoparticles (FNPs) and quantum dots (QDs) for instance, can carry many fluorophores for aptamer labelling and have already demonstrated to improve the detection limit for DNA aptamer reporters [39, 40]. Additionally, application of RNA aptamer reporters towards other signal transduction methods that can provide lower background signal, may also improve the detection limit. Electrochemical-based detection for example [264, 265], has already demonstrated to lower the detection limit for DNA aptamer reporters [56, 252].

Furthermore, for more effective application of RNA structure-switching reporters towards other signal transduction methods, integration of a QC element, or internal control that can distinguish between true-positive and false-positive signals would be important to ensure high quality detection. While work in this thesis has already

successfully tested fluorescent RNA aptamer reporters in human serum (discussed in Chapter 3), further testing using a range of real-life samples (eg. urine, saliva, food, water), and implementing a variety of different RNA and DNA aptamers will demonstrate broader applicability. Expectedly, the complexity of real-life samples can interfere with the detection strategies used (eg. fluorescence quenching), rendering our sensor ineffective. However, we have discovered that remedy methods such as sample filtration, and the use of nuclease inhibitors are effective in removing nucleases, and signal interfering agents for our fluorescence-based design. These solutions may be useful for other signal transduction methods as well.

RNA structure-switching reporters may also be expanded for in vivo applications, particularly for therapeutics. One possibility is to implement the RNA aptamer sensors based on regulated GO adsorption, which have already been demonstrated for in vitro sensing in this thesis (discussed in Chapter 4). These systems may be suitable for intracellular sensing for a number of reasons. Firstly, graphene is an appropriate material for the transport of RNA aptamer reporters into relevant cells, as the biocompatibility of graphene has already been well established in a range of mammalian cell types [266-270], as well as a mouse model for cancer [271]. Additionally, previous studies have also demonstrated that graphene enables high transfection efficiency of therapeutic agents into cells [272, 273], and also confers protection of aptamers against nuclease degradation [269, 270]. Similarly, aptamers have also been well-tested for in vivo applications. Pegaptanib sodium (commercially known as Macugen) is the most marketable aptamer that is clinically used to treat macular degeneration, a common cause of vision loss in

elderly people [202, 274]. When injected into the eyes, the therapeutic DNA aptamer specifically binds to vascular endothelial growth factor (VEGF) to inhibit blood vessel formation in the retina, where leakage of fluid causes cloudiness in the eye. Moreover, many DNA and RNA aptamers are currently in advanced stages of clinical studies and may become the next examples of commercialized aptamers [275]. Among these aptamers, several are therapeutic candidates, and others have been successful for targeted drug delivery. A notable example of the latter, is an RNA aptamer that recognizes prostate-specific membrane antigen (PSMA) [151], a biomarker found on prostate tumors. While conjugated to a cancer fighting drug, the aptamer binds PSMA to trigger cell internalization through endocytosis [276-278]. This results in site-specific delivery of the drug, which can potentially reduce many side-effects that are characteristic of traditional cancer treatments. Together, the useful properties of graphene and diverse range of aptamers may prove to be an effective combination for intracellular detection.

Our work exploring the glmS ribozyme as a potential drug target for antibiotic development may also benefit from future in vivo application. Our study resulted in the synthesis of one particular GlcN6P analogue, carba-sugar 1, which was able to induce self-cleavage of the ribozyme, and may be a potential lead for drug design. As discussed in Chapter 6, carba-sugar 1 produces different activation levels of glmS self-cleavage depending on which bacterium the ribozyme is derived from. Consequently, testing the effects of carba-sugar 1 on glmS ribozyme sequences from a wider range of bacteria, particularly from pathogens such as *Bacillus anthracis* would be important to determine the extent of drug applicability. Particularly, determination of drug potency ( $EC_{50}$ , half

maximal effective concentration), target specificity and cleave rate constant ( $k_{obs}$ ) will help characterize drug effect on each glmS sequence. The glmS sequences that demonstrate the best drug response can be further tested in vivo to verify drug lethality on the target bacterium.

In conclusion, this thesis provides generalizable structure-switching strategies to make use of the abundance of RNA aptamers, monitor the quality of detection and correct detection error, enhance aptamer sensing capability, as well as protect aptamers against nucleases and chemical instability. Additionally, work in this thesis further validates the use of riboswitches/ribozymes as potential targets for drug discovery. Future studies that lead to a better understanding of the fundamentals of structure-switching, and further efforts to overcome limitations required for effective in vitro, as well as in vivo applications, will enable the continued success of RNA structure-switching reporters.

## APPENDIX 1

### CHAPTER 2. SUPPLEMENTARY INFORMATION

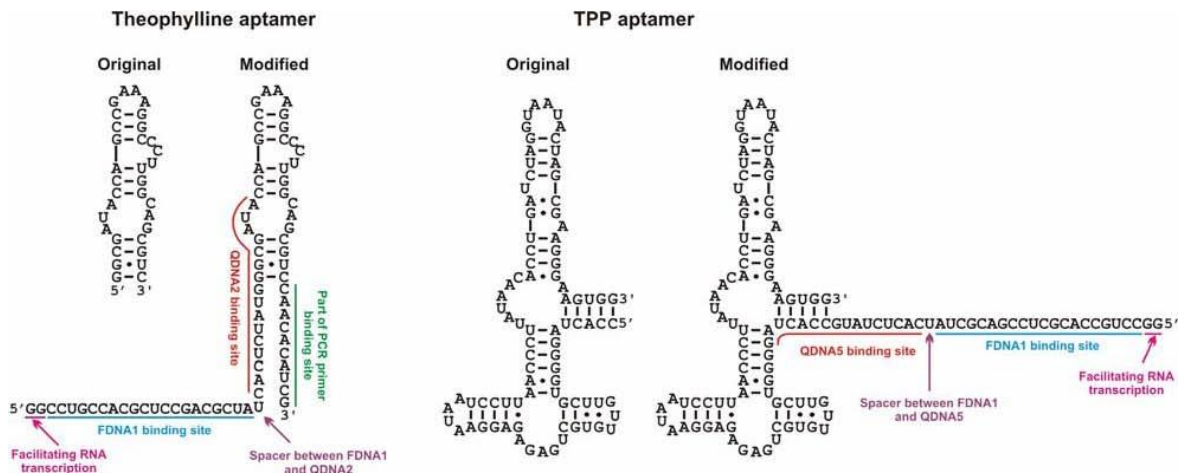


**Figure S2-1.** Secondary structures of the theophylline aptamer and the TPP aptamer. The secondary structure of the original theophylline aptamer is adopted from Ref 1, and that of the original TPP aptamer is adopted from Ref. 2. The sequence of each aptamer is modified in this study to contain additional sequence elements for the indicated purposes. See the main text for details.

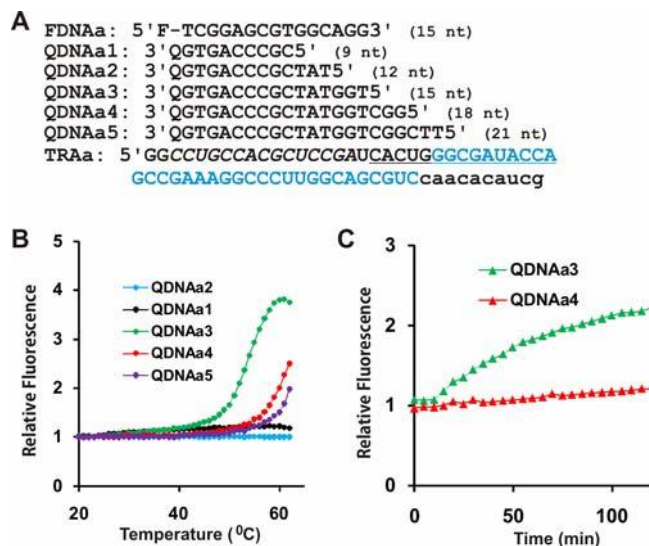


**Figure S2-2.** The initially designed structure-switching reporter from the theophylline RNA aptamer. **A)** The sequences of FDNA, QDNAs and TRAa (extended theophylline aptamer version a). **B)** Thermal denaturation profiles of the duplexes made from TRAa, FDNAa along with QDNAa1 (light blue), QDNAa2 (black), QDNAa3 (green), QDNAa4 (red) and QDNAa5 (purple). **C)** Theophylline-induced fluorescence response of two reporters made from QDNAa3 (green) and QDNAa4 (red) in the duplex with FDNAa and TRAa. Each duplex was incubated at 37°C for 5 min followed by the addition of 1 mM theophylline. **Brief discussion:** The initial design of the theophylline reporter followed the identical strategy that was used to produce structure-switching reporters from DNA aptamers. However, we discovered that QDNA sequences less than 13 nt (QDNAa1 and QDNAa2) could not effectively anneal with the extended theophylline aptamer because both systems exhibited near-flat thermal denaturation profiles. QDNAa3 (15 nt) exhibited a nice thermal denaturation profile (green curve in panel B) and some structure-switching activity upon the addition of 1 mM theophylline at 37°C but the switching activity was fairly weak, needing more than 2 hours to reach ~2-fold fluorescence increase (green data set in panel C). Longer QDNAs (such as QDNAa4) appeared to bind the aptamer very strongly (red curve in panel B) and did not produce significant fluorescence increase upon target addition (red data set in panel C). Based on this observation, we abandoned this system.

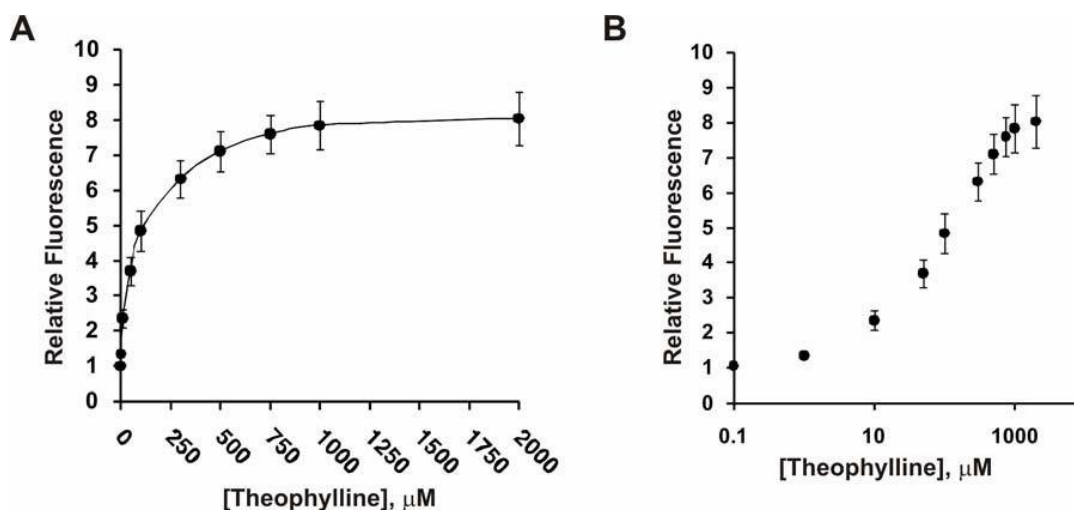


**Figure S2-3.** Detection sensitivity of the theophylline reporter made of FDNA1, QDNA2 and TRA1. **A)** Relative fluorescence vs. theophylline concentration. **B)** Relative fluorescence vs. theophylline concentration in logarithmic scale. Relative fluorescence of each sample was taken at the 20th minute incubation. The theophylline concentration was varied between 0.1-2000 µM. The detection limit was found to be 1 µM (which produced a signal that is above 3× standard deviation of the fluorescence in the absence of the target).

```

TPPRA:
5'GGCCU GCCAC GCUCC GACGC UAUCA CUCUA UGCCA CUAGG GGUGC UUGUU
  GUGCU GAGAG AGGAA UAAUC CUUAA CCCUU AUAAC ACCUG AUCUA GGUAA
  UACUA GCGAA GGGAA GUGG3'

TPPRA mutant:
5'GGCCU GCCAC GCUCC GACGC UAUCA CUCUA UGCCA CUAGG GcUGC UUGUU
  GUGCU cAuUG AGGAA UAAUC CUUAA CCCUU AUAAC ACCUG AUCUA GGUAA
  UACUA GcUAA GGGAA GUGG3'
    
```

**Figure S2-4.** Nucleotide sequences of TPP aptamer (TPPRA) and a mutant aptamer. The nucleotides indicated in red and lower-case letters are altered nucleotides in relation to the wildtype sequence. Mutation was introduced at four critical nucleotides required for TPP-binding (see Ref 2 and 3).

## References for Chapter 2 Supplementary Information

1. a) R. D. Jenison, S. C. Gill, A. Pardi, B. Polisky, *Science* 1994, 263, 1425; b) G. R. Zimmermann, R. D. Jenison, C. L. Wick, J. P. Simorre, A. Pardi, *Nat Struct Biol* 1997, 4, 644.
2. R. Welz, R. R. Breaker, *RNA* 2007, 13, 573.
3. a) S. Thore, M. Leibundgut, N. Ban. *Science* 2006, 312: 1208. b) A. Serganov, A. Polonskaia, A. T. Phan, R. R. Breaker, D. J. Patel. *Nature* 2006, 441, 1167. c) T. E. Edwards, A. R. Ferré-D'Amaré. *Structure* 2006, 14, 1459.

## CHAPTER 3. SUPPLEMENTARY INFORMATION

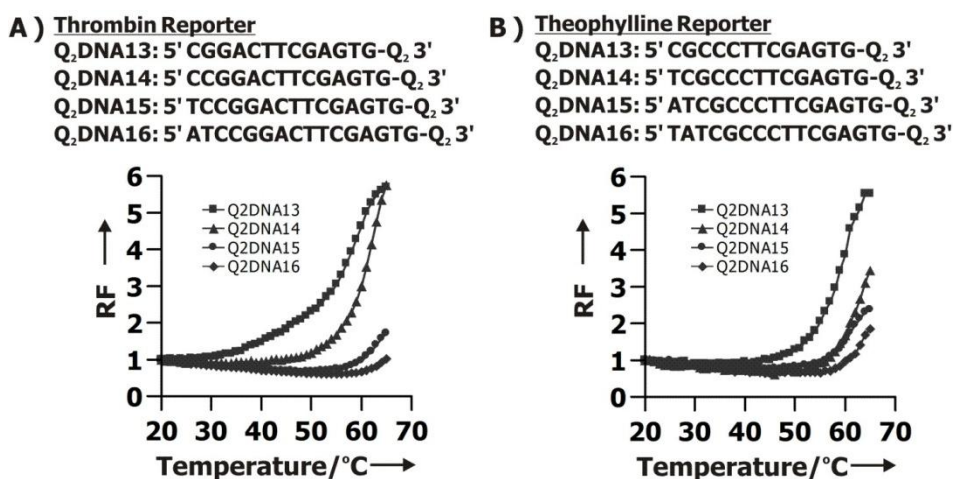


**Figure S3-1.** Thermal denaturation profiles of duplexes made from Q<sub>2</sub>DNA13-16 with mfRNA, F<sub>1</sub>DNAF<sub>2</sub> and Q<sub>1</sub>DNA for **A)** thrombin and **B)** theophylline reporters. F<sub>2</sub>-fluorescence associated with the aptamer domain (red emission) is depicted.

- A) thrombin mfRNA:** 5' GGGAGACACGUCGUGCGUACUCCUGC  
CACGCUCCGACGCUAGCUGAUCACUCGAAGUCCGGGAUCGAA  
GUUAGUAGGCCGGA 3'  
**Mut1:** 5'GGGAGACACGUCGUGCGUACUCCUGCCACGCUCCG  
ACGCUAGCUGAUCACUCGAAGUCCGGAgCGAAGUUCGUcGGC  
GGA 3'  
**Mut2:** 5' GGGAGACACGUCGUGCGUACUCCUGCCACGCUCCG  
ACGCUAGCUGAUCACUCGAAGUCCGGAUcUAAGUUUAUAuGC  
GGA 3'
- B) theophylline mfRNA:** 5'GGGAGACACGUCGUGCGUACUCC  
UGCCACGCUCCGACGCUAGCUGAUCACUCGAAGGGCGAUAC  
CAGCCGAAAGGCCUUGGCAGCGUCCAACACAUCG 3'  
**Mut1:** 5'GGGAGACACGUCGUGCGUACUCCUGCCACGCUCCG  
ACGCUAGCUGAUCACUCGAAGGGCGAUACaAGCCGAAAGGCC  
CUUGGCuGCGUCCAACACAUCG 3'  
**Mut2:** 5'GGGAGACACGUCGUGCGUACUCCUGCCACGCUCCG  
ACGCUAGCUGAUCACUCGAAGGGCGAUAgAAGCCGAAAGGCC  
CUUGGCAGCGUCCAACACAUCG 3'

**Figure S3-2.** Wildtype multifunctional RNA aptamer sequences (mfRNA) and their mutated aptamer sequences (Mut1, Mut2) for both **A)** thrombin and **B)** theophylline reporters. Aptamer domains are underlined.<sup>[1]</sup> Mutated nucleotides are shown in gray, lowercase.

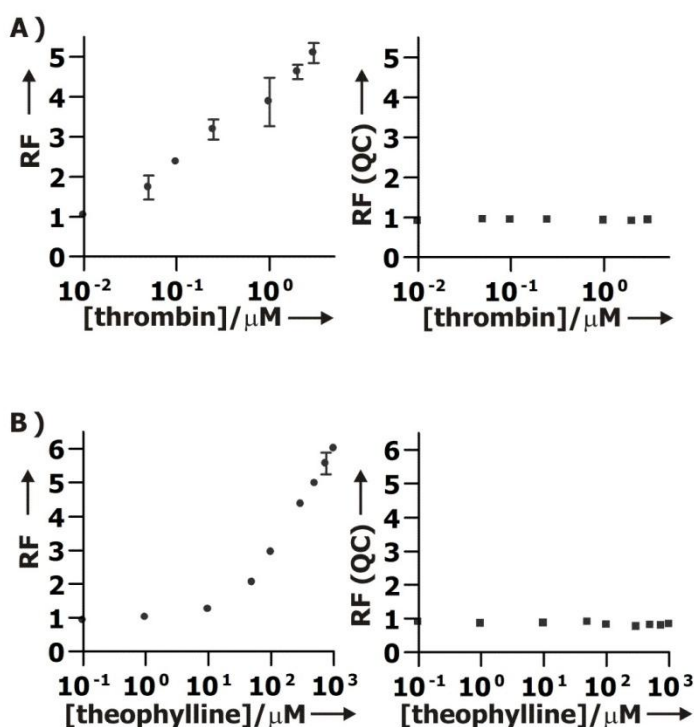


**Figure S3-3.** Detection sensitivity of structure-switching RNA aptamer reporters made up of corresponding mfRNA, Q<sub>1</sub>DNA, F<sub>1</sub>DNAF<sub>2</sub>, and Q<sub>2</sub>DNA13. Relative fluorescence (RF) vs. target concentration presented in logarithmic scale. RF of each sample was taken at the 15<sup>th</sup> minute of incubation. RF from F<sub>2</sub> (sensor module) and F<sub>1</sub> (quality control module) presented on the left and right, respectively. Results are representative of two independent experiments. **A)** Thrombin reporter. The thrombin concentration was varied between 0.01-3  $\mu\text{M}$ . The detection limit was determined to be 0.01  $\mu\text{M}$  (signal produced that is 3x the standard deviation of fluorescence in the absence of target). **B)** Theophylline reporter. The theophylline concentration was varied between 0.1-1000  $\mu\text{M}$ . The detection limit was found to be 1  $\mu\text{M}$ .

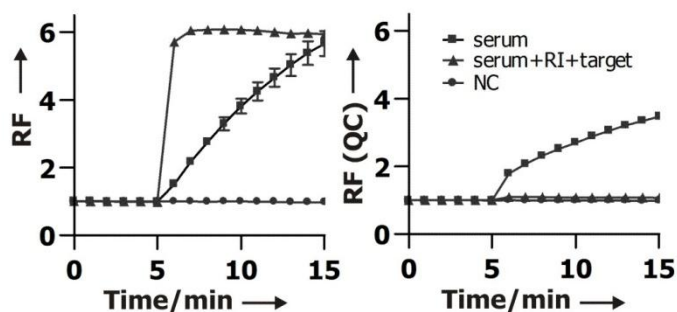


**Figure S3-4.** Error detection and correction using thrombin structure-switching reporter with a quality control element. Relative fluorescence (RF for F<sub>2</sub>; RF (QC) for F<sub>1</sub>) was measured as the signalling duplex was incubated at 37°C for 5 min, before the addition of serum (square data set). The addition of RiboLock RNase inhibitor (RI) largely inactivates nucleases and facilitates the target detection (triangle data set). Negative control (NC, circle): no thrombin. The experiment was performed in duplicate.

### References for Chapter 3 Supplementary Information

- [1] a) M. F. Kubik, A. W. Stephens, D. Schneider, R. A. Marlar, D. Tasset, *Nucleic Acids Res.* **1994**, *22*, 2619-2626; b) R. D. Jenison, S. C. Gill, A. Pardi, B. Polisky, *Science* **1994**, *263*, 1425-1429.

## CHAPTER 4. SUPPLEMENTARY INFORMATION

**General procedure.** Unless stated otherwise, the following conditions were used for Figure S4-1. For FDNA-RNA aptamer duplex assembly, a mixture of FDNA (200 nM) and RNA aptamer (200 nM) in a reaction buffer (50  $\mu$ L total volume) of Tris-HCl (25 mM, pH 7.5) and  $MgCl_2$  (10 mM) was first heated at 65°C for 2 min, then cooled at room temperature for 10 min, and finally cooled at 4°C for 10 min. GO (20  $\mu$ L from 100  $\mu$ g/mL stock) was then mixed into the FDNA-RNA aptamer mixture, and an aliquot (50  $\mu$ L) was taken for analysis. All fluorescence readings were measured at 37°C on Cary Eclipse (Varian) with an  $\lambda_{ex}/\lambda_{em}$  of 490/520 nm.

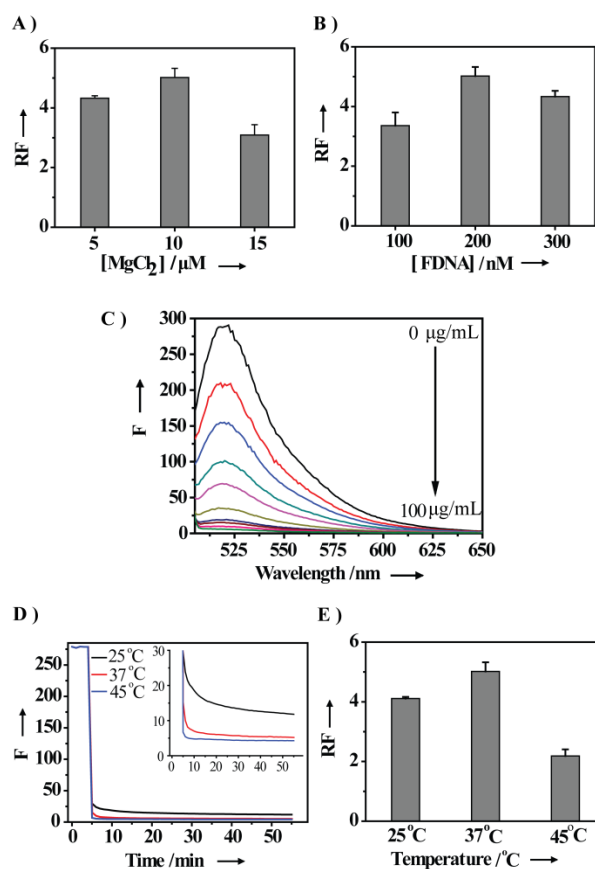


**Figure S4-1.** Optimization of conditions for RNA aptamer sensor using classic GO adsorption method. **A)** Testing divalent metal ion concentration. FDNA-RNA aptamer-GO assembly was tested in Tris-HCl (25 mM, pH 7.5) with different concentrations of MgCl<sub>2</sub> (5-15 μM). **B)** Testing FDNA concentration (100-300 nM). [For A) and B), after incubation of FDNA-RNA aptamer-GO for 30 min to reach stable background, theophylline (800 μM) was then added, and RF was recorded 1 hr after]. **C)** Testing GO concentration for fluorescence quenching. FDNA-RNA aptamer duplex was treated with different GO concentrations (0, 20, 30, 40, 50, 60, 70, 80, 90, 100 μg/mL). Fluorescence spectra were measured after 30 min. **D)** Testing effect of temperature on fluorescence quenching (25-45°C). FDNA-RNA aptamer duplex was incubated for 5 min, before the addition of GO. **E)** Testing effect of temperature on fluorescence recovery (25-45°C). FDNA-RNA aptamer-GO assembly was treated with theophylline (800 μM), and RF was recorded 1 hr later. [Higher temperatures produced lower background (shown in D), and the highest signal enhancement was produced at 37°C (shown in E); 37°C provided the optimal balance of low background and high signal enhancement, so was chosen for subsequent analysis]. All experiments were performed in duplicate.

**A)** Theophylline mutant aptamer:  
5' - GGCCUGCCACGCUCCGACGCUAUGGCGAU  
AGAAAGCCGAAAGGCCCUUGGCAGCGUC - 3'

**B)** TPP mutant aptamer:  
5' - GGCCUGCCACGCUCCGACGCUAUCCACUA  
GGGCUGCUUGUUGUGCUCAUUGAGGAAU  
AAUCCUUAACCCUUAUAACACCUGAUCUA  
GGUAAUACUAGCUAAGGGAAGUGG - 3'

**Figure S4-2.** Sequences of **A)** theophylline, and **B)** TPP mutant aptamers. Nucleotide substitutions are shown in red.

## APPENDIX 2

### DEVELOPMENT OF TANDEM DNA APTAMERS FOR THE DETECTION OF *L. MONOCYTOGENES*

#### Author's Preface

The work presented here is still in progress. Dr. Yingfu Li and I conceived the project idea together. I was principally responsible for designing and performing experiments, as well as interpreting data. Uyen T. Nguyen taught me how to grow *L. monocytogenes* biofilm and she also conducted the biofilm SEM imaging. Dr. Yingfu Li, Dr. Brian K. Coombes and Dr. Lori L. Burrows provided helpful advice and suggestions.

Lau PS, Nguyen UT, Burrows LL, Coombes BK, Li Y. Development of tandem DNA aptamers for the detection of *L. monocytogenes*.

## **Abstract**

Foodborne pathogens cause illness in millions of people around the world, everyday. Due to the limitations of current pathogen detection methods, there is a need for alternative biosensing strategies for better food safety. Aptamers are single-stranded DNA or RNA molecules that can fold into a defined tertiary structure to bind a designated target. These unique molecular probes have been widely implemented for biosensor development due to their inherent sensing capabilities. Our goal is to develop “tandem DNA aptamers” to detect *L. monocytogenes*, an emerging foodborne pathogen. These tandem aptamers are molecular probes made up of two or three aptamer units linked together consecutively within a sequence and may bind to multiple sites on the pathogen for enhanced overall binding affinity and selectivity. Herein, we present a SELEX-based approach to create tandem aptamers, and discuss directions for further development in future studies.

## **Introduction**

Foodborne acquired illnesses affect millions of people everyday worldwide. If not safeguarded against microbial and chemical contamination, food products can transmit more than 250 known diseases, resulting in numerous hospitalizations and deaths annually [1]. In the United States alone, 76 million cases of foodborne illnesses, 32 500 cases of hospitalization, and 5000 deaths are reported every year. Globally, foodborne diseases are estimated to cost healthcare approximately \$5-6 billion annually [1]. In recent years, outbreaks caused by *L. monocytogenes* have been on the rise [2-4]. As an

opportunistic pathogen, *L. monocytogenes* frequently affects immune-compromised patients and infection carries a notably high mortality rate [5, 6]. The difficulty in combating *L. monocytogenes*, is further aggravated by the ability of these cells to form biofilm (protective bacterial communities), which allows the pathogen to persist in different environmental conditions, and provides increased tolerance to antibiotics and attack from the host immune system [7-9]. Consequently, having effective methods of pathogen detection is critical in controlling and possibly preventing widespread infection. Cell culturing, PCR and antibody-based methods are currently used and are well-established strategies. However, several limitations still exist including long analysis time, intensive labour, expensive reagents, extensive sample purification steps, and limited accuracy [10-12]. There is a need for an alternative method of detection that can address these limitations for better food safety.

Aptamers are single-stranded DNA or RNA molecules that fold into a defined tertiary structure to bind a designated target [13, 14]. These unique molecular probes have been widely implemented for biosensor development due to their useful properties such as the chemical stability of DNA, intricate folding capability of RNA and DNA, high binding affinity and specificity, ease of immobilization, and amenability to various chemical modifications [15, 16]. Furthermore, the versatility of SELEX (Systematic Evolution of Ligands by EXponential enrichment) enables the development of aptamers that can bind to a desired target for customized applications [13, 14]. In recent years, several research groups have enhanced the affinity and specificity of aptamers through polyvalent binding, whereby a linker is used to join together two different aptamers,

which recognize distinct epitopes of a target molecule [17-19]. However, the focus of these studies has mainly relied upon the use of model aptamers for proof-of-concept purposes, as well as some degree of rational design for sensor development. Development of polyvalent aptamers directly through SELEX has yet to be demonstrated, and may provide enhanced sensing, which is crucial for more real-life applications such as detection of foodborne pathogens.

To address some of the current limitations in food monitoring, our goal is to develop an alternative sensing method based on polyvalent aptamers to detect *L. monocytogenes*. Specifically, our purpose is to develop “tandem aptamers”, which are DNA probes made up of two or three aptamer units linked together consecutively within a sequence (Figure 1). Advantageously, a single tandem probe may recognize multiple binding sites on the pathogen target. Hence, the overall binding affinity and selectivity of the tandem probe can be significantly enhanced (compared to an aptamer monomer) [17-19]. Our goal is broken down into three aims. The first aim is to create randomized, tandem DNA libraries using a procedure based on rolling circle amplification (Figure 1A). Sequences composed of two tandem aptamer repeats make up the dimeric DNA library, while sequences composed of three tandem aptamer repeats make up the trimeric DNA library. The second aim is to use these tandem DNA libraries in SELEX to develop tandem aptamers to detect *L. monocytogenes* (Figure 1B). In this procedure of in vitro evolution [13, 14], a selective pressure is exerted on the tandem DNA libraries to isolate only the sequences that recognize the pathogen. The strongest tandem aptamer candidates are subsequently amplified by PCR after each round of selection. Through multiple

rounds of isolation and amplification, nucleic acid sequences are allowed to evolve and compete with each other so that only the most capable tandem aptamer candidates are selected and copied. Development of these tandem aptamer candidates then leads to the third aim, which is to couple these sequences with a signal transduction method such as fluorescence for biosensor development (Figure 1C).

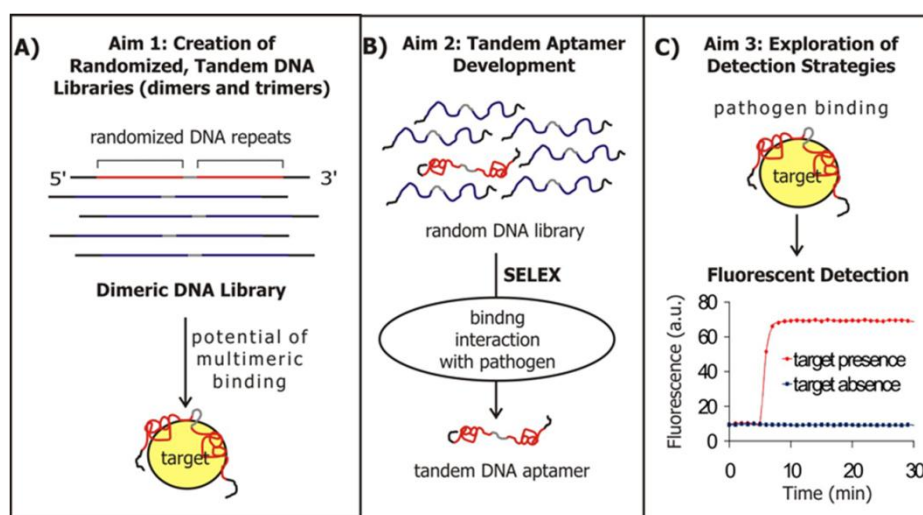


**Figure 1.** Overview of objectives to develop tandem DNA aptamers for detection of *L. monocytogenes*. (For simplicity, only dimeric DNA is presented here)

## Materials and Methods

**Materials.** All DNA oligonucleotides were synthesized by using automated DNA synthesis (W. M. Keck Oligonucleotide Synthesis Facility, Yale University, New Haven, CT, USA) and were purified by 10% denaturing PAGE before use. All radioisotopes were purchased from PerkinElmer (Woodbridge, ON, Canada). Unless otherwise noted, all reaction enzymes were purchased from Thermo Scientific (Ottawa, ON, Canada) and all other materials were purchased from Sigma-Aldrich and used without further purification.

**Growth of bacterial strains.** *L. monocytogenes* 568 (serotype 1/2a) was a gift from Lisbeth Truelstrup-Hansen (Dalhousie University, Halifax, NS, Canada). *L. innocua*, *B. subtilis* 168, *E. coli* K12 (MG1655) were gifts from Gerry Wright (McMaster University, Hamilton, ON, Canada). The glycerol stocks were streaked onto Difco tryptic soy agar (BD Biosciences) and incubated overnight at 37°C. After plating, a single colony from each respective bacterial strain was used to inoculate 5 ml of tryptic soy broth (TSB; BD Biosciences) at 37°C with agitation overnight. The overnight cultures were 200X-diluted in TSB and further incubated with agitation until an optical density at 600 nm (OD600) of 0.5 (VersaMax microplate reader, Molecular Devices, Sunnyvale, CA, USA) was obtained.

**Growth of *L. monocytogenes* biofilm.** The procedure to grow *L. monocytogenes* biofilm was adapted from a previously reported study [20]. In brief, a single colony from a plated culture was used to inoculate 10 ml of TSB at 37°C with agitation overnight and standardized to an OD600 of ~0.03 in TSB (Thermo Scientific BioMate3, Canada). The wells of a 96-well plate, were filled with the bacterial culture (150 µL) and wells along the periphery of the plate were filled with ddH<sub>2</sub>O (150µL) to prevent edge effects due to dehydration. Biofilm was grown on polystyrene pegs by placing a 96-peg lid (Nunc, VWR, Mississauga, ON, Canada) on the 96-well plate, sealing with parafilm to prevent evaporation and then incubating for 24 hrs at 37°C, 200 rpm. After 24 hrs of incubation, the planktonic growth in the 96-well plate was measured at OD600, and the peg lid was transferred to a new 96-well plate with fresh TSB (150 µL) and water (150 µL) in the peripheral wells. The plate was resealed with parafilm and incubated at 37°C, with

shaking at 200 rpm, for 24 hrs. This step was repeated again for a total incubation time of 72 hrs (three passages in total, once every 24 hrs). To quantify the amount of biofilm formed, any loosely adhered bacterial cells on the pegs were first washed off by transferring the peg lid to a new 96-well plate containing 1X phosphate-buffered saline (PBS, 200  $\mu$ L) per well for 10 min. The peg lid was then transferred to a 96-well plate filled with crystal violet (CV, 0.1% [wt/vol], 200  $\mu$ L) for 15 min. To wash off excess CV, the lid was transferred to a single well tray of ddH<sub>2</sub>O (70 mL), for 10 min. This wash step was repeated four times. For CV elution off of the pegs, the peg lid was then transferred to a 96-well plate containing 95% ethanol (200  $\mu$ L) per well for 15 min and the CV absorbance was measured at 600 nm (BioTek ELx800, Winooski, VT, USA) to quantify biofilm growth on each peg.

***Preparation of dimeric/trimeric DNA libraries.*** The synthetic DNA template for the dimeric and trimeric DNA libraries began as a sequence of 5'-TGGTCC-N50-GTGTCGATC-3' (N50 = equimolar randomized region of 50 nucleotides; italicized represents site of TaqI restriction digestion). The 5'-terminus of the template (2400 pmol) was phosphorylated using the standard T4 polynucleotide kinase reaction (T4 PNK) in PNK buffer A (240  $\mu$ L, 50 mM Tris-HCl [pH7.6] 10 mM MgCl<sub>2</sub>, 5 mM DTT, 0.1 mM spermidine), ATP (10 mM), T4 PNK (0.5 units/ $\mu$ L). The reaction mixture was incubated at 37°C for 30 min, then heated at 90°C for 5 min, and finally cooled at room temperature for 10 min. The phosphorylated DNA template (800 pmol) was circularized using the DNA ligation procedure in DNA ligase buffer (400  $\mu$ L, 40 mM Tris-HCl, 10 mM MgCl<sub>2</sub>, 10 mM DTT, 0.5 mM ATP [pH 7.8]), using ligation template (1000 pmol, 5' GGACC

AGATC GACAC 3'; TaqI restriction digestion site is italicized), and T4 DNA ligase (0.1 units/ $\mu$ L). The reaction mixture was incubated at room temperature for 4 hrs, then heated at 90°C for 10 min, and finally cooled at room temperature for 5 min. The circularized DNA mixture was concentrated through ethanol precipitation and purified by 10% denaturing PAGE. Rolling circle amplification (RCA) was performed according to manufacturer's protocol. In brief, a mixture of circular DNA template (150 pmol), and RCA primer (150 pmol, 5' GGACC AGATC GACAC 3'; TaqI restriction digestion site is italicized) in 300  $\mu$ L of ddH<sub>2</sub>O was heated at 90°C for 1 min and then cooled at room temperature for 20 min. The following were introduced to the mixture: dNTPs (0.5 mM of each), phi29 DNA polymerase (0.4 units/ $\mu$ L) in a final reaction buffer of Tris-acetate (360  $\mu$ L, 33 mM, [pH 7.9]), Mg-acetate (10 mM), K-acetate (66 mM), Tween 20 [0.1% (v/v)], DTT (1 mM). The reaction was incubated at 30°C for 3 hrs and the RCA products were then concentrated through ethanol precipitation. To generate dimeric and trimeric DNA sequences, the RCA products were restriction digested according to manufacturer's protocol (New England BioLabs, Ipswich, MA, USA) using Taq I ( $3 \times 10^6$  units/ $\mu$ L) in a reaction buffer (150  $\mu$ L) of K-acetate (50 mM), Tris-acetate (20 mM, pH 7.9), Mg-acetate (10 mM), BSA (100  $\mu$ g/ml). In brief, reaction mixtures were incubated at 65°C for 1 hr and stopped by the addition of EDTA (20 mM, pH8). Samples were then concentrated through ethanol precipitation and purified by 10% denaturing PAGE to isolate dimeric and trimeric DNA sequences. Due to the tandem nature of the dimeric/trimeric DNA sequences, unique forward and reverse primer segments needed to be ligated to the ends of each sequence group to prepare for subsequent PCR steps. The sequences of the oligos

involved in ligation appear as follows: forward primer segment (5' GCACA TTACG GTT 3'), reverse primer segment (5' GCTGA CTATG GC 3'), forward primer ligation template (5' GTGTC GAACC GTAAT GTGC 3') and reverse primer ligation template (5' GCCAT AGTCA GCATC 3'). Through the standard T4 PNK reaction (Thermo Scientific, Canada), dimeric/trimeric DNA sequences were radioactively phosphorylated at the 5'-termini using [ $\alpha$ -<sup>32</sup>P]ATP, while the reverse primer segment was non-radioactively phosphorylated. For T4 DNA ligation reaction, a mixture of radioactively labeled dimeric/trimeric DNA (14 pmol), forward primer segment (14 pmol), forward primer ligation template (16 pmol), reverse primer segment (14 pmol), and reverse primer ligation template (16 pmol) was heated at 90°C, for 1 min, and then cooled at room temperature for 10 min. T4 DNA ligase (0.1 units/ $\mu$ L) was then added to the mixture in a final reaction buffer (100  $\mu$ L, 40 mM Tris-HCl, 10 mM MgCl<sub>2</sub>, 10 mM DTT, 0.5 mM ATP [pH 7.8]). After incubation at room temperature for 3 hrs, the reaction was stopped by EDTA addition (20 mM). Dimeric/trimeric DNA sequences (now ligated with specific primers) were purified using 10% denaturing PAGE.

***Polymerase Chain Reaction (PCR).*** After design and preparation, the DNA library sequences appear as follows: dimeric library (5' GCACA TTACG GTTCG ACAC – N50 – GGACC AGATC GACAC – N50 – GGACC AGATG CTGAC TATGG C 3'), trimeric library (5' GCACA TTACG GTTCG ACAC – N50 – GGACC AGATC GACAC – N50 – GGACC AGATC GACAC – N50 – GGACC AGATG CTGAC TATGG C 3'). For PCR1 (enrichment of target-binding sequences), the template was amplified using forward primer 5' GCACA TTACG GTTCG 3' and reverse primer 5' GCCAT AGTCA GCATC

3'. For PCR2 (isolation of target-binding, sense DNA strand), the template was amplified using forward primer 5' GCACA TTACG GTTCG 3' and reverse primer 5' AAAAA AAAAA AAAAA spacer GCCAT AGTCA GCATC 3' (spacer = 9-O-Dimethoxytrityl-triethylene glycol, 1-[(2-cyanoethyl)-(N,N-diisopropyl)]-phosphoramidite). PCR1 was conducted in Tris·HCl (pH 9.0, 75 mM), MgCl<sub>2</sub> (2 mM), KCl (50 mM), (NH<sub>4</sub>)<sub>2</sub>SO<sub>4</sub> (20 mM), primers (0.5 μM of each), DNA template (~3 nM), dNTPs (0.2 mM of each) and Taq DNA polymerase (five units, Biotools, Madrid, Spain). PCR2 followed the same conditions except the following were added: [ $\alpha$ -<sup>32</sup>P]dGTP (0.5 μL of 3000 Ci/mmol) and dNTPs (0.2 mM of dCTP, dATP and dTTP, 0.02 mM dGTP). Thermal cycling conditions varied depending on target type (biofilm/planktonic cells) and elution method (NaOH/EDTA) used. Generally, thermal cycling steps for the dimeric DNA were as follows: PCR1 (94°C for 1 min, 5-18 cycles of 94–49/52–72°C [30 s for each temperature], and finally 72°C for 8 min), PCR2 (same steps, except only 10 cycles were needed). Thermal cycling steps for the trimeric DNA were as follows: PCR1 (94°C for 1 min, 5-18 cycles of 94–43–72°C [30 s for each temperature], and finally 72°C for 8 min), PCR2 (same steps, except only 13 cycles were needed).

**Biofilm SELEX procedure.** For the first 7 rounds, *L. monocytogenes* biofilm was used as the target. After 72 hrs of growth, the biofilm peg lid was first transferred to a 96-well plate of 1X PBS (200 μL) for 20 min to remove loosely adhered cells. The peg-lid was then transferred to a new 96-well plate to interact with radioactively labeled DNA libraries (200 pmol, 2 wells contained the dimeric and trimeric DNA libraries respectively, and the remaining wells not involved in target-binding step contained 1X

PBS only). DNA libraries were allowed to interact with biofilm for 40 min. The peg lid was transferred to a new 96-well plate filled with 1X PBS (200  $\mu$ L per well) for 10 min to wash away DNA sequences that non-specifically bound to biofilm target. This step was repeated three times. To elute DNA sequences from the target, peg lid was then placed in a 96-well plate filled with NaOH (0.2 M, 200  $\mu$ L) for 15 min. Eluted dimeric and trimeric DNA were concentrated through ethanol precipitation for subsequent PCR steps and the next round of SELEX. Biofilm growth on pegs that interacted with DNA libraries were quantified as discussed above. Percent of target binding for each round was calculated using the following: % binding = (target/target+background) x 100% whereby “target” is radioactivity measured from DNA sequences eluted from the target, and “background” is radioactivity measured from DNA sequences obtained from all wash steps. Radioactivity was measured using a liquid scintillation counter (Beckman Coulter, LS6000, Mississauga, ON, Canada).

***Cell SELEX procedure.*** For rounds 8-17, planktonic cells of *L. monocytogenes* were used as the target. *L. monocytogenes* subculture (200  $\mu$ L, OD600 = 0.5,  $\sim 1 \times 10^9$  CFU/mL) was first washed three times by spinning down the cells (5000 g, 2 min), removing the supernatant and resuspending in binding buffer (200  $\mu$ L, 1X PBS, 20 mM MgCl<sub>2</sub>). Washed cells were then incubated with radioactively labeled dimeric or trimeric DNA libraries (200 pmol) in binding buffer (200  $\mu$ L) for 10 min. Non-specific binding DNA sequences were washed with wash buffer (200  $\mu$ L, 1X PBS, 20 mM MgCl<sub>2</sub>, Tween 20 [0.01% (v/v)]) three times. Specific binding DNA sequences were eluted from the cells by incubating in elution buffer (200  $\mu$ L, 10 mM EDTA) for 30 min. Eluted DNA was

then concentrated through ethanol precipitation for subsequent PCR steps and the next round of SELEX. Percent of target binding for each round was calculated using the same equation noted for biofilm-SELEX, and radioactivity was measured using a geiger counter (GSM-500, WB Johnson Instruments, Idaho Falls, ID, USA). As an internal control and assessment of target-binding specificity, for rounds 8-11 of SELEX, *L. innocua* (200  $\mu$ L, OD600 = 0.5,  $\sim 1 \times 10^9$  CFU/mL) was also tested for binding with the dimeric/trimeric DNA libraries and was subjected to pre-wash, target-binding, wash, and DNA elution steps alongside the samples treated with *L. monocytogenes* target. For rounds 9-17, a mixture of *E. coli* and *B. subtilis* (200  $\mu$ L of each, OD600 = 0.5,  $\sim 1 \times 10^9$  CFU/mL) were used as the internal control to assess binding specificity. Counter-SELEX was carried out for rounds 13 and 17, whereby a mixture of *E. coli* and *B. subtilis* subculture (200  $\mu$ L of each, OD600 = 0.5,  $\sim 1 \times 10^9$  CFU/mL) was incubated with the dimeric/trimeric DNA libraries respectively for 10 min, before spinning down and collecting unbound DNA sequences. Unbound DNA sequences were then incubated with *L. monocytogenes* and the usual SELEX steps followed afterwards. Additional modifications were made along the way to enhance binding specificity including: changing the DNA elution method from NaOH (0.2 M) to the more effective EDTA (10 mM, implemented from round 9 and onwards), spiking the DNA libraries with the original library (to accommodate for any loss sequences from previous rounds of NaOH elution (200 pmol, implemented at round 10), reducing concentration of target cells ( $\sim 5 \times 10^8$  CFU/mL, implemented round 12 and onwards), as well as DNA pool (100 pmol, implemented round 15 and onwards). After 17 rounds, dimeric and trimeric DNA pools

were cloned (InsTAclone PCR Cloning Kit, Thermo Scientific, Canada) and sequenced (Functional Biosciences Inc., Madison, WI, USA).

## **Results and Discussion**

### *Creation of dimeric and trimeric DNA libraries*

Homo-tandem DNA libraries were generated through rolling circle amplification (RCA) (Figure 2) [21, 22]. A circular, single-stranded (ss) DNA template encoding the TaqI restriction digestion site (5' TCGA 3') was created by: i) phosphorylating the 5' terminus of monomeric DNA with a randomized region of 50 nucleotides (N50) through a T4 polynucleotide kinase (PNK)-mediated reaction, and then ii) self-circularizing these DNA sequences by carrying out a T4 ligase-mediated reaction. An appropriately designed DNA primer was then annealed to the circular template, and phi29 DNA polymerase extended this primer by incorporating incoming dNTPs, while displacing the newly synthesized, complementary strand [21, 22]. A polymeric sequence composed of thousands of randomized DNA repeats along with TaqI restriction digest sites was generated through this process (Figure 3A). To create dimeric and trimeric sequences, TaqI restriction digestion for 30 and 60 min resulted in digested fragments [23]. Dimeric and trimeric DNA repeats were isolated from 10% denaturing PAGE for further analysis (Figure 3A). Afterwards, we ligated unique primer binding sequences to both 5' and 3' termini of the dimeric and trimeric libraries to facilitate subsequent PCR amplification (Figure 3B). The tandem DNA libraries were ready for SELEX.

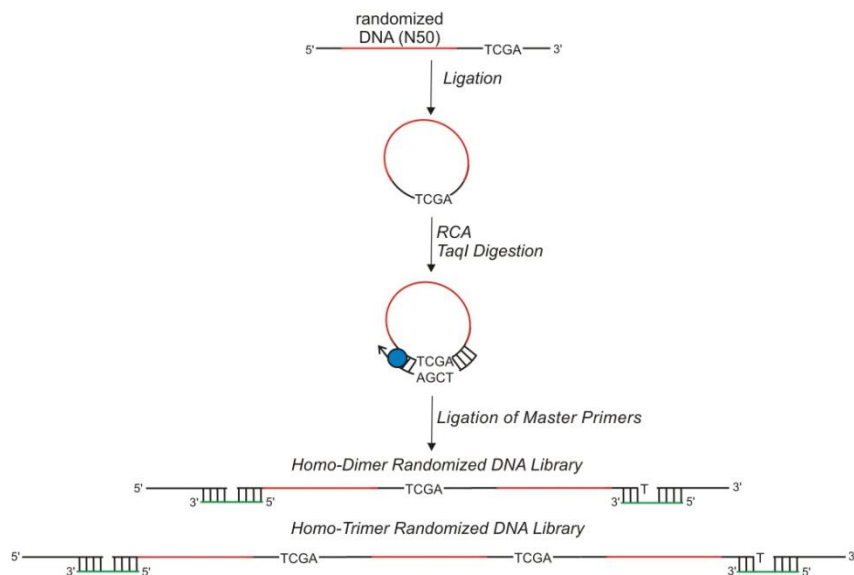


**Figure 2.** Scheme of creating the homo-tandem DNA library. Randomized DNA sequences that include a restriction enzyme site were ligated to form circular templates. Through rolling circle amplification (RCA), tandem repeats of the DNA library were generated. Restriction digestion was used to limit the number of repeats to form only dimeric and trimeric DNA libraries. Ligation of master primers prepared these random, tandem sequences for subsequent PCR amplification and SELEX.

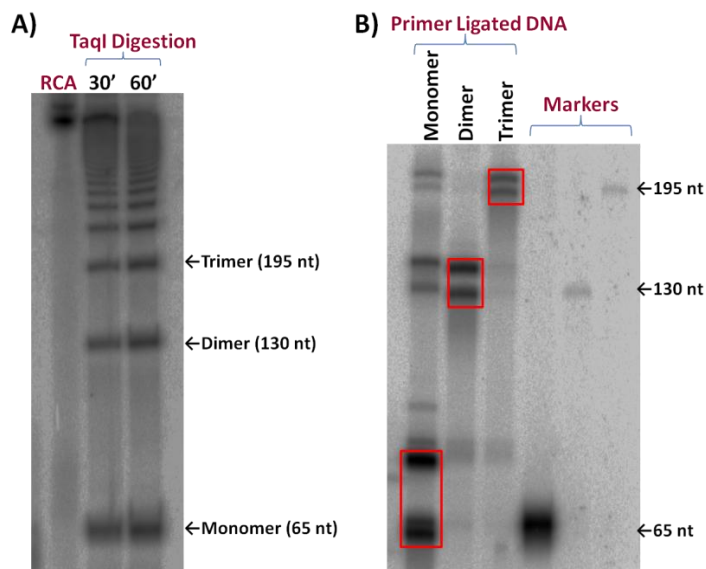


**Figure 3.** Creation of the homo-tandem DNA library (10% urea PAGE, [ $\alpha$ - $^{32}$ P]dGTP-labeled DNA). **A)** The RCA product generated was subjected to TaqI digestion at different time points to create the indicated monomeric, dimeric and trimeric DNA repeats. **B)** Tandem DNA repeats were subsequently ligated with unique primer binding

sequences to prepare for PCR amplification. Bands of interest are boxed (top band signifies ligated product, bottom band indicates unligated DNA).

### *Optimization of biofilm growth of L. monocytogenes*

Biofilm was grown on polystyrene pegs. By measuring the OD600 every 24 hrs, our results show that the most biofilm formed after 3 days (Figure 4A). A longer incubation time could possibly generate more biofilm. However, this may also lead to greater variability in growth as a mature biofilm is more prone to cell shedding. To confirm biofilm growth, an SEM image of 3-day old biofilm was taken (Figure 4B).

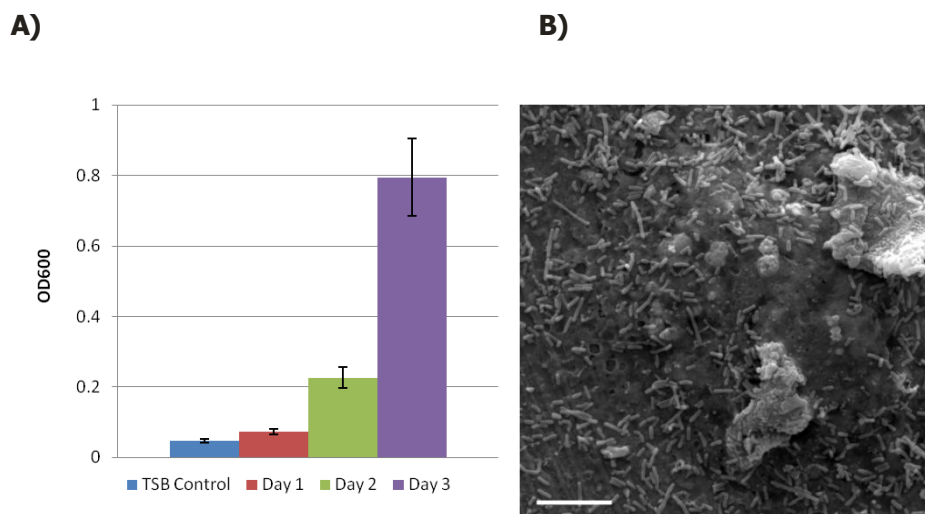


**Figure 4.** Biofilm growth of *L. monocytogenes* 568. **A)** Optimization of biofilm growth (TSB = tryptic soy broth; average of 48 replicates for biofilm samples, average of 12 replicates for TSB control). **B)** Scanning electron micrograph of *L. monocytogenes* biofilm. Image was taken by Uyen Nguyen from the Burrows' lab at McMaster University (magnification at 5 000x, bar represents 10 μm).

### ***Progress of SELEX***

For the first 7 rounds of SELEX, *L. monocytogenes* biofilm was used as the target. The experimental setup for biofilm-SELEX appears in Figure 5. For convenience and ease in handling, many steps involved in this process were carried out on 96-well plates. In brief, sample pegs with three-day old biofilm growth were first washed in a plate of 1X phosphate buffered saline (PBS) to remove any loosely associated planktonic cells. The sample pegs were then transferred to a new plate for incubation with the radiolabelled tandem DNA libraries. This biofilm-DNA binding step took place in a reaction buffer of 20 mM MgCl<sub>2</sub>, 1X PBS. The addition of MgCl<sub>2</sub> was necessary since previous studies have shown that divalent metal ions facilitate nucleic acid folding for target binding [24, 25]. Our experimental data also show that there is no detrimental effect to biofilm integrity at this metal ion concentration in a two hour incubation period (Figure 6A). Any sequences that bound non-specifically were then removed from the biofilm by washing the sample pegs in 20 mM MgCl<sub>2</sub>, 0.01% Tween20, 1X PBS. Our results show that this low percentage of detergent does not disrupt the biofilm in a test period of two hours (Figure 6B). Any DNA sequences that remained specifically bound to the biofilm were then eluted in NaOH solution. Our results show that at concentrations of 0.2-1 M NaOH, all biofilm was disrupted after two hours of incubation (Figure 6C). For the purpose of simply removing any biofilm-binding sequences, the lowest test concentration was chosen for use at a shorter incubation time. Eluted DNA was then subjected to PCR amplification to enrich the target-binding sequences and regenerate the DNA library for

the next round of SELEX. Percent binding to target was measured for each round (see experimental section for full details).

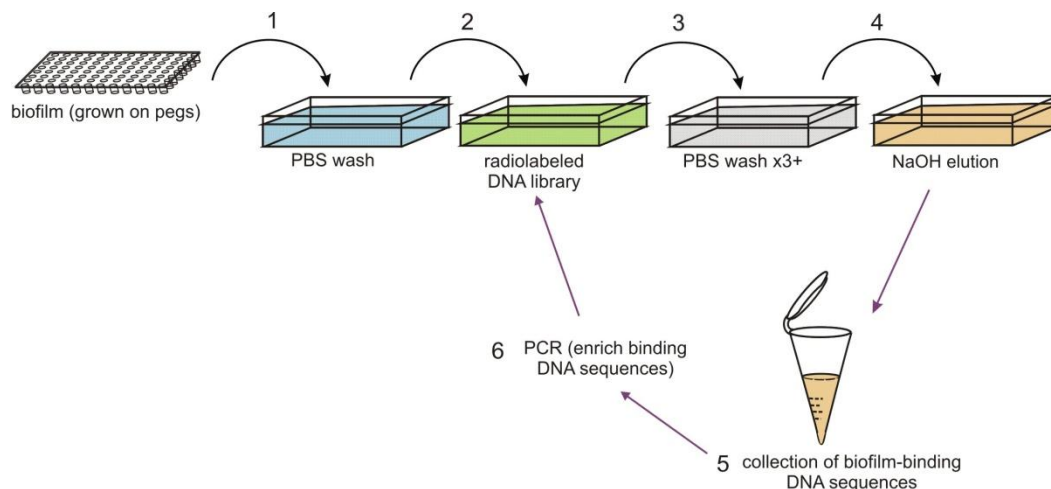


**Figure 5.** Overview of biofilm-SELEX.

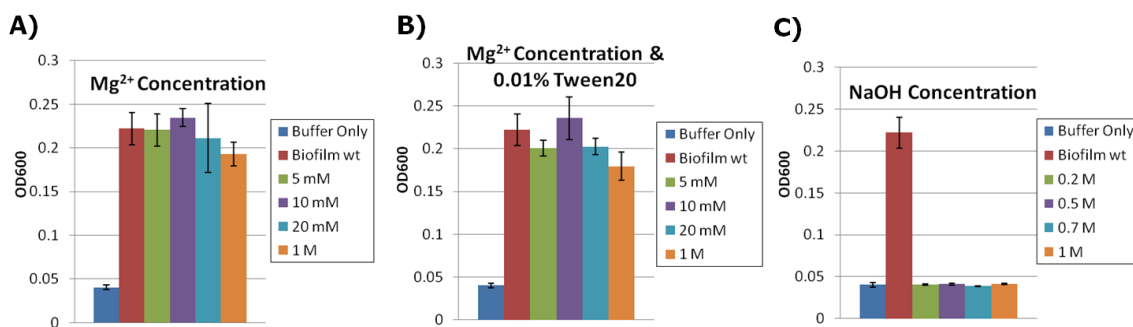


**Figure 6.** Finding optimal conditions for biofilm-SELEX. Effect of varying chemical concentrations on the integrity of biofilm required for **A)** binding, **B)** wash and **C)** elution steps of SELEX. All test concentrations were allowed to incubate with the biofilm for two hours at room temperature. Data is shown in triplicate.

At round 7, a small, but notable increase in percent binding to biofilm was observed for the dimeric DNA pool (~0.5%). In further testing of binding of dimeric and trimeric DNA pools to *L. monocytogenes* in planktonic and biofilm states, we discovered that the enriched DNA sequences were binding distinctly to the exposed free cells of the pathogen, as opposed to the matrix components of the biofilm (Figure 7A). To streamline the procedure and further develop these DNA sequences for *L. monocytogenes* detection, we decided to continue SELEX using free cells of the pathogen as the target (Figure 8).

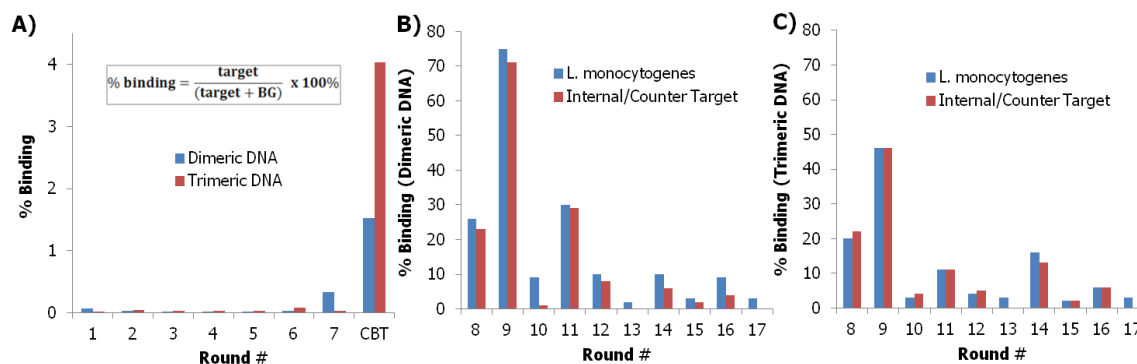


**Figure 7.** Progress of SELEX using tandem dimeric and trimeric DNA pools. **A)** The first 7 rounds were performed using *L. monocytogenes* biofilm as the target. Radioactively labeled DNA sequences were measured using liquid scintillation counting and % binding was calculated using target binding DNA and background (BG) DNA obtained from wash steps. Cell binding test (CBT) showed strong binding of DNA pools to free cells, as opposed to the biofilm matrix. Results pertaining to **B)** Dimeric DNA and **C)** Trimeric DNA pools: Planktonic cells of *L. monocytogenes* were used as the target for subsequent rounds and DNA sequences were measured with a geiger counter. In rounds 8-11, a separate *L. innocua* sample was implemented as an internal target to compare binding to that of the desired target and gage target specificity. In rounds 12-17, *E. coli* and *B. subtilis* were used as the internal targets for binding comparison, which also served as counter-SELEX targets for rounds 13 and 17 (no corresponding data for these rounds). See main text for full details.

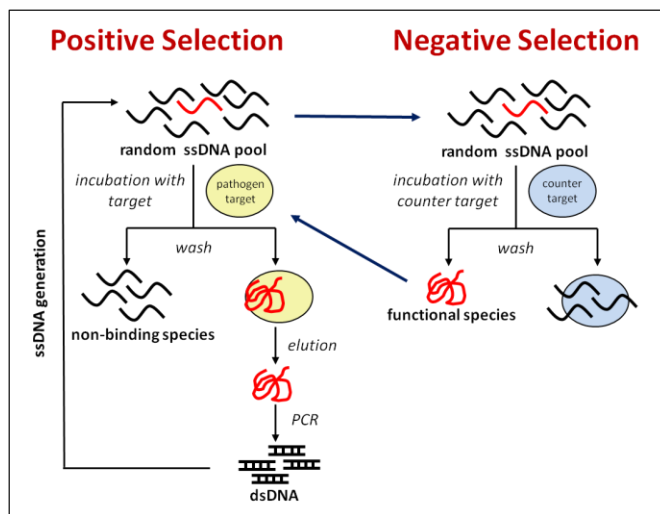


**Figure 8.** Overview of cell-SELEX.

From round 8 and onwards, we also tested binding of the tandem DNA libraries to an internal control target in parallel to *L. monocytogenes* to assess the level of target-binding specificity. For rounds 8-11, we implemented *L. innocua*, a closely related strain to *L. monocytogenes* as the internal control. No significant differences were found in binding to *L. monocytogenes* and *L. innocua* for either the dimeric (Figure 7B) or trimeric DNA pools (Figure 7C), which signifies that the tandem libraries cannot discriminate between closely related *Listeria* strains at this point in development. In effect, for subsequent rounds, we chose to use a mixture of *B. subtilis*, a Gram positive bacterium, and *E. coli*, a Gram negative bacterium as an internal control that is less closely related to *L. monocytogenes*. However, we also found that no significant differences were found in binding to *L. monocytogenes* and the internal control for either the dimeric (Figure 7B) or trimeric DNA pools (Figure 7C). To enhance binding specificity of the tandem DNA pools, we conducted negative selection for rounds 13 and 17, whereby a mixture of *E.*

*coli* and *B. subtilis* subculture was incubated with the dimeric/trimeric DNA libraries respectively to remove any sequences that recognize these counter targets (Figure 8). DNA sequences that did not bind the counter targets were then collected and incubated with *L. monocytogenes*. The usual SELEX steps followed afterwards for further enrichment of these sequences. Additional modifications were made along the way to enhance binding specificity including: changing the DNA elution method from NaOH to the more effective EDTA (increased DNA elution by up to 65%, data not shown; implemented from round 9 and onwards), spiking the DNA libraries with the original library to accommodate for any loss sequences from previous rounds of NaOH elution (implemented at round 10), reducing concentration of target cells (round 12 and onwards), as well as DNA pool (round 15 and onwards).

#### ***Analysis of dimeric and trimeric sequence data***

After completion of 17 rounds of SELEX, we suspect that we have developed DNA sequences that bind strongly to *L. monocytogenes* cells, but not specifically to this pathogen (Figure 7). To verify these results, we have cloned and sequenced our DNA pools from round 17. For the dimeric DNA pool, a distinct class of 8 sequences has emerged (Figure 9). Interestingly for this class of sequences, the central DNA spacer region, which was initially a fixed sequence, has been completely altered. Instead, the fixed spacer sequence (5' GGACC AGATG ACAC 3') has emerged in both of the designated binding domains. Quite possibly, this new sequence arrangement may have evolved out of binding necessity. Depending on the parameters of the cell surface molecule(s) these sequences bind to, the central region may have evolved to become the

new binding domain for the target, whereas the randomized regions evolved to become the new spacer regions that are inert of binding ability. Notably, the designated binding domains for all sequences have remained virtually identical. Differences between the two domains range from 0 to 6 point mutations. This finding is surprising given that PCR mutations were expected to accumulate after so many rounds of SELEX. Furthermore, many sequences contain repetitive regions of 5 to 7 nucleotides in length. Perhaps, the maintenance of homo-tandemness is required for target-binding. Similar observations were also found for the trimeric DNA pool (data not presented). There was only a minor loss of homo-tandemness among binding domains, and many sequences possess repetitive regions. However, no distinct class was found.

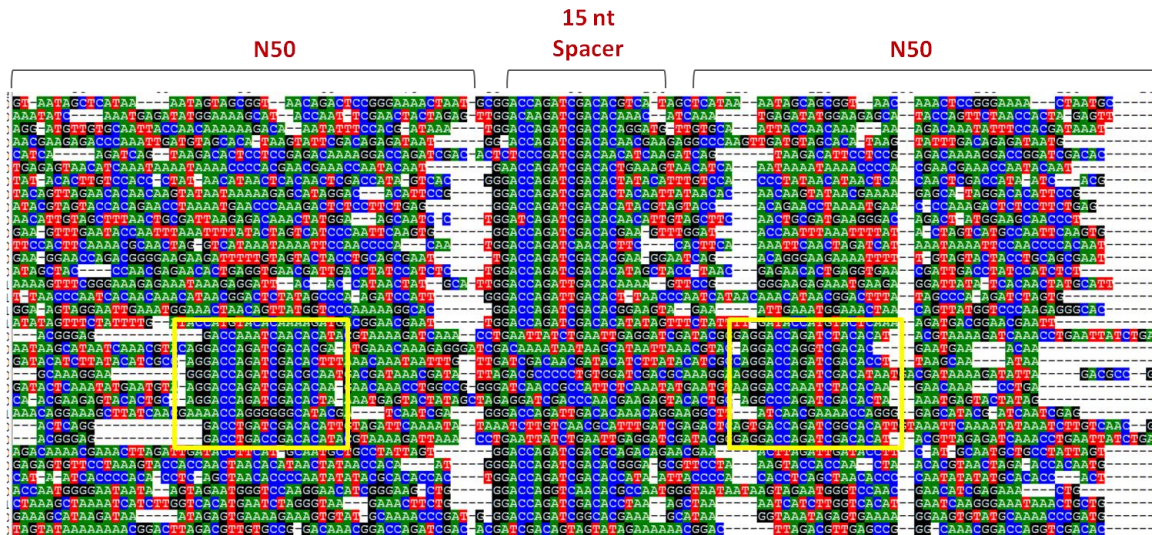


**Figure 9.** Sequencing results of the dimer DNA pool after 17 round of SELEX. N50 denotes each designated binding domain. Boxed areas signify conserved regions that have emerged. BioEdit software was used for sequence alignment.

## Future Directions

Subsequent work should focus on the distinct class that has emerged from the dimeric pool. The immediate next step would be to verify the target-binding ability of sequences from this class (ie. radioactive binding assays). It would also be important to compare the binding ability of the monomer, and central spacer regions to the full-length dimeric sequences to determine which elements are responsible for pathogen recognition. Additionally, conducting assays such as DNase footprinting would also help identify the precise binding site to further characterize these tandem aptamer candidates. To determine the binding specificity and affinity of these sequences, assays such as radioactive titration experiments using different bacterial strains as targets for binding can be performed. If the tandem aptamer candidates demonstrate non-specific binding to *L. monocytogenes*, then perhaps incorporation of rational design may enhance specificity. For instance, linking together monomer regions from different sequences in the dimeric class through PNK-mediated ligation may create customized, hetero-tandem aptamers that possess greater overall binding specificity to *L. monocytogenes*. Furthermore, optimizing the central linker length may also enhance the binding affinity, as many other studies have previously demonstrated [17-19].

If efforts through rational design do not enhance the binding ability of these tandem aptamer candidates, then redesign of the tandem DNA libraries and/or the SELEX strategy may be required. One possibility may be to use a simpler target such as a surface or regulatory protein of *L. monocytogenes* (ie. internalins A & B, positive regulatory factor A) that still serves as a biomarker for detection. These smaller, well-studied targets

have defined dimensions to accommodate optimal and more rational tandem library design. Another possibility may be to design a SELEX procedure that requires tandem binding to the target before sequence enrichment at the end of each round. For example in the case of dimeric DNA sequences, the requirement of two separate target-binding events during the functional step of SELEX would ensure the isolation of only the desired sequences to be carried on to subsequent rounds. Weaker sequences (ie. sequences that bind to only one target site) would be eliminated during the earlier stages of SELEX.

While further steps are required to characterize and optimize these tandem aptamer candidates, we can envision integration of these sequences for biosensor development in future studies (Figure 1C). For instance, tandem aptamers can be incorporated into a fluorescent structure-switching design, which we have already demonstrated is compatible with multiple fluorophore and quencher pairs [26]. We can adopt this design to include our dimeric aptamers, whereby aptamer-target binding results in two structure-switching events and enhanced signal generation. Regardless of the signal transduction method implemented, the polyvalent nature of tandem aptamers, may provide higher affinity and selective target recognition, as well as signal amplification, which may be beneficial for food detection.

### **Acknowledgements**

This work was supported by research grants from the Canadian Food Inspection Agency (CFIA), and the Natural Sciences and Engineering Research Council of Canada (NSERC).

## References for Appendix 2

1. Arora P, Sindhu A, Dilbaghi N, Chaudhury A (2011) Biosensors as innovative tools for the detection of food borne pathogens. *Biosens Bioelectron* 28: 1-12.
2. FDA (2005) *Listeria monocytogenes* Outbreaks. Website: <http://www.fda.gov/Food/FoodSafety/Product-SpecificInformation/MilkSafety/ConsumerInformationAboutMilkSafety/ucm165468.htm>
3. PHAC (2008) *Listeria monocytogenes* Outbreak. Website: <http://www.phac-aspc.gc.ca/media/cpho-acsp/listeria080820-eng.php>
4. Farber J (2010) Listeriosis in Canada: Anatomy of an Outbreak, Lessons-Learned and Path Forward. Health Canada.
5. Farber JM, Peterkin PI (1991) *Listeria monocytogenes*, a food-borne pathogen. *Microbiol Rev* 55: 476-511.
6. Mead PS, Slutsker L, Dietz V, McCaig LF, Bresee JS, Shapiro C, Griffin PM, Tauxe RV (1999) Food-related illness and death in the United States. *Emerg Infect Dis* 5: 607-625.
7. Harvey J, Keenan KP, Gilmour A (2007) Assessing biofilm formation by *Listeria monocytogenes* strains. *Food Microbiol* 24: 380-392.
8. Jaakohuhta S, Harma H, Tuomola M, Lovgren T (2007) Sensitive *Listeria* spp. immunoassay based on europium(III) nanoparticulate labels using time-resolved fluorescence. *Int J Food Microbiol* 114: 288-294.
9. Willis C, Greenwood M (2003) Wessex shopping basket survey - a structured approach to local food sampling. *Int J Environ Health Res* 13: 349-359.
10. Hussong D, Colwell RR, O'Brien M, Weiss E, Pearson AD, Weiner RM, Burge WD (1987) Viable *Legionella pneumophila* not detectable by culture on agar media. *Nat Biotechnol* 5: 947-950.
11. Koziol-Montewka M, Magrys A, Stojek N, Palusinska-Szys M, Danielak M, Wojtowicz M, Niewiedziol J, Koncewicz R, Niedzwiadek J, Paluch-Oles J, Trzeciak H, Drozanski W, Dutkiewicz J (2008) Monitoring *Legionella* species in hospital water systems. Link with disease and evaluation of different detection methods. *Ann Agric Environ Med* 15: 143-147.
12. Liu Y, Gilchrist A, Zhang J, Li XF (2008) Detection of viable but nonculturable *Escherichia coli* O157:H7 bacteria in drinking water and river water. *Appl Environ Microbiol* 74: 1502-1507.
13. Ellington AD, Szostak JW (1990) In vitro selection of RNA molecules that bind specific ligands. *Nature* 346: 818-822.
14. Tuerk C, Gold L (1990) Systematic evolution of ligands by exponential enrichment: RNA ligands to bacteriophage T4 DNA polymerase. *Science* 249: 505-510.
15. Klussmann S (2006) *The Aptamer Handbook*. Wiley-VCH: Weinheim.
16. Li Y, Lu Y (2009) *Functional Nucleic Acids for Analytical Applications*. Springer: New York.

17. Muller J, Wulffen B, Potzsch B, Mayer G (2007) Multidomain targeting generates a high-affinity thrombin-inhibiting bivalent aptamer. *Chembiochem* 8: 2223-2226.
18. Rinker S, Ke Y, Liu Y, Chhabra R, Yan H (2008) Self-assembled DNA nanostructures for distance-dependent multivalent ligand-protein binding. *Nat Nanotechnol* 3: 418-422.
19. Tian L, Heyduk T (2009) Bivalent ligands with long nanometer-scale flexible linkers. *Biochemistry* 48: 264-275.
20. Nguyen UT, Wenderska IB, Chong MA, Koteva K, Wright GD, Burrows LL (2012) Small-molecule modulators of *Listeria monocytogenes* biofilm development. *Appl Environ Microbiol* 78: 1454-1465.
21. Fire A, Xu SQ (1995) Rolling replication of short DNA circles. *Proc Natl Acad Sci USA* 92: 4641-4645.
22. Liu D, Daubendiek SL, Zillman MA, Ryan K, Kool ET (1996) Rolling circle DNA synthesis: Small circular oligonucleotides as efficient templates for DNA polymerases. *J Am Chem Soc* 118: 1587-1594.
23. Zhao W, Gao Y, Kandadai SA, Brook MA, Li Y (2006) DNA polymerization on gold nanoparticles through rolling circle amplification: towards novel scaffolds for three-dimensional periodic nanoassemblies. *Angew Chem Int Ed Engl* 45: 2409-2413.
24. Zimmermann GR, Wick CL, Shields TP, Jenison RD, Pardi A (2000) Molecular interactions and metal binding in the theophylline-binding core of an RNA aptamer. *RNA* 6: 659-667.
25. Rupcich N, Chiuman W, Nutiu R, Mei S, Flora KK, Li Y, Brennan JD (2006) Quenching of fluorophore-labeled DNA oligonucleotides by divalent metal ions: implications for selection, design, and applications of signaling aptamers and signaling deoxyribozymes. *J Am Chem Soc* 128: 780-790.
26. Lau PS, Lai CK, Li Y (2013) Quality control certification of RNA aptamer-based detection. *Chembiochem* 14: 987-992.

## REFERENCES

1. Gerstein M, Krebs W (1998) A database of macromolecular motions. *Nucleic Acids Res* 26: 4280-4290.
2. Nahvi A, Sudarsan N, Ebert MS, Zou X, Brown KL, et al. (2002) Genetic control by a metabolite binding mRNA. *Chem Biol* 9: 1043.
3. Roth A, Breaker RR (2009) The structural and functional diversity of metabolite-binding riboswitches. *Annu Rev Biochem* 78: 305-334.
4. Tucker BJ, Breaker RR (2005) Riboswitches as versatile gene control elements. *Curr Opin Struct Biol* 15: 342-348.
5. Mandal M, Breaker RR (2004) Gene regulation by riboswitches. *Nat Rev Mol Cell Biol* 5: 451-463.
6. Topp S, Gallivan JP (2010) Emerging applications of riboswitches in chemical biology. *ACS Chem Biol* 5: 139-148.
7. Werstuck G, Green MR (1998) Controlling gene expression in living cells through small molecule-RNA interactions. *Science* 282: 296-298.
8. Thompson KM, Syrett HA, Knudsen SM, Ellington AD (2002) Group I aptazymes as genetic regulatory switches. *BMC Biotechnol* 2: 21-32.
9. Suess B, Hanson S, Berens C, Fink B, Schroeder R, et al. (2003) Conditional gene expression by controlling translation with tetracycline-binding aptamers. *Nucleic Acids Res* 31: 1853-1858.
10. Suess B, Fink B, Berens C, Stentz R, Hillen W (2004) A theophylline responsive riboswitch based on helix slipping controls gene expression in vivo. *Nucleic Acids Res* 32: 1610-1614.
11. Desai SK, Gallivan JP (2004) Genetic screens and selections for small molecules based on a synthetic riboswitch that activates protein translation. *J Am Chem Soc* 126: 13247-13254.
12. Weigand JE, Sanchez M, Gunnesch EB, Zeiher S, Schroeder R, et al. (2008) Screening for engineered neomycin riboswitches that control translation initiation. *RNA* 14: 89-97.
13. Topp S, Gallivan JP (2007) Guiding bacteria with small molecules and RNA. *J Am Chem Soc* 129: 6807-6811.
14. Topp S, Gallivan JP (2008) Random walks to synthetic riboswitches--a high-throughput selection based on cell motility. *Chembiochem* 9: 210-213.
15. Ellington AD, Szostak JW (1990) In vitro selection of RNA molecules that bind specific ligands. *Nature* 346: 818-822.
16. Tuerk C, Gold L (1990) Systematic evolution of ligands by exponential enrichment: RNA ligands to bacteriophage T4 DNA polymerase. *Science* 249: 505-510.
17. Bunka DH, Stockley PG (2006) Aptamers come of age - at last. *Nat Rev Microbiol* 4: 588-596.
18. Lee JF, Hesselberth JR, Meyers LA, Ellington AD (2004) Aptamer database. *Nucleic Acids Res* 32: D95-100.

19. Lau PS, Li Y (2011) Functional nucleic acids as molecular recognition elements for small organic and biological molecules. *Curr Org Chem* 15: 557-575.
20. Vallee-Belisle A, Plaxco KW (2010) Structure-switching biosensors: inspired by nature. *Curr Opin Struct Biol* 20: 518-526.
21. Klussmann S, editor (2006) *The Aptamer Handbook*. Weinheim: Wiley-VCH.
22. Nutiu R, Li Y (2003) Structure-switching signaling aptamers. *J Am Chem Soc* 125: 4771-4778.
23. Huizenga DE, Szostak JW (1995) A DNA aptamer that binds adenosine and ATP. *Biochemistry* 34: 656-665.
24. Bock LC, Griffin LC, Latham JA, Vermaas EH, Toole JJ (1992) Selection of single-stranded DNA molecules that bind and inhibit human thrombin. *Nature* 355: 564-566.
25. Han K, Liang Z, Zhou N (2010) Design strategies for aptamer-based biosensors. *Sensors* 10: 4541-4557.
26. White RJ, Rowe AA, Plaxco KW (2010) Re-engineering aptamers to support reagentless, self-reporting electrochemical sensors. *Analyst* 135: 589-594.
27. Nutiu R, Li YF (2005) In vitro selection of structure-switching signaling aptamers. *Angew Chem Int Ed Engl* 44: 1061-1065.
28. Lin CH, Patel DJ (1997) Structural basis of DNA folding and recognition in an AMP-DNA aptamer complex: distinct architectures but common recognition motifs for DNA and RNA aptamers complexed to AMP. *Chem Biol* 4: 817-832.
29. Wang Z, Heon Lee J, Lu Y (2008) Highly sensitive "turn-on" fluorescent sensor for Hg<sup>2+</sup> in aqueous solution based on structure-switching DNA. *Chem Commun (Camb)*: 6005-6007.
30. Wu DH, Zhang Q, Chu X, Wang HB, Shen GL, et al. (2010) Ultrasensitive electrochemical sensor for mercury (II) based on target-induced structure-switching DNA. *Biosens Bioelectron* 25: 1025-1031.
31. Taylor SK, Pei RJ, Moon BC, Damera S, Shen AH, et al. (2009) Triggered release of an active peptide conjugate from a DNA device by an orally administrable small molecule. *Angew Chem Int Ed Engl* 48: 4394-4397.
32. Liu J, Lu Y (2005) Fast colorimetric sensing of adenosine and cocaine based on a general sensor design involving aptamers and nanoparticles. *Angew Chem Int Ed Engl* 45: 90-94.
33. Null EL, Lu Y (2010) Rapid determination of enantiomeric ratio using fluorescent DNA or RNA aptamers. *Analyst* 135: 419-422.
34. Feng KJ, Sun CH, Jiang JH, Yu RQ (2011) An aptamer-based competitive fluorescence quenching assay for IgE. *Anal Lett* 44: 1301-1309.
35. Zhu ZY, Schmidt T, Mahrous M, Guieu V, Perrier S, et al. (2011) Optimization of the structure-switching aptamer-based fluorescence polarization assay for the sensitive tyrosinamide sensing. *Anal Chim Acta* 707: 191-196.
36. Niu WZ, Jiang N, Hu YH (2007) Detection of proteins based on amino acid sequences by multiple aptamers against tripeptides. *Anal Biochem* 362: 126-135.

37. Liu DY, Zhao Y, He XW, Yin XB (2011) Electrochemical aptasensor using the tripropylamine oxidation to probe intramolecular displacement between target and complementary nucleotide for protein array. *Biosens Bioelectron* 26: 2905-2910.
38. Yang LT, Fung CW, Cho EJ, Ellington AD (2007) Real-time rolling circle amplification for protein detection. *Anal Chem* 79: 3320-3329.
39. Song YJ, Zhao C, Ren JS, Qu XG (2009) Rapid and ultra-sensitive detection of AMP using a fluorescent and magnetic nano-silica sandwich complex. *Chem Commun*: 1975-1977.
40. Levy M, Cater SF, Ellington AD (2005) Quantum-dot aptamer beacons for the detection of proteins. *Chembiochem* 6: 2163-2166.
41. Liu JW, Lee JH, Lu Y (2007) Quantum dot encoding of aptamer-linked nanostructures for one-pot simultaneous detection of multiple analytes. *Anal Chem* 79: 4120-4125.
42. Elowe NH, Nutiu R, Allah-Hassani A, Cechetto JD, Hughes DW, et al. (2006) Small-molecule screening made simple for a difficult target with a signaling nucleic acid aptamer that reports on deaminase activity. *Angew Chem Int Ed Engl* 45: 5648-5652.
43. Aldrich MB, Blackburn MR, Kellems RE (2000) The importance of adenosine deaminase for lymphocyte development and function. *Biochem Biophys Res Commun* 272: 311-315.
44. Fowler CC, Brown ED, Li Y (2008) A FACS-based approach to engineering artificial riboswitches. *Chembiochem* 9: 1906-1911.
45. Huang PJJ, Liu JW (2010) Flow cytometry-assisted detection of adenosine in serum with an immobilized aptamer sensor. *Anal Chem* 82: 4020-4026.
46. Zheng D, Seferos DS, Giljohann DA, Patel PC, Mirkin CA (2009) Aptamer Nanoflares for Molecular Detection in Living Cells. *Nano Lett* 9: 3258-3261.
47. Rupcich N, Nutiu R, Li YF, Brennan JD (2005) Entrapment of fluorescent signaling DNA aptamers in sol-gel-derived silica. *Anal Chem* 77: 4300-4307.
48. Carrasquilla C, Li YF, Brennan JD (2011) Surface Immobilization of Structure-Switching DNA Aptamers on Macroporous Sol-Gel-Derived Films for Solid-Phase Biosensing Applications. *Anal Chem* 83: 957-965.
49. El-Hamed F, Dave N, Liu J (2011) Stimuli-responsive releasing of gold nanoparticles and liposomes from aptamer-functionalized hydrogels. *Nanotechnology* 22: 494011.
50. Su SX, Nutiu R, Filipe CDM, Li YF, Pelton R (2007) Adsorption and covalent coupling of ATP-binding DNA aptamers onto cellulose. *Langmuir* 23: 1300-1302.
51. Radi AE, Acero Sanchez JL, Baldrich E, O'Sullivan CK (2006) Reagentless, reusable, ultrasensitive electrochemical molecular beacon aptasensor. *J Am Chem Soc* 128: 117-124.
52. Luong JH, Male KB, Glennon JD (2008) Biosensor technology: technology push versus market pull. *Biotechnol Adv* 26: 492-500.
53. Yoshizumi J, Kumamoto S, Nakamura M, Yamana K (2008) Target-induced strand release (TISR) from aptamer-DNA duplex: A general strategy for electronic

- detection of biomolecules ranging from a small molecule to a large protein. *Analyst* 133: 323-325.
54. Zuo XL, Song SP, Zhang J, Pan D, Wang LH, et al. (2007) A target-responsive electrochemical aptamer switch (TREAS) for reagentless detection of nanomolar ATP. *J Am Chem Soc* 129: 1042-1043.
  55. Wang JL, Wang F, Dong SJ (2009) Methylene blue as an indicator for sensitive electrochemical detection of adenosine based on aptamer switch. *J Electroanal Chem* 626: 1-5.
  56. Du Y, Li BL, Wang F, Dong SJ (2009) Au nanoparticles grafted sandwich platform used amplified small molecule electrochemical aptasensor. *Biosens Bioelectron* 24: 1979-1983.
  57. Guo SJ, Du Y, Yang X, Dong SJ, Wang EK (2011) Solid-state label-free integrated aptasensor based on graphene-mesoporous silica-gold nanoparticle hybrids and silver microspheres. *Anal Chem* 83: 8035-8040.
  58. Zhang SS, Xia JP, Li XM (2008) Electrochemical biosensor for detection of adenosine based on structure-switching aptamer and amplification with reporter probe DNA modified Au nanoparticles. *Anal Chem* 80: 8382-8388.
  59. Li W, Nie Z, Xu XH, Shen QP, Deng CY, et al. (2009) A sensitive, label free electrochemical aptasensor for ATP detection. *Talanta* 78: 954-958.
  60. Zhang XR, Zhao YQ, Li SG, Zhang SS (2010) Photoelectrochemical biosensor for detection of adenosine triphosphate in the extracts of cancer cells. *Chem Commun* 46: 9173-9175.
  61. Du Y, Li BL, Wei H, Wang YL, Wang EK (2008) Multifunctional label-free electrochemical biosensor based on an integrated aptamer. *Anal Chem* 80: 5110-5117.
  62. Clark LC, Jr., Lyons C (1962) Electrode systems for continuous monitoring in cardiovascular surgery. *Ann N Y Acad Sci* 102: 29-45.
  63. Montagnana M, Caputo M, Giavarina D, Lippi G (2009) Overview on self-monitoring of blood glucose. *Clin Chim Acta* 402: 7-13.
  64. Xiang Y, Lu Y (2011) Using personal glucose meters and functional DNA sensors to quantify a variety of analytical targets. *Nat Chem* 3: 697-703.
  65. Liu JW, Lu Y (2006) Fast colorimetric sensing of adenosine and cocaine based on a general sensor design involving aptamers and nanoparticles. *Angew Chem Int Ed* 45: 90-94.
  66. Zhao WA, Chiunan W, Brook MA, Li YF (2007) Simple and rapid colorimetric biosensors based on DNA aptamer and noncrosslinking gold nanoparticle aggregation. *Chembiochem* 8: 727-731.
  67. Wang J, Wang LH, Liu XF, Liang ZQ, Song SP, et al. (2007) A gold nanoparticle-based aptamer target binding readout for ATP assay. *Adv Mater* 19: 3943-+.
  68. Liu JW, Lu Y (2006) Smart nanomaterials responsive to multiple chemical stimuli with controllable cooperativity. *Adv Mater* 18: 1667-+.
  69. Liu JW, Mazumdar D, Lu Y (2006) A simple and sensitive "dipstick" test in serum based on lateral flow separation of aptamer-linked nanostructures". *Angew Chem Int Ed Engl* 45: 7955-7959.

70. Stoddard CD, Batey RT (2006) Mix-and-match riboswitches. *ACS Chem Biol* 1: 751-754.
71. Winkler WC, Breaker RR (2003) Genetic control by metabolite-binding riboswitches. *ChemBiochem* 4: 1024-1032.
72. Johansen LE, Nygaard P, Lassen C, Agerso Y, Saxild HH (2003) Definition of a second *Bacillus subtilis* pur regulon comprising the pur and xpt-pbuX operons plus pbuG, nupG (yxjA), and pbuE (ydhL). *J Bacteriol* 185: 5200-5209.
73. Mandal M, Breaker RR (2004) Adenine riboswitches and gene activation by disruption of a transcription terminator. *Nat Struct Mol Biol* 11: 29-35.
74. Mandal M, Boese B, Barrick JE, Winkler WC, Breaker RR (2003) Riboswitches control fundamental biochemical pathways in *Bacillus subtilis* and other bacteria. *Cell* 113: 577-586.
75. Roth A, Winkler WC, Regulski EE, Lee BW, Lim J, et al. (2007) A riboswitch selective for the queuosine precursor preQ1 contains an unusually small aptamer domain. *Nat Struct Mol Biol* 14: 308-317.
76. Meyer MM, Roth A, Chervin SM, Garcia GA, Breaker RR (2008) Confirmation of a second natural preQ1 aptamer class in *Streptococcaceae* bacteria. *RNA* 14: 685-695.
77. Mironov AS, Gusarov I, Rafikov R, Lopez LE, Shatalin K, et al. (2002) Sensing small molecules by nascent RNA: a mechanism to control transcription in bacteria. *Cell* 111: 747-756.
78. Rodionov DA, Vitreschak AG, Mironov AA, Gelfand MS (2002) Comparative genomics of thiamin biosynthesis in prokaryotes. New genes and regulatory mechanisms. *J Biol Chem* 277: 48949-48959.
79. Cheah MT, Wachter A, Sudarsan N, Breaker RR (2007) Control of alternative RNA splicing and gene expression by eukaryotic riboswitches. *Nature* 447: 497-500.
80. Wachter A, Tunc-Ozdemir M, Grove BC, Green PJ, Shintani DK, et al. (2007) Riboswitch control of gene expression in plants by splicing and alternative 3' end processing of mRNAs. *Plant Cell* 19: 3437-3450.
81. Croft MT, Moulin M, Webb ME, Smith AG (2007) Thiamine biosynthesis in algae is regulated by riboswitches. *Proc Natl Acad Sci U S A* 104: 20770-20775.
82. Bocobza S, Adato A, Mandel T, Shapira M, Nudler E, et al. (2007) Riboswitch-dependent gene regulation and its evolution in the plant kingdom. *Genes Dev* 21: 2874-2879.
83. Winkler WC, Cohen-Chalamish S, Breaker RR (2002) An mRNA structure that controls gene expression by binding FMN. *Proc Natl Acad Sci U S A* 99: 15908-15913.
84. Sudarsan N, Lee ER, Weinberg Z, Moy RH, Kim JN, et al. (2008) Riboswitches in eubacteria sense the second messenger cyclic di-GMP. *Science* 321: 411-413.
85. Mandal M, Lee M, Barrick JE, Weinberg Z, Emilsson GM, et al. (2004) A glycine-dependent riboswitch that uses cooperative binding to control gene expression. *Science* 306: 275-279.

86. Grundy FJ, Lehman SC, Henkin TM (2003) The L box regulon: lysine sensing by leader RNAs of bacterial lysine biosynthesis genes. *Proc Natl Acad Sci U S A* 100: 12057-12062.
87. Rodionov DA, Vitreschak AG, Mironov AA, Gelfand MS (2003) Regulation of lysine biosynthesis and transport genes in bacteria: yet another RNA riboswitch? *Nucleic Acids Res* 31: 6748-6757.
88. Sudarsan N, Wickiser JK, Nakamura S, Ebert MS, Breaker RR (2003) An mRNA structure in bacteria that controls gene expression by binding lysine. *Genes Dev* 17: 2688-2697.
89. Gilbert SD, Rambo RP, Van Tyne D, Batey RT (2008) Structure of the SAM-II riboswitch bound to S-adenosylmethionine. *Nat Struct Mol Biol* 15: 177-182.
90. Corbino KA, Barrick JE, Lim J, Welz R, Tucker BJ, et al. (2005) Evidence for a second class of S-adenosylmethionine riboswitches and other regulatory RNA motifs in alpha-proteobacteria. *Genome Biol* 6: R70.
91. Epshtein V, Mironov AS, Nudler E (2003) The riboswitch-mediated control of sulfur metabolism in bacteria. *Proc Natl Acad Sci U S A* 100: 5052-5056.
92. Fuchs RT, Grundy FJ, Henkin TM (2006) The S(MK) box is a new SAM-binding RNA for translational regulation of SAM synthetase. *Nat Struct Mol Biol* 13: 226-233.
93. McDaniel BA, Grundy FJ, Artsimovitch I, Henkin TM (2003) Transcription termination control of the S box system: direct measurement of S-adenosylmethionine by the leader RNA. *Proc Natl Acad Sci U S A* 100: 3083-3088.
94. Winkler WC, Nahvi A, Sudarsan N, Barrick JE, Breaker RR (2003) An mRNA structure that controls gene expression by binding S-adenosylmethionine. *Nat Struct Biol* 10: 701-707.
95. Wang JX, Lee ER, Morales DR, Lim J, Breaker RR (2008) Riboswitches that sense S-adenosylhomocysteine and activate genes involved in coenzyme recycling. *Mol Cell* 29: 691-702.
96. Borovok I, Gorovitz B, Schreiber R, Aharonowitz Y, Cohen G (2006) Coenzyme B12 controls transcription of the *Streptomyces* class Ia ribonucleotide reductase *nrdABS* operon via a riboswitch mechanism. *J Bacteriol* 188: 2512-2520.
97. Warner DF, Savvi S, Mizrahi V, Dawes SS (2007) A riboswitch regulates expression of the coenzyme B12-independent methionine synthase in *Mycobacterium tuberculosis*: implications for differential methionine synthase function in strains H37Rv and CDC1551. *J Bacteriol* 189: 3655-3659.
98. Winkler WC, Nahvi A, Roth A, Collins JA, Breaker RR (2004) Control of gene expression by a natural metabolite-responsive ribozyme. *Nature* 428: 281-286.
99. Cromie MJ, Shi Y, Latifi T, Groisman EA (2006) An RNA sensor for intracellular Mg(2+). *Cell* 125: 71-84.
100. Baker JL, Sudarsan N, Weinberg Z, Roth A, Stockbridge RB, et al. (2012) Widespread genetic switches and toxicity resistance proteins for fluoride. *Science* 335: 233-235.

101. Welz R, Breaker RR (2007) Ligand binding and gene control characteristics of tandem riboswitches in *Bacillus anthracis*. *RNA* 13: 573-582.
102. Wang JX, Breaker RR (2008) Riboswitches that sense S-adenosylmethionine and S-adenosylhomocysteine. *Biochem Cell Biol* 86: 157-168.
103. Ciampi MS (2006) Rho-dependent terminators and transcription termination. *Microbiology* 152: 2515-2528.
104. Grate D, Wilson C (2001) Inducible regulation of the *S. cerevisiae* cell cycle mediated by an RNA aptamer-ligand complex. *Bioorg Med Chem* 9: 2565-2570.
105. Buskirk AR, Landrigan A, Liu DR (2004) Engineering a ligand-dependent RNA transcriptional activator. *Chem Biol* 11: 1157-1163.
106. Sharma V, Nomura Y, Yokobayashi Y (2008) Engineering complex riboswitch regulation by dual genetic selection. *J Am Chem Soc* 130: 16310-16315.
107. Famulok M (2005) Allosteric aptamers and aptazymes as probes for screening approaches. *Curr Opin Mol Ther* 7: 137-143.
108. Lynch SA, Desai SK, Sajja HK, Gallivan JP (2007) A high-throughput screen for synthetic riboswitches reveals mechanistic insights into their function. *Chem Biol* 14: 173-184.
109. Lauhon CT, Szostak JW (1995) RNA aptamers that bind flavin and nicotinamide redox cofactors. *J Am Chem Soc* 117: 1246-1257.
110. Burke DH, Hoffman DC (1998) A novel acidophilic RNA motif that recognizes coenzyme A. *Biochemistry* 37: 4653-4663.
111. Burgstaller P, Famulok M (1994) Isolation of RNA aptamers for biological cofactors by in-vitro selection. *Angew Chem Int Ed Engl* 33: 1084-1087.
112. Roychowdhury-Saha M, Lato SM, Shank ED, Burke DH (2002) Flavin recognition by an RNA aptamer targeted toward FAD. *Biochemistry* 41: 2492-2499.
113. Gebhardt K, Shokraei A, Babaie E, Lindqvist BH (2000) RNA aptamers to S-adenosylhomocysteine: kinetic properties, divalent cation dependency, and comparison with anti-S-adenosylhomocysteine antibody. *Biochemistry* 39: 7255-7265.
114. Wilson C, Nix J, Szostak J (1998) Functional requirements for specific ligand recognition by a biotin-binding RNA pseudoknot. *Biochemistry* 37: 14410-14419.
115. Jenison RD, Gill SC, Pardi A, Polisky B (1994) High-resolution molecular discrimination by RNA. *Science* 263: 1425-1429.
116. Lau JL, Baksh MM, Fiedler JD, Brown SD, Kussrow A, et al. (2011) Evolution and protein packaging of small-molecule RNA aptamers. *ACS Nano* 5: 7722-7729.
117. Lorsch JR, Szostak JW (1994) In vitro selection of RNA aptamers specific for cyanocobalamin. *Biochemistry* 33: 973-982.
118. Win MN, Klein JS, Smolke CD (2006) Codeine-binding RNA aptamers and rapid determination of their binding constants using a direct coupling surface plasmon resonance assay. *Nucleic Acids Res* 34: 5670-5682.
119. Lato SM, Boles AR, Ellington AD (1995) In vitro selection of RNA lectins: using combinatorial chemistry to interpret ribozyme evolution. *Chem Biol* 2: 291-303.
120. Kwon M, Chun SM, Jeong S, Yu J (2001) In vitro selection of RNA against kanamycin B. *Mol Cells* 11: 303-311.

121. Burke DH, Hoffman DC, Brown A, Hansen M, Pardi A, et al. (1997) RNA aptamers to the peptidyl transferase inhibitor chloramphenicol. *Chem Biol* 4: 833-843.
122. Wallace ST, Schroeder R (1998) In vitro selection and characterization of streptomycin-binding RNAs: recognition discrimination between antibiotics. *RNA* 4: 112-123.
123. Berens C, Thain A, Schroeder R (2001) A tetracycline-binding RNA aptamer. *Bioorg Med Chem* 9: 2549-2556.
124. Wang Y, Rando RR (1995) Specific binding of aminoglycoside antibiotics to RNA. *Chem Biol* 2: 281-290.
125. Wallis MG, von Ahsen U, Schroeder R, Famulok M (1995) A novel RNA motif for neomycin recognition. *Chem Biol* 2: 543-552.
126. Wallis MG, Streicher B, Wank H, von Ahsen U, Clodi E, et al. (1997) In vitro selection of a viomycin-binding RNA pseudoknot. *Chem Biol* 4: 357-366.
127. Famulok M (1994) Molecular recognition of amino acids by RNA aptamers: an L-citrulline binding RNA motif and its evolution into an L-arginine binder. *J Am Chem Soc* 116: 1698-1706.
128. Geiger A, Burgstaller P, von der Eltz H, Roeder A, Famulok M (1996) RNA aptamers that bind L-arginine with sub-micromolar dissociation constants and high enantioselectivity. *Nucleic Acids Res* 24: 1029-1036.
129. Majerfeld I, Puthenvedu D, Yarus M (2005) RNA affinity for molecular L-histidine; genetic code origins. *J Mol Evol* 61: 226-235.
130. Majerfeld I, Yarus M (2005) A diminutive and specific RNA binding site for L-tryptophan. *Nucleic Acids Res* 33: 5482-5493.
131. Famulok M, Szostak JW (1992) Stereospecific recognition of tryptophan agarose by in vitro selected RNA. *J Am Chem Soc* 114: 3990-3991.
132. Majerfeld I, Yarus M (1998) Isoleucine: RNA sites with associated coding sequences. *RNA* 4: 471-478.
133. Mannironi C, Scerch C, Fruscoloni P, Tocchini-Valentini GP (2000) Molecular recognition of amino acids by RNA aptamers: the evolution into an L-tyrosine binder of a dopamine-binding RNA motif. *RNA* 6: 520-527.
134. Majerfeld I, Yarus M (1994) An RNA pocket for an aliphatic hydrophobe. *Nat Struct Biol* 1: 287-292.
135. Mannironi C, Di Nardo A, Fruscoloni P, Tocchini-Valentini GP (1997) In vitro selection of dopamine RNA ligands. *Biochemistry* 36: 9726-9734.
136. Illangasekare M, Yarus M (2002) Phenylalanine-binding RNAs and genetic code evolution. *J Mol Evol* 54: 298-311.
137. Kiga D, Futamura Y, Sakamoto K, Yokoyama S (1998) An RNA aptamer to the xanthine/guanine base with a distinctive mode of purine recognition. *Nucleic Acids Res* 26: 1755-1760.
138. Sazani PL, Larralde R, Szostak JW (2004) A small aptamer with strong and specific recognition of the triphosphate of ATP. *J Am Chem Soc* 126: 8370-8371.
139. Meli M, Vergne J, Decout JL, Maurel MC (2002) Adenine-aptamer complexes: a bipartite RNA site that binds the adenine nucleic base. *J Biol Chem* 277: 2104-2111.

140. Haller AA, Sarnow P (1997) In vitro selection of a 7-methyl-guanosine binding RNA that inhibits translation of capped mRNA molecules. *Proc Natl Acad Sci U S A* 94: 8521-8526.
141. Rink SM, Shen JC, Loeb LA (1998) Creation of RNA molecules that recognize the oxidative lesion 7,8-dihydro-8-hydroxy-2'-deoxyguanosine (8-oxodG) in DNA. *Proc Natl Acad Sci U S A* 95: 11619-11624.
142. Koizumi M, Breaker RR (2000) Molecular recognition of cAMP by an RNA aptamer. *Biochemistry* 39: 8983-8992.
143. Holeman LA, Robinson SL, Szostak JW, Wilson C (1998) Isolation and characterization of fluorophore-binding RNA aptamers. *Fold Des* 3: 423-431.
144. Grate D, Wilson C (1999) Laser-mediated, site-specific inactivation of RNA transcripts. *Proc Natl Acad Sci U S A* 96: 6131-6136.
145. Brockstedt U, Uzarowska A, Montpetit A, Pfau W, Labuda D (2004) In vitro evolution of RNA aptamers recognizing carcinogenic aromatic amines. *Biochem Biophys Res Commun* 313: 1004-1008.
146. Hofmann HP, Limmer S, Hornung V, Sprinzl M (1997) Ni<sup>2+</sup>-binding RNA motifs with an asymmetric purine-rich internal loop and a G-A base pair. *RNA* 3: 1289-1300.
147. Ciesiolka J, Gorski J, Yarus M (1995) Selection of an RNA domain that binds Zn<sup>2+</sup>. *RNA* 1: 538-550.
148. Shigdar S, Lin J, Yu Y, Pastuovic M, Wei M, et al. (2011) RNA aptamer against a cancer stem cell marker epithelial cell adhesion molecule. *Cancer Sci* 102: 991-998.
149. Chen CHB, Chernis GA, Hoang VQ, Landgraf R (2003) Inhibition of heregulin signaling by an aptamer that preferentially binds to the oligomeric form of human epidermal growth factor receptor-3. *Proc Natl Acad Sci U S A* 100: 9226-9231.
150. Kang HS, Huh YM, Kim S, Lee D (2009) Isolation of RNA aptamers targeting HER-2- overexpressing breast cancer cells using cell-SELEX. *Bull Korean Chem Soc* 30: 1827-1831.
151. Lupold SE, Hicke BJ, Lin Y, Coffey DS (2002) Identification and characterization of nuclease-stabilized RNA molecules that bind human prostate cancer cells via the prostate-specific membrane antigen. *Cancer Res* 62: 4029-4033.
152. Ylera F, Lurz R, Erdmann VA, Furste JP (2002) Selection of RNA aptamers to the Alzheimer's disease amyloid peptide. *Biochem Biophys Res Commun* 290: 1583-1588.
153. Binkley J, Allen P, Brown DM, Green L, Tuerk C, et al. (1995) RNA ligands to human nerve growth factor. *Nucleic Acids Res* 23: 3198-3205.
154. Daniels DA, Sohal AK, Rees S, Grisshammer R (2002) Generation of RNA aptamers to the G-protein-coupled receptor for neurotensin, NTS-1. *Anal Biochem* 305: 214-226.
155. Nieuwlandt D, Wecker M, Gold L (1995) In vitro selection of RNA ligands to substance P. *Biochemistry* 34: 5651-5659.
156. Huang Z, Pei W, Jayaseelan S, Shi H, Niu L (2007) RNA aptamers selected against the GluR2 glutamate receptor channel. *Biochemistry* 46: 12648-12655.

157. Huang Z, Pei W, Han Y, Jayaseelan S, Shekhtman A, et al. (2009) One RNA aptamer sequence, two structures: a collaborating pair that inhibits AMPA receptors. *Nucleic Acids Res* 37: 4022-4032.
158. Rhie A, Kirby L, Sayer N, Wellesley R, Disterer P, et al. (2003) Characterization of 2'-fluoro-RNA aptamers that bind preferentially to disease-associated conformations of prion protein and inhibit conversion. *J Biol Chem* 278: 39697-39705.
159. Ko J, Lee Y, Park I, Cho B (2001) Identification of a structural motif of 23S rRNA interacting with 5S rRNA. *FEBS Lett* 508: 300-304.
160. Sando S, Ogawa A, Nishi T, Hayami M, Aoyama Y (2007) In vitro selection of RNA aptamer against *Escherichia coli* release factor 1. *Bioorg Med Chem Lett* 17: 1216-1220.
161. Homann M, Goringer HU (1999) Combinatorial selection of high affinity RNA ligands to live African trypanosomes. *Nucleic Acids Res* 27: 2006-2014.
162. Pan Q, Zhang XL, Wu HY, He PW, Wang F, et al. (2005) Aptamers that preferentially bind type IVB pili and inhibit human monocytic-cell invasion by *Salmonella enterica* serovar typhi. *Antimicrob Agents Chemother* 49: 4052-4060.
163. Hyeon JY, Chon JW, Choi IS, Park C, Kim DE, et al. (2012) Development of RNA aptamers for detection of *Salmonella Enteritidis*. *J Microbiol Methods* 89: 79-82.
164. Tahiri-Alaoui A, Frigotto L, Manville N, Ibrahim J, Romby P, et al. (2002) High affinity nucleic acid aptamers for streptavidin incorporated into bi-specific capture ligands. *Nucleic Acids Res* 30: e45.
165. Hirao I, Harada Y, Nojima T, Osawa Y, Masaki H, et al. (2004) In vitro selection of RNA aptamers that bind to colicin E3 and structurally resemble the decoding site of 16S ribosomal RNA. *Biochemistry* 43: 3214-3221.
166. Yamamoto R, Katahira M, Nishikawa S, Baba T, Taira K, et al. (2000) A novel RNA motif that binds efficiently and specifically to the Tat protein of HIV and inhibits the trans-activation by Tat of transcription in vitro and in vivo. *Genes Cells* 5: 371-388.
167. Allen P, Worland S, Gold L (1995) Isolation of high-affinity RNA ligands to HIV-1 integrase from a random pool. *Virology* 209: 327-336.
168. Berglund JA, Charpentier B, Rosbash M (1997) A high affinity binding site for the HIV-1 nucleocapsid protein. *Nucleic Acids Res* 25: 1042-1049.
169. Tuerk C, MacDougall S, Gold L (1992) RNA pseudoknots that inhibit human immunodeficiency virus type 1 reverse transcriptase. *Proc Natl Acad Sci U S A* 89: 6988-6992.
170. Khati M, Schuman M, Ibrahim J, Sattentau Q, Gordon S, et al. (2003) Neutralization of infectivity of diverse R5 clinical isolates of human immunodeficiency virus type 1 by gp120-binding 2'-F-RNA aptamers. *J Virol* 77: 12692-12698.
171. Gopinath SCB, Misono TS, Kawasaki K, Mizuno T, Imai M, et al. (2006) An RNA aptamer that distinguishes between closely related human influenza viruses and inhibits haemagglutinin-mediated membrane fusion. *J Gen Virol* 87: 479-487.

172. Gopinath SC, Sakamaki Y, Kawasaki K, Kumar PK (2006) An efficient RNA aptamer against human influenza B virus hemagglutinin. *J Biochem* 139: 837-846.
173. Feng H, Beck J, Nassal M, Hu KH (2011) A SELEX-screened aptamer of human hepatitis B virus RNA encapsidation signal suppresses viral replication. *PLoS One* 6: e27862.
174. Urvil PT, Kakiuchi N, Zhou DM, Shimotohno K, Kumar PK, et al. (1997) Selection of RNA aptamers that bind specifically to the NS3 protease of hepatitis C virus. *Eur J Biochem* 248: 130-138.
175. Biroccio A, Hamm J, Incitti I, De Francesco R, Tomei L (2002) Selection of RNA aptamers that are specific and high-affinity ligands of the hepatitis C virus RNA-dependent RNA polymerase. *J Virol* 76: 3688-3696.
176. Chen H, Gold L (1994) Selection of high-affinity RNA ligands to reverse transcriptase: inhibition of cDNA synthesis and RNase H activity. *Biochemistry* 33: 8746-8756.
177. Park SY, Kim S, Yoon H, Kim KB, Kalme SS, et al. (2011) Selection of an antiviral RNA aptamer against hemagglutinin of the subtype H5 avian influenza virus. *Nucleic Acid Ther* 21: 395-402.
178. Jang KJ, Lee NR, Yeo WS, Jeong YJ, Kim DE (2008) Isolation of inhibitory RNA aptamers against severe acute respiratory syndrome (SARS) coronavirus NTPase/Helicase. *Biochem Biophys Res Commun* 366: 738-744.
179. Bryant KF, Cox JC, Wang H, Hogle JM, Ellington AD, et al. (2005) Binding of herpes simplex virus-1 US11 to specific RNA sequences. *Nucleic Acids Res* 33: 6090-6100.
180. Baskerville S, Zapp M, Ellington AD (1999) Anti-Rex aptamers as mimics of the Rex-binding element. *J Virol* 73: 4962-4971.
181. Chen H, McBroom DG, Zhu YQ, Gold L, North TW (1996) Inhibitory RNA ligand to reverse transcriptase from feline immunodeficiency virus. *Biochemistry* 35: 6923-6930.
182. Schneider D, Tuerk C, Gold L (1992) Selection of high affinity RNA ligands to the bacteriophage R17 coat protein. *J Mol Biol* 228: 862-869.
183. Mori Y, Nakamura Y, Ohuchi S (2012) Inhibitory RNA aptamer against SP6 RNA polymerase. *Biochem Biophys Res Commun* 420: 440-443.
184. Rusconi CP, Yeh A, Lysterly HK, Lawson JH, Sullenger BA (2000) Blocking the initiation of coagulation by RNA aptamers to factor VIIa. *Thromb Haemost* 84: 841-848.
185. Rusconi CP, Scardino E, Layzer J, Pitoc GA, Ortel TL, et al. (2002) RNA aptamers as reversible antagonists of coagulation factor IXa. *Nature* 419: 90-94.
186. Gal SW, Amontov S, Urvil PT, Vishnuvardhan D, Nishikawa F, et al. (1998) Selection of a RNA aptamer that binds to human activated protein C and inhibits its protease function. *Eur J Biochem* 252: 553-562.
187. Ulrich H, Magdesian MH, Alves MJ, Colli W (2002) In vitro selection of RNA aptamers that bind to cell adhesion receptors of *Trypanosoma cruzi* and inhibit cell invasion. *J Biol Chem* 277: 20756-20762.

188. White RR, Shan S, Rusconi CP, Shetty G, Dewhirst MW, et al. (2003) Inhibition of rat corneal angiogenesis by a nuclease-resistant RNA aptamer specific for angiopoietin-2. *Proc Natl Acad Sci U S A* 100: 5028-5033.
189. White R, Rusconi C, Scardino E, Wolberg A, Lawson J, et al. (2001) Generation of species cross-reactive aptamers using "toggle" SELEX. *Mol Ther* 4: 567-573.
190. Burnette AD, Nimjee SM, Batchvarova M, Zennadi R, Telen MJ, et al. (2011) RNA aptamer therapy for vaso-occlusion in Sickle cell disease. *Nucleic Acid Ther* 21: 275-283.
191. Blind M, Kolanus W, Famulok M (1999) Cytoplasmic RNA modulators of an inside-out signal-transduction cascade. *Proc Natl Acad Sci U S A* 96: 3606-3610.
192. Lee HK, Choi YS, Park YA, Jeong S (2006) Modulation of oncogenic transcription and alternative splicing by beta-catenin and an RNA aptamer in colon cancer cells. *Cancer Res* 66: 10560-10566.
193. Jenison RD, Jennings SD, Walker DW, Bargatze RF, Parma D (1998) Oligonucleotide inhibitors of P-selectin-dependent neutrophil-platelet adhesion. *Antisense Nucleic Acid Drug Dev* 8: 265-279.
194. O'Connell D, Koenig A, Jennings S, Hicke B, Han HL, et al. (1996) Calcium-dependent oligonucleotide antagonists specific for L-selectin. *Proc Natl Acad Sci U S A* 93: 5883-5887.
195. Nazarenko IA, Uhlenbeck OC (1995) Defining a smaller RNA substrate for elongation factor Tu. *Biochemistry* 34: 2545-2552.
196. Klug SJ, Huttenhofer A, Kromayer M, Famulok M (1997) In vitro and in vivo characterization of novel mRNA motifs that bind special elongation factor SelB. *Proc Natl Acad Sci U S A* 94: 6676-6681.
197. Scarabino D, Crisari A, Lorenzini S, Williams K, Tocchini-Valentini GP (1999) tRNA prefers to kiss. *EMBO J* 18: 4571-4578.
198. Hirao I, Madin K, Endo Y, Yokoyama S, Ellington AD (2000) RNA aptamers that bind to and inhibit the ribosome-inactivating protein, pepocin. *J Biol Chem* 275: 4943-4948.
199. Pagratis NC, Bell C, Chang YF, Jennings S, Fitzwater T, et al. (1997) Potent 2'-amino-, and 2'-fluoro-2'-deoxyribonucleotide RNA inhibitors of keratinocyte growth factor. *Nat Biotechnol* 15: 68-73.
200. Kimoto M, Shirouzu M, Mizutani S, Koide H, Kaziro Y, et al. (2002) Anti-(Raf-1) RNA aptamers that inhibit Ras-induced Raf-1 activation. *Eur J Biochem* 269: 697-704.
201. Vuyisich M, Beal PA (2002) Controlling protein activity with ligand-regulated RNA aptamers. *Chem Biol* 9: 907-913.
202. Ruckman J, Green LS, Beeson J, Waugh S, Gillette WL, et al. (1998) 2'-Fluoropyrimidine RNA-based aptamers to the 165-amino acid form of vascular endothelial growth factor (VEGF165). Inhibition of receptor binding and VEGF-induced vascular permeability through interactions requiring the exon 7-encoded domain. *J Biol Chem* 273: 20556-20567.
203. Biesecker G, Dihel L, Enney K, Bendele RA (1999) Derivation of RNA aptamer inhibitors of human complement C5. *Immunopharmacology* 42: 219-230.

204. Hicke BJ, Marion C, Chang YF, Gould T, Lynott CK, et al. (2001) Tenascin-C aptamers are generated using tumor cells and purified protein. *J Biol Chem* 276: 48644-48654.
205. Bridonneau P, Chang YF, O'Connell D, Gill SC, Snyder DW, et al. (1998) High-affinity aptamers selectively inhibit human nonpancreatic secretory phospholipase A2 (hnp-PLA2). *J Med Chem* 41: 778-786.
206. Ohuchi SP, Ohtsu T, Nakamura Y (2006) Selection of RNA aptamers against recombinant transforming growth factor-beta type III receptor displayed on cell surface. *Biochimie* 88: 897-904.
207. Seiwert SD, Stines Nahreini T, Aigner S, Ahn NG, Uhlenbeck OC (2000) RNA aptamers as pathway-specific MAP kinase inhibitors. *Chem Biol* 7: 833-843.
208. Jellinek D, Lynott CK, Rifkin DB, Janjic N (1993) High-affinity RNA ligands to basic fibroblast growth factor inhibit receptor binding. *Proc Natl Acad Sci U S A* 90: 11227-11231.
209. Bell SD, Denu JM, Dixon JE, Ellington AD (1998) RNA molecules that bind to and inhibit the active site of a tyrosine phosphatase. *J Biol Chem* 273: 14309-14314.
210. Haraguchi Y, Kuwasako K, Muto Y, Bessho Y, Nishimoto M, et al. (2009) Characterization of RNA aptamers against SRP19 protein having sequences different from SRP RNA. *Nucleic Acids Symp Ser (Oxf)*: 265-266.
211. Hyun S, Lee KH, Han A, Yu J (2011) An RNA aptamer that selectively recognizes symmetric dimethylation of arginine 8 in the histone H3 N-terminal peptide. *Nucleic Acid Ther* 21: 157-163.
212. Bini A, Centi S, Tombelli S, Minunni M, Mascini M (2008) Development of an optical RNA-based aptasensor for C-reactive protein. *Anal Bioanal Chem* 390: 1077-1086.
213. Tesmer VM, Lennarz S, Mayer G, Tesmer JJ (2012) Molecular mechanism for inhibition of G protein-coupled receptor kinase 2 by a selective RNA aptamer. *Structure* 20: 1300-1309.
214. Jeong S, Eom T, Kim S, Lee S, Yu J (2001) In vitro selection of the RNA aptamer against the Sialyl Lewis X and its inhibition of the cell adhesion. *Biochem Biophys Res Commun* 281: 237-243.
215. Cox JC, Ellington AD (2001) Automated selection of anti-protein aptamers. *Bioorg Med Chem* 9: 2525-2531.
216. Levesque D, Beaudoin JD, Roy S, Perreault JP (2007) In vitro selection and characterization of RNA aptamers binding thyroxine hormone. *Biochem J* 403: 129-138.
217. Davis KA, Lin Y, Abrams B, Jayasena SD (1998) Staining of cell surface human CD4 with 2'-F-pyrimidine-containing RNA aptamers for flow cytometry. *Nucleic Acids Res* 26: 3915-3924.
218. Kubik MF, Bell C, Fitzwater T, Watson SR, Tasset DM (1997) Isolation and characterization of 2'-fluoro-, 2'-amino-, and 2'-fluoro-/amino-modified RNA ligands to human IFN-gamma that inhibit receptor binding. *J Immunol* 159: 259-267.

219. Wiegand TW, Williams PB, Dreskin SC, Jouvin MH, Kinet JP, et al. (1996) High-affinity oligonucleotide ligands to human IgE inhibit binding to Fc epsilon receptor I. *J Immunol* 157: 221-230.
220. Santulli-Marotto S, Nair SK, Rusconi C, Sullenger B, Gilboa E (2003) Multivalent RNA aptamers that inhibit CTLA-4 and enhance tumor immunity. *Cancer Res* 63: 7483-7489.
221. Watanabe T, Ito K, Matsumoto M, Seya T, Nishikawa S, et al. (2006) Isolation of RNA aptamers against human Toll-like receptor 3 ectodomain. *Nucleic Acids Symp Ser (Oxf)*: 251-252.
222. Doudna JA, Cech TR, Sullenger BA (1995) Selection of an RNA molecule that mimics a major autoantigenic epitope of human insulin receptor. *Proc Natl Acad Sci U S A* 92: 2355-2359.
223. Hwang B, Lee SW (2002) Improvement of RNA aptamer activity against myasthenic autoantibodies by extended sequence selection. *Biochem Biophys Res Commun* 290: 656-662.
224. Kim YM, Choi KH, Jang YJ, Yu J, Jeong S (2003) Specific modulation of the anti-DNA autoantibody-nucleic acids interaction by the high affinity RNA aptamer. *Biochem Biophys Res Commun* 300: 516-523.
225. Chen CH, Dellamaggiore KR, Ouellette CP, Sedano CD, Lizadjohry M, et al. (2008) Aptamer-based endocytosis of a lysosomal enzyme. *Proc Natl Acad Sci U S A* 105: 15908-15913.
226. Lebruska LL, Maher LJ, 3rd (1999) Selection and characterization of an RNA decoy for transcription factor NF-kappa B. *Biochemistry* 38: 3168-3174.
227. Meyer C, Eydeler K, Magbanua E, Zivkovic T, Piganeau N, et al. (2012) Interleukin-6 receptor specific RNA aptamers for cargo delivery into target cells. *RNA Biol* 9: 67-80.
228. Berezhnoy A, Stewart CA, McNamara JO, Thiel W, Giangrande P, et al. (2012) Isolation and optimization of murine IL-10 receptor blocking oligonucleotide aptamers using high-throughput sequencing. *Molecular Therapy* 20: 1242-1250.
229. Kim S, Kim JH, Yoon S, Kim KS, Yoon MY, et al. (2010) Generation of antagonistic RNA aptamers specific to proinflammatory cytokine interleukin-32. *Bull Korean Chem Soc* 31: 3561-3566.
230. Zhai LJ, Wang TJ, Kang K, Zhao Y, Shrotriya P, et al. (2012) An RNA aptamer-based microcantilever sensor to detect the inflammatory marker, mouse lipocalin-2. *Anal Chem* 84: 8763-8770.
231. Fowler CC, Navani NK, Brown ED, Li Y (2008) Aptamers and their potential as recognition elements for the detection of bacteria. In: Zourob M, Elwary S, Turner A, editors. *Principles of Bacterial Detection: Biosensors, Recognition Receptors and Microsystems*. Montreal, Canada: Springer. pp. 689-714.
232. Li Y, Breaker RR (1999) Kinetics of RNA degradation by specific base catalysis of transesterification involving the 2'-hydroxyl group. *J Am Chem Soc* 121: 5364-5372.

233. Oivanen M, Kuusela S, Lonnberg H (1998) Kinetics and mechanisms for the cleavage and isomerization of the phosphodiester bonds of RNA by Bronsted acids and bases. *Chem Rev* 98: 961-990.
234. Westheimer FH (1968) Pseudo-rotation in the hydrolysis of phosphate esters. *Acc Chem Res* 1: 70-78.
235. Lightstone FC, Bruice TC (1996) Ground state conformations and entropic and enthalpic factors in the efficiency of intramolecular and enzymatic reactions. 1. Cyclic anhydride formation by substituted glutarates, succinate, and 3,6-Endoxo- $\Delta^4$ -tetrahydrophthalate monophenyl esters. *J Am Chem Soc* 118: 2595-2605.
236. Soukup GA, Breaker RR (1999) Relationship between internucleotide linkage geometry and the stability of RNA. *RNA* 5: 1308-1325.
237. Cech TR, Golden BL (1999) Building a catalytic active site using only RNA. In: Gesteland RF, Cech TR, Atkins JF, editors. *The RNA World*. Cold Spring Harbor, New York: Cold Spring Harbor Laboratory Press. pp. 321-349.
238. Ciesiolka J, Lorenz S, Erdmann VA (1992) Different conformational forms of *Escherichia coli* and rat liver 5S rRNA revealed by Pb(II)-induced hydrolysis. *Eur J Biochem* 204: 583-589.
239. Reynolds MA, Beck TA, Say PB, Schwartz DA, Dwyer BP, et al. (1996) Antisense oligonucleotide containing an internal, non-nucleotide-based linker promote site-specific cleavage of RNA. *Nucleic Acids Res* 24: 760-765.
240. Welch M, Majerfeld I, Yarus M (1997) 23S rRNA similarity from selection for peptidyl transferase mimicry. *Biochemistry* 36: 6614-6623.
241. Usher DA, McHale AH (1976) Hydrolytic stability of helical RNA: a selective advantage for the natural 3',5'-bond. *Proc Natl Acad Sci U S A* 73: 1149-1153.
242. Jin R, Chapman WH, Jr., Srinivasan AR, Olson WK, Breslow R, et al. (1993) Comparative spectroscopic, calorimetric, and computational studies of nucleic acid complexes with 2',5"-versus 3',5"-phosphodiester linkages. *Proc Natl Acad Sci U S A* 90: 10568-10572.
243. Puglisi EV, Puglisi JD, Williamson JR, RajBhandary UL (1994) NMR analysis of tRNA acceptor stem microhelices: discriminator base change affects tRNA conformation at the 3' end. *Proc Natl Acad Sci U S A* 91: 11467-11471.
244. Gerlt JA (1993) Mechanistic principles of enzyme-catalyzed cleavage of phosphodiester bonds. In: Linn SM, Lloyd RS, Roberts RJ, editors. *The Nucleases*. Cold Spring Harbor, New York: Cold Spring Harbor Laboratory Press. pp. 1-34.
245. Carlson WD (1976) X-ray diffraction studies of bovine pancreatic ribonuclease-S and *E. Coli* alkaline phosphatase. New Haven, Connecticut: Yale University.
246. Thompson JE, Kutateladze TG, Schuster MC, Venegas FD, Messmore JM, et al. (1995) Limits to catalysis by ribonuclease A. *Bioorg Chem* 23: 471-481.
247. Nutiu R, Yu JMY, Li YF (2004) Signaling aptamers for monitoring enzymatic activity and for inhibitor screening. *ChemBiochem* 5: 1139-1144.
248. Nutiu R, Li YF (2005) A DNA-protein nanoengine for "On-Demand" release and precise delivery of molecules. *Angew Chem Int Ed Engl* 44: 5464-5467.

249. Rupcich N, Nutiu R, Li YF, Brennan JD (2006) Solid-phase enzyme activity assay utilizing an entrapped fluorescence-signaling DNA aptamer. *Angew Chem Int Ed* 45: 3295-3299.
250. Liu JW, Lu Y (2007) Non-base pairing DNA provides a new dimension for controlling aptamer-linked nanoparticles and sensors. *J Am Chem Soc* 129: 8634-8643.
251. Zhu Z, Wu C, Liu H, Zou Y, Zhang X, et al. (2010) An aptamer cross-linked hydrogel as a colorimetric platform for visual detection. *Angew Chem Int Ed Engl* 49: 1052-1056.
252. Wu ZS, Guo MM, Zhang SB, Chen CR, Jiang JH, et al. (2007) Reusable electrochemical sensing platform for highly sensitive detection of small molecules based on structure-switching signaling aptamers. *Anal Chem* 79: 2933-2939.
253. Zayats M, Huang Y, Gill R, Ma CA, Willner I (2006) Label-free and reagentless aptamer-based sensors for small molecules. *J Am Chem Soc* 128: 13666-13667.
254. Sugimoto N, Nakano S, Katoh M, Matsumura A, Nakamuta H, et al. (1995) Thermodynamic parameters to predict stability of RNA/DNA hybrid duplexes. *Biochemistry* 34: 11211-11216.
255. Lesnik EA, Freier SM (1995) Relative thermodynamic stability of DNA, RNA, and DNA:RNA hybrid duplexes: relationship with base composition and structure. *Biochemistry* 34: 10807-10815.
256. Paladino A, Zangi R (2013) Propensities for loop structures of RNA & DNA backbones. *Biophys Chem* 180-181: 110-118.
257. Pley HW, Flaherty KM, McKay DB (1994) Model for an RNA tertiary interaction from the structure of an intermolecular complex between a GAAA tetraloop and an RNA helix. *Nature* 372: 111-113.
258. Cate JH, Gooding AR, Podell E, Zhou K, Golden BL, et al. (1996) Crystal structure of a group I ribozyme domain: principles of RNA packing. *Science* 273: 1678-1685.
259. Nissen P, Ippolito JA, Ban N, Moore PB, Steitz TA (2001) RNA tertiary interactions in the large ribosomal subunit: the A-minor motif. *Proc Natl Acad Sci U S A* 98: 4899-4903.
260. Tamura M, Holbrook SR (2002) Sequence and structural conservation in RNA ribose zippers. *J Mol Biol* 320: 455-474.
261. Collie GW, Haider SM, Neidle S, Parkinson GN (2010) A crystallographic and modelling study of a human telomeric RNA (TERRA) quadruplex. *Nucleic Acids Res* 38: 5569-5580.
262. Butcher SE, Pyle AM (2011) The molecular interactions that stabilize RNA tertiary structure: RNA motifs, patterns, and networks. *Acc Chem Res* 44: 1302-1311.
263. Sassanfar M, Szostak JW (1993) An RNA motif that binds ATP. *Nature* 364: 550-553.
264. Willner I, Zayats M (2007) Electronic aptamer-based sensors. *Angew Chem Int Ed Engl* 46: 6408-6418.

265. Cheng AKH, Sen D, Yu HZ (2009) Design and testing of aptamer-based electrochemical biosensors for proteins and small molecules. *Bioelectrochemistry* 77: 1-12.
266. Zhang L, Lu Z, Zhao Q, Huang J, Shen H, et al. (2011) Enhanced chemotherapy efficacy by sequential delivery of siRNA and anticancer drugs using PEI-grafted graphene oxide. *Small* 7: 460-464.
267. Liu Z, Robinson JT, Sun X, Dai H (2008) PEGylated nanographene oxide for delivery of water-insoluble cancer drugs. *J Am Chem Soc* 130: 10876-10877.
268. Sun X, Liu Z, Welsher K, Robinson JT, Goodwin A, et al. (2008) Nano-graphene oxide for cellular imaging and drug delivery. *Nano Res* 1: 203-212.
269. Wang Y, Li ZH, Hu DH, Lin CT, Li JH, et al. (2010) Aptamer/graphene oxide nanocomplex for in situ molecular probing in living cells. *J Am Chem Soc* 132: 9274-9276.
270. Wang Y, Li Z, Weber TJ, Hu D, Lin CT, et al. (2013) In situ live cell sensing of multiple nucleotides exploiting DNA/RNA aptamers and graphene oxide nanosheets. *Anal Chem* 85: 6775-6782.
271. Yang K, Zhang S, Zhang G, Sun X, Lee ST, et al. (2010) Graphene in mice: ultrahigh in vivo tumor uptake and efficient photothermal therapy. *Nano Lett* 10: 3318-3323.
272. Chen BA, Liu M, Zhang LM, Huang J, Yao JL, et al. (2011) Polyethylenimine-functionalized graphene oxide as an efficient gene delivery vector. *J Mater Chem* 21: 7736-7741.
273. Kim H, Namgung R, Singha K, Oh IK, Kim WJ (2011) Graphene oxide-polyethylenimine nanoconstruct as a gene delivery vector and bioimaging tool. *Bioconjugate Chem* 22: 2558-2567.
274. Sultan MB, Zhou D, Loftus J, Dombi T, Ice KS, et al. (2011) A phase 2/3, multicenter, randomized, double-masked, 2-year trial of pegaptanib sodium for the treatment of diabetic macular edema. *Ophthalmology* 118: 1107-1118.
275. Ni X, Castanares M, Mukherjee A, Lupold SE (2011) Nucleic acid aptamers: clinical applications and promising new horizons. *Curr Med Chem* 18: 4206-4214.
276. Meyer C, Hahn U, Rentmeister A (2011) Cell-specific aptamers as emerging therapeutics. *J Nucleic Acids* 2011: 904750.
277. Bagalkot V, Zhang L, Levy-Nissenbaum E, Jon S, Kantoff PW, et al. (2007) Quantum dot-aptamer conjugates for synchronous cancer imaging, therapy, and sensing of drug delivery based on bi-fluorescence resonance energy transfer. *Nano Lett* 7: 3065-3070.
278. Zhang L, Radovic-Moreno AF, Alexis F, Gu FX, Basto PA, et al. (2007) Co-delivery of hydrophobic and hydrophilic drugs from nanoparticle-aptamer bioconjugates. *ChemMedChem* 2: 1268-1271.